UNIVERSITÉ LAVAL

Hybrid modeling of aboveground biomass carbon using disturbance history over large areas of boreal forest in eastern Canada

Thèse

Dinesh Babu Irulappa Pillai Vijayakumar

Doctorat en sciences forestières
Philosophiae doctor (Ph.D.)

Québec, Canada

Résumé

Le feu joue un rôle important dans la succession de la forêt boréale du nord-est de l'Amérique et le temps depuis le dernier feu (TDF) devrait être utile pour prédire la distribution spatiale du carbone. Les deux premiers objectifs de cette thèse sont: (1) la spatialisation du TDF pour une vaste région de forêt boréale de l'est du Canada (217,000 km^2) et (2) la prédiction du carbone de la biomasse aérienne (CBA) à l'aide du TDF à une échelle liée aux perturbations par le feu.

Un modèle non paramétrique a d'abord été développé pour prédire le TDF à partir d'historiques de feu, des données d'inventaire et climatiques à une échelle de 2 km^2. Cette échelle correspond à la superficie minimale d'un feu pour être inclus dans la base de données canadienne des grands feux. Nous avons trouvé un ajustement substantiel à l'échelle de la région d'étude et à celle de paysages régionaux, mais la précision est restée faible à l'échelle de cellules individuelles de 2 km^2.

Une modélisation hiérarchique a ensuite été développée pour spatialiser le CBA des placettes d'inventaire à la même échelle de 2 km^2. Les proportions des classes de densité du couvert étaient les variables les plus importantes pour prédire le CBA. Le CBA co-variait également avec la vitesse de récupération du couvert au travers de laquelle le TDF intervient indirectement.

Finalement, nous avons comparé des estimations de CBA obtenues par télédétection satellitaire avec celles obtenues précédemment. Les résultats indiquent que les proportions des classes de densité du couvert et des types de dépôts ainsi que le TDF pourraient servir comme variables auxiliaires pour augmenter substantiellement la précision des estimés de CBA par télédétection.

Les résultats de cette étude ont montré: 1) l'importance d'allonger la profondeur temporelle des historiques de feu pour donner une meilleure perspective des changements actuels du régime de feu; 2) l'importance d'intégrer l'information sur la reprise du couvert après feu aux courbes de rendement de CBA dans les modèles de bilan de carbone; et 3) l'importance de l'historique des feux et de la récupération de la végétation pour améliorer la précision de la cartographie de la biomasse à partir de la télédétection.

Abstract

Fire is as a main succession driver in northeastern American boreal forests and time since last fire (TSLF) is seen as a useful covariate to infer the spatial variation of carbon. The first two objectives of this thesis are: (1) to elaborate a TSLF map over an extensive region in boreal forests of eastern Canada (217,000 km^2) and (2) to predict aboveground carbon biomass (ABC) as a function of TSLF at a scale related to fire disturbances.

A non-parametric model was first developed to predict TSLF using historical records of fire, forest inventory data and climate data at a 2-km^2 scale. Two kilometer square is the minimum size for fires to be considered important enough and included in the Canadian large fire database. Overall, we found a substantial agreement at the scale of both the study area and landscape units, but the accuracy remained fairly low at the scale of individual 2-km^2 cells.

A hierarchical modeling approach is then presented for scaling-up ABC from inventory plots to the same 2 km^2 scale. The proportions of cover density classes were the most important variables to predict ABC. ABC was also related to the speed of post-fire canopy recovery through which TSLF acts indirectly upon ABC.

Finally, we compared remote sensing based aboveground biomass estimates with our inventory based estimates to provide insights on improving their accuracy. The results indicated again that abundances of canopy cover density classes of surficial deposits, and TSLF may serve as ancillary variables for improving substantially the accuracy of remotely sensed biomass estimates.

The study results have shown: 1) the importance of lengthening the historical records of fire records to provide a better perspective of the actual changes of fire regime; 2) the importance of incorporating post-fire canopy recovery information together with ABC yield curves in carbon budget models at a spatial scale related to fire disturbances; 3) the importance of adding disturbance history and vegetation recovery trends with remote sensing reflectance data to improve accuracy for biomass mapping

Table of contents

Résumé iii
Abstract v
Table of contents vii
List of Tables xi
List of Figures xiii
Acknowledgements xvii
Preface xix
1. General Introduction 1
1.01 What is a forest carbon stock? 1
1.02 Carbon stocks in Canadian boreal ecosystems 1
1.03 Dynamics of the black spruce forest 4
1.04 Why map TSLF? 5
1.05 Research problem and motivation 5
1.06 Objectives 7
1.07 References 9
2. Chapter 1: Lengthening the historical records of fire history over large areas of boreal forest in eastern Canada using empirical relationships 15
2.01 Abstract 16
2.02 Introduction 17
2.03 Methods 18
2.03.01 Study Area 18
2.03.02 Characterization of study units 19
2.03.03 Modelling TSLF 22
2.03.04 TSLF extrapolation to the entire study area 26
2.03.05 Relating forest composition with past disturbances at the landscape scale 26
2.04 Results 27
2.04.01 Accuracy of TSLF models 27
2.04.02 Temporal changes in the decadal burn rate during the 20th century 29
2.04.03 Forest composition in relation to fire regime as derived from the TSLF map 29
2.05 Discussion 31
2.05.01 Estimation of TSLF over a large spatial extent with Random Forest models 31

2.05.02 Interpretation of TSLF predictors 32
2.05.03 Impacts of spatial scale on TSLF modelling 32
2.05.04 Temporal changes in regional burn rate 33
2.05.05 Management and conservation implications 33
2.06 Conclusion 33
2.07 Acknowledgements 34
2.08 References 35
2.09 Supplementary material 41
3. Chapter 2: Cover density recovery after fire disturbance controls landscape aboveground biomass carbon in the boreal forest of eastern Canada 45
3.01 Abstract 46
3.02 Introduction 47
3.03 Material and Methods 48
3.03.01 Study region 48
3.03.02 Datasets and study units 49
3.03.03 Scaling framework 52
3.03.04 Quantifying information loss due to scaling-up 54
3.03.05 Result synthesis and visualization 54
3.04 Results 55
3.04.01 Estimation of aboveground biomass carbon 55
3.04.02 Variation of cover density and ABC yield curves at a regional scale 57
3.05 Discussion 61
3.05.01 Interpretation of ABC predictors at plot level 61
3.05.02 Relationship between ABC and TSLF at the 2-km^2 scale 61
3.05.03 Comparing accuracy with previous studies 62
3.05.04 Implications for C budget modelling 62
3.06 Conclusion 63
3.07 Acknowledgements 64
3.08 References 65
4. Chapter 3: Fire disturbance history improves the consistency of remotely sensed aboveground biomass estimates for boreal forests in eastern Canada 73
4.01 Abstract 74
4.02 Introduction 75
4.03 Methods 78

4.03.01 Study area 78
4.03.02 Estimation of AGB based on inventory data 79
4.03.03 Estimations of AGB from remote sensing data 80
4.03.04 Comparison of biomass maps 82
4.04 Results 84
4.04.01 Estimation of AGB using GLAS canopy height data 84
4.04.02 Spatial distribution and covariation of remotely sensed and inventory based biomass estimates 85
4.04.03 Spatial analysis of differences between inventory and remotely sensed biomass estimates 88
4.04.04 Detecting potential ancillary variables for remotely sensed AGB estimation 88
4.04.05 AGB yield curves with remotely sensed products 89
4.05 Discussion 94
4.05.01 Interpreting covariation and spatial distribution of biomass estimates 94
4.05.02 Consistency of results among comparable studies 96
4.05.03 Potential ancillary variables for remotely sensed AGB estimation 96
4.06 Conclusion 98
4. 07 Acknowledgements 98
4.08 References 100
4.09 Supplementary material 108
5. General Conclusion 111
5.01 References 113

List of Tables

Table 2-1. List of explanatory variables considered for the training of the random forest models 21

Table 2-2. Sources used to generate the response variable for the training dataset for the random forest TSLF models 24

Table 2-3. Average proportions of tree species by vegetation cluster after a clustering analysis to explain the homogeneity of landscape units by vegetation composition. Species names are provided in Table 2.1. Bold numbers indicate the dominant species 30

Table 3-1. Mean proportions of the relative abundances of surficial deposits classes: very abundant, very coarse (VAVC); abundant, coarse (AC); rock (ROC); and organic (ORG) (Mansuy et al., 2010), and the means of degree-days by each cluster, which were used to explain homogeneity of the landscape units. Bold numbers indicate the maximum value of variables that were used for clustering (values are normalized). 58

Table 4-1. List of explanatory variables used in estimating AGB 83

Table 4-2. Pearson correlations between each of MODIS, GLAS, ASAR and inventory based AGB estimates after accounting for spatial autocorrelation* 86

List of Figures

Figure 2.1. Location of study area (outlined in dark black) and fire history maps (numbered grayed areas, refer to Table 2.2). Inventory plots used for the training of the TSLF models are not shown. 19

Figure 2.2. For the top six variables (Table 2.1), ranked by the random forest models for the classification of 2-km^2 cells into TSLF ≤ 120 years and TSLF > 120 years, (a) normalized mean decrease in Gini coefficient, and (b) normalized mean decrease in mean square error in predicted cell-level TSLF for cells in which TSLF is predicted to be less than 120 years; c) density plot of observed vs predicted year of stand origin for cells for which TSLF is predicted ≤ 120 years; d) box-and-whisker plots of margins of error for predicted TSLF values grouped by decade class; e) Decadal burn rates between 1880 and 2000 for the study region (dark grey: burn rate correction due to survival analyses, light grey: highest values of burn rate, hatching: burn rates between 1970 and 2000). 28

Figure 2.3. Map of predicted time since last fire by decade class (between1880 and 2000). The map was generalized by aggregating 2-km^2 cells of identical period of fire activity (1880-1920, 1920-1940, 1940-1970 and 1970-2000) and by removing any object smaller than 4 km^2. 29

Figure 2.4. a) Vegetation map of landscape units (ecological districts) derived from a cluster analysis based on species abundance. Average proportions of species and names for each cluster are presented in Table 2.3; b) box-and-whisker plots of mean time since last fire by ecological district across the vegetation clusters; c) frequency of 2-km^2 cells with a TSLF value above or below 120 years by vegetation cluster. 31

Figure 3.1. Panel a) Location of the study area (dark outline) with training areas for which time-since-last-fire was available from published studies. Panel b) Distribution of forest inventory plots used in the analysis. 51

Figure 3.2. Top six variables ranked by the random forest models for the prediction of ABC at plot level (a) and at scale of 2-km^2 cells (d). Density plot of estimated ABC vs predicted ABC at plot level (b) and at 2-km^2 scale (e). c) Map of ABC predicted with RF modelling at the scale of 2 km^2. 56

Figure 3.3. (a) Box-and-whisker plots of the coefficient of variation of residual variance for individual 2-km^2 cells as a function of the number of repetitions of RF model training for ABC prediction. (b) Density plot of estimated vs predicted ABC values at 2-km^2 scale when variability of predicted values at SIFORT tile centroid level is considered for ABC predictions. (c) Density plot of predicted values of ABC at 2-km^2 scale when variability of predicted values at SIFORT tile centroid level is considered (B) or not (A). 57

Figure 3.4. Cluster map ("organic," "coarse," and "typical" zones) of ecological districts based on centroid degree-days and their relative abundances of marginal surficial deposit groups (organic, stony and coarse-textured, and rock surficial deposits). 59

Figure 3.5. Box-and-whisker plots of ABC as a function of time-since-last-fire at 2-km^2 scale cells in "organic" (a), "coarse" (b), and "typical" (c) zones; box-and-whisker plots of the abundance of closed-density cover (> 81%, 61-80%, and 41-60%) as a function of time-since-last-fire for 2-km^2 scale cells "organic" (d), "coarse" (e), and "typical" (f) zones. 60

Figure 4.1. General flow diagram 78

Figure 4.2. Locations of the study area (dark outline) and training datasets (grey areas) from the published studies. 79

Figure 4.3. Top six variables ranked by a random forest model for the estimation of AGB based on observed canopy height at plot level (a); (b) density plot of estimated vs predicted AGB by the model based on observed canopy height at plot level 85

Figure 4.4. Maps of AGB at the scale of 2 km^2 based on: inventory data (a); MODIS data obtained from Beaudoin et al. (2014) (b); GLAS data (c); ASAR data obtained from Thurner et al. (2014) (d) 87

Figure 4.5 Top-six variables ranked by RF models used to explain the differences observed between remotely sensed and inventory based AGB estimates with relative frequencies of SIFORT attributes (Table 4.1) and observed TSLF: MODIS (a); GLAS (b); and ASAR (c); density plots of observed vs predicted AGB differences between inventories based and remotely sensed AGB estimates: MODIS (d), GLAS (e), and ASAR data (f). 90

Figure 4.6. Box-and-whisker plots of differences observed between inventory based AGB estimates and biomass estimates of MODIS (a), GLAS (b), and ASAR (c), regrouped by abundance classes of canopy closed cover density. 91

Figure 4.7. Top-six variables ranked by RF models used to explain the differences observed between remotely sensed and inventory based AGB estimates when abundances of cover canopy density classes are removed from the list of potential explanatory variables: MODIS, (a); GLAS, (b); and ASAR, (c); density plots of observed vs predicted AGB differences between remotely sensed and inventory based AGB estimates: MODIS (d); GLAS (e); and ASAR data (f). 92

Figure 4.8. Box-and-whisker plots of AGB estimates based on inventory data (a), MODIS (b), GLAS (c), and ASAR data (d) as a function of TSLF at the 2-km^2 scale. 93

Acknowledgements

I would like to express my sincere gratitude to my PhD supervisor, Dr. Frédéric Raulier (Professor, Université Laval), who supported me from the initial start of defining my research proposal to the end of this study. I started PhD without any knowledge on boreal forests and today I have learned many things from my PhD supervisor with his critical and helpful comments.

I would like to thank my co-supervisor Dr. Pierre Bernier (senior scientist, Canadian Forest Service, Laurentian Forestry Center) for guiding me in my study and helping a lot while writing manuscripts.

I would like to thank Dr. Sylvie Gauthier (senior scientist, Canadian Forest Service, Laurentian Forestry Center), Dr. Yves Bergeron (Chaire industrielle CRSNG-UQAT-UQAM en aménagement forestier durable, Université du Québec en Abitibi-Témiscamingue, UQAT) and Dr. David Pothier (Professor, Université Laval) for graciously providing fire history maps. They also helped for writing manuscripts. I also thank Dr. Dominic Cyr, Dr. Héloïse Le Goff, Dr. Annie-Claude Bélisle and Daniel Lesieur for their fire history maps. Without these precious and expensive data, this study would not have been possible. Thanks a lot everybody!!!

I also thank Dr. David Paré (senior scientist, Canadian Forest Service, Laurentian Forestry Center) who was part of my doctoral committee for very useful comments on this study and particularly chapter 2. I am very much grateful to Hakim Ouzenou (Research professional, Université Laval) for helping with SAS programming and also for French translation. I would also like to appreciate Dr. Steven cumming (Professor, Université Laval) and Dr. Alain Leduc (Professor, Université du Québec à Montréal) for their comments to improve the final version of this thesis.

I also thank Dr. Narayan Prasad Dhital, Dr. Kenneth Agbesi Anyomi, Dr. Julien Beguin, Guillaume Cyr, Baburam and Gina for social gathering and discussions beyond the lab work.

I have to thank God Lord Jesus Christ first for his blessings and grace.

Preface

This thesis consists of five sections; General Introduction, Chapter 1, Chapter 2, Chapter 3, and General Conclusion.

Chapter 1 to 3 correspond to the following (published, submitted or under preparation) articles:

1) Irulappa Pillai Vijayakumar, D.B., Raulier, F., Bernier, P. Y., Gauthier, S., Bergeron, Y., & Pothier, D. 2015. Lengthening the historical records of fire history over large areas of boreal forest in eastern Canada using empirical relationships. Forest Ecology and Management, 347, 30-39.

2) Irulappa Pillai Vijayakumar, D.B., Raulier, F., Bernier, P. Y., Paré, D., Gauthier, S., Bergeron, Y., & Pothier, D. 2016. Cover density recovery after fire disturbance controls landscape aboveground biomass carbon in the boreal forest of eastern Canada. Forest Ecology and Management, 360, 170–180.

3) Irulappa Pillai Vijayakumar, D.B., Raulier, F., Bernier, P. Y., Gauthier, S., Bergeron, Y., & Pothier, D. Fire disturbance history improves the consistency of remotely sensed aboveground biomass estimates for boreal forests in eastern Canada (Manuscript under preparation)

Forest inventory data, SIFORT and SOPFEU fire polygons data for this study were provided by Ministère de la Forêt, de la Faune et des Parcs. Dr. Sylvie Gauthier (senior scientist, Canadian Forest Service, Laurentian Forestry Center), Dr. Yves Bergeron (Chaire industrielle CRSNG-UQAT-UQAM en aménagement forestier durable, Université du Québec en Abitibi-Témiscamingue, UQAT) and Dr. David Pothier (Professor, Université Laval) provided fire history maps for this study. Dr. David Paré (senior scientist, Canadian Forest Service, Laurentian Forestry Center) was part of our project, and provided suggestions and comments on this study.

1. General Introduction

1.01 What is a forest carbon stock?

The carbon cycle can be defined as "the constant movement of carbon from the land and water through the atmosphere and living organisms" (Natural Resources Canada, 2015). Carbon is an abundant element that is a constituent of all terrestrial life. Several reservoirs make up the carbon (C) cycle. Among these, forests cover ~32 million km^2 (Hansen et al., 2010) in tropical, temperate, and boreal biomes and play an important role in tempering terrestrial climatic variations (Schimel, 1995). "A forest ecosystem includes the living organisms of the forest, and it extends vertically upward into the atmospheric layer enveloping forest canopies and downward to the lowest soil layers affected by roots and biotic processes" (Waring and Running, 2007). In forest ecosystems, C begins its cycle through photosynthesis. Atmospheric C is transformed into carbohydrates using solar energy and water. Trees release part of their carbohydrates through respiration and store another part in their biomass (foliage, stems, and roots) which constitute carbon stocks. Tree biomass contains approximately 50% carbon. Through senescence, litterfall and mortality, organic matter accumulates on soil and is either released during its decomposition by biological organisms or accumulates in soil carbon stocks.

Aboveground biomass (AGB) is an important biophysical parameter for understanding terrestrial carbon stocks dynamics (Houghton et al., 2009). AGB corresponds to the total oven-dried biological material or mass present above the soil including stump, stem, branches, and foliage in a given area at a given time. Most of C stocks are in the tropical forests (55% of total C stocks, including in soil to 1m depth and live biomass), whereas 32% of C stock is present in boreal forests (Pan et al., 2011). The allocation of C stocked between the vegetation and soils of all ecosystems varies with latitude (Dixon et al., 1994). For example, boreal ecosystems store large amount of the carbon in the soils rather than in vegetation, i.e., 84% of the carbon lies in soil organic matter and the remaining in the living biomass (Malhi et al., 1999). Deforestation is the main driver of carbon dynamics in tropical forests, whereas in boreal forests, natural disturbance and harvesting are the most prominent disturbances that influence carbon stocks (Houghton, 2005). With an increasing interest in the effects of human alteration on the global carbon cycle, knowledge of forest carbon content on a regional and extended-time scale becomes important (Houghton, 2003).

1.02 Carbon stocks in Canadian boreal ecosystems

The boreal forest consists of coniferous and deciduous tree species that covers 11% of the earth's terrestrial surface (Bonan and Shugart, 1989). Twelve percent of the global boreal biome is found within Canada (Burton et al., 2010). Canada's forests therefore play a role in global C cycle for its size and enormous quantity of C stored in vegetation, deep soil, and permafrost pools (Natural Resources Canada, 2012). Canada's managed forest stocks about 28 Pg of carbon in biomass, dead organic matter and soil

pools (Kurz et al., 2013). Improving accuracy in quantifying carbon stocks with an enhanced knowledge of the boreal ecosystems is a key objective of carbon science in Canada (Natural Resources Canada, 2012). Still, capturing spatial variability of carbon stocks at a large scale in the boreal forest remains a challenging issue.

The boreal forests of Canada are the largest supplier of forest products to the world markets (Golden et al., 2011). Intergovernmental panel on climate change (IPCC) recognises that the use of harvested wood products for construction instead of concrete, steel, aluminum and plastic materials could generate carbon emissions reductions (Watson, 2009). The use of forest products for energy also provides a sustainable and renewable resource of energy (Barker, 2007). In recent years, the Canadian forest sector has been facing difficult times and it is in the view of diversifying its markets through the sale of harvest residues and biomass for energy to increase revenue (Paré et al., 2011). To make a profitable forest based products business, it is a responsibility of forest managers to follow an ecosystem-based forest management approach. Ecosystem-based forest management approach is defined as "a management approach that aims to maintain healthy and resilient forest ecosystems by focusing on a reduction of differences between natural and managed landscapes to ensure long term maintenance of ecosystem functions and thereby retain the social and economic benefits they provide to society" (Gauthier et al., 2009). In this approach, the management practices should emulate natural disturbances and maintain biodiversity and forest ecosystem functions (Bergeron et al., 1999). The underlying concept is that species are usually adapted to their natural environmental conditions, including the range of natural variability. This basic concept entails that "past conditions and processes provide a context and the guidance for managing ecological systems today, and that disturbance-driven spatial and temporal variability is a vital attribute of nearly all ecological systems" (Landres et al., 2007). In this context, understanding ecosystem processes and functions including disturbance regimes, is essential to reduce the differences between natural and managed landscapes (Gauthier et al., 2002). This ecosystem-based management approach is based on coarse filter principles. Under a coarse-filter approach, forest management should ensure the conservation of most species through the preservation of habitat diversity (North and Keeton, 2008). At the landscape level, forest age structure (i.e. age class distribution) is targeted within the natural range of variability. Determination of the harvest rate is based on the rate of natural disturbance (Armstrong, 1999). "The closer an ecosystem is managed to allow for natural ecological processes to function, the more successful that management strategy will be" (Elmore and Kauffman, 1994).

Forest carbon cycle is also an important forest ecological process (Landsberg & Sands, 2010). A coarse filter approach should also tend to reduce the differences between carbon storage in managed and natural landscapes (Henschel and Gray, 2007). Stand carbon content is the sum of the organic carbon (C) present in the overstory biomass, organic soil floor (litter, understory bryophytes, and sphagnum peat

mosses) and inorganic or mineral layer. The fundamental elements of the stand-level C contents are the tree species composition, size of trees, canopy cover density, understory, litter, including coarse woody debris and soil substrate (Liu et al., 2011). In Canadian boreal forests, natural disturbance such as fire or insect outbreaks and logging influence the forest C pool. Disturbance is defined as "any relatively discrete event in time that disrupts ecosystem, community, or population structure and changes resources, substrate availability or the physical environment" (Kasischke & Stocks, 2000). Natural disturbances alter forest structure and disturb carbon dynamics in ecosystems (Kurz et al., 2008b). They transfer carbon from the living pool biomass to dead coarse woody debris, forest floor litter and subsurface soil pools. Disturbances modify forest soil's physical and chemical factors and microclimatic environments. They impact forest structure and reset forest succession transfer (Liu et al., 2011). For example, by altering forest structure, fire also controls soil thermal and moisture regimes, and indirectly controls metabolic processes that drive forest succession, photosynthesis and soil microbial processes (Kasischke & Stocks, 2000).

The important processes which are directly linked to sequestration of carbon are; 1) the rate of photosynthesis which is determined by site productivity, species composition, climate and age of the forest (Kurz et al., 2013); and 2) the rate of decomposition of organic matter (Kasischke and Stocks, 2000). These processes are mostly influenced by climate, physiography and soil factors (Banfield et al., 2002). The rate of C accumulation in the biomass pools depends on the temporal scale; on a short time frame, it is a function of the net ecosystem exchange (daily to weekly to yearly) and on a longer time frame, on the dynamics of forest succession (yearly to decadal time scales) (Kasischke & Stocks, 2000). Following a stand replacing disturbance, C stock in boreal forests first gets reduced and then reaches a maximum during intermediate stand ages that depends on the type and intensity of the last stand replacing disturbance and also of post-fire tree regeneration (Kurz et al., 2013). At landscape level, C stocks are therefore determined by the age class distribution that is the proportion of forest area in different age classes. The forest age-class structure is left shifted with predominately young forests in recently disturbed areas, which has a low C density, whereas it reaches a point of maximum C density with a right shifted age class structure (Kurz and Apps, 1999) in infrequently disturbed forests. In this way, C stays for a certain period of time before it escapes the forest ecosystem due to decomposition and respiration processes and natural disturbances. This residence time of carbon is related to the stability of forest ecosystems (Henschel and Gray, 2007). This residence time further conditions the resistance and resilience qualities which are related to the ability of ecosystem to recover from disturbances (Thompson et al., 2009). The quantity of carbon stocks is also an index of forest ecosystem productivity (Simard et al., 2007, Malhi 2012) and timber production (Simard et al., 2007).

1.03 Dynamics of the black spruce forest

The black spruce (*Picea mariana* (Mill.) BSP) - moss forest (closed-crown forest) is the dominant North American boreal ecosystem (De Lafontaine and Payette, 2011), and such a forest in eastern Canada is the focus of this study. These forests make a large belt at the boundary between closed-canopy and open-canopy (taiga) boreal forests. In this ecosystem, fire is a natural driver of the ecological processes (succession) that dictate forest structure and function (Lecomte et al., 2006, Cyr et al., 2007). Disturbances and succession are key ecological processes that structure landscapes as a mosaic of forest stands of different ages and compositions. Natural black spruce stands originate from fire, after killing the previously established trees, developing into even-aged and closed-crown stands (Kneeshaw and Gauthier, 2003). High severity burns release the nutrients from soil organic carbon content supporting the regeneration of black spruce. In the absence of fire after 120-200 years approximately (Rossi et al., 2009), black spruce trees reach maturity and the death and falling of trees create gaps in the canopy (Grandpré et al., 2000; Harper et al., 2006). Long fire return intervals of approximately 300-1000 years in black spruce forest of eastern Canada (Bergeron et al., 2004b; Bouchard et al., 2008) exceed the life expectancy of black spruce and favors the presence of uneven old-aged stands with unbalanced stand structure (Harper et al., 2006; Bouchard et al., 2008). Black spruce stands are able to maintain for thousands of years in the absence of fire (stable state) (Pollock and Payette, 2010). This represents up to 70% of stands of the eastern black spruce-moss forest in the Province of Quebec (Boucher et al., 2003). The age distribution of black spruce stands is therefore highly skewed towards old stands in this ecosystem and has profound influence on the storage of carbon in soils and living biomass.

Forest age distribution has to be considered for the extrapolation of stand-level carbon budgets to landscapes or regions (Kurz et al., 2008b). In these forests, successional changes are related less to tree species succession but more to structural changes (Harper et al., 2005). The replacement of even-aged closed stands to uneven-aged open canopy stands corresponds to a gradual decline in stand productivity, and is followed by a steady-state phase (Garet et al., 2009). In this way, the stand carbon yield curve is slow at first and then rapidly increases before reaching a maximum near canopy closure, and declines when stands become old and then stabilizes or reduces in the absence of fire (Wang et al., 2003, Martin et al., 2005). Thus, the age structure of the stands conditions the size of carbon stocks stored in forest biomass (Kurz et al., 2008). In fact, TSLF is the right temporal variable to explain the long term dynamics of forest age structure in this region, when the mean longevity of the dominant species can be lower than the time elapsed since the last stand-initiating disturbance (Garet et al., 2012) and also to infer successional patterns (Bouchard et al., 2008). In such case, the mean canopy age will underestimate time since last fire. In this region, the empirical relationship existing between mean canopy age and carbon stocks and the use of mean canopy age to comprehend successional patterns may not be valid. TSLF is also the primary determinant of the accumulation of stand biomass and the soil organic carbon layer

depth and its distribution (Simard et al., 2007, Pollock and Payette, 2010). For these reasons, generating wall to wall information of TSLF becomes important in this region for the quantification of biomass.

1.04 Why map TSLF?

Producing a map of TSLF allows us to understand long-term relationships between vegetation, fire and climate for analysing the impact of changes in fire regimes on forest composition. Understanding the extent of change in fire regimes due to climate variability can be used to quantify past ecosystem changes and to compute typical fire return intervals. A TSLF map could also help understand the influence of TSLF on carbon stocks at a regional scale and also aid forest managers for finding insights on ecosystem change for natural resources management planning. Biomass maps integrated with TSLF information can help landscape forest managers to devise management strategies for reducing differences in carbon storage between natural and managed landscapes.

Boreal forest productivity is not only under the control of permanent physical factors but also of transient factors related to forest succession, notably species compositional (Anyomi et al., 2014) and stand structural changes (Boucher et al., 2006). These successional traits are linked to TSLF and thus to past fire activity. Furthermore, landscape productivity is related to its forest age structure, not only because stand productivity is related to its age, but also because tree sensitivity to drought events or to the length of growing seasons is related to its age (Girardin et al., 2012). As a result, past fire activity has a role in forest management and conservation plans for enhancing sustainability and also a significant impact on the actual productivity of the forest.

1.05 Research problem and motivation

Mapping TSLF across a large area over a long temporal scale is inherently challenging in heterogeneous forest environments (Morgan et al., 2001). Existing methods employed to provide TSLF information are either temporally or spatially limited. For example, dendroecological sampling (Girardin et al., 2006) and dating may provide TSLF for longer time spans (Bergeron and Brisson, 1990) but are labour intensive and provide only a spatially-coarse representation of past fire activities (Cyr et al., 2010). The delineation of recent fire scars using aerial photographs provides spatial data of recent burns (Gauthier et al., 2002, Le Goff et al., 2007, Bélisle et al., 2011), but the delineation of fire boundaries remains ambiguous (Cyr et al. 2010). A disadvantage of all these methods is that only present standing trees are measured (recent TSLF), and the information is also spatially restricted over time (Niklasson and Granström, 2000). Analysis of charcoal in lake sediments can be used to determine TSLF over much longer periods of time (Carcaillet et al., 2007, Hély et al., 2010, Payette et al., 2012), but gathering the information is costly and remains limited in space (Niklasson and Granström, 2000).

“Time since last fire” requires making the assumption of complete stand replacement (Johnson and Wagner, 1985). This assumption is only partially valid, since burned areas are expected to be

heterogeneous, with residual unburned patches and islands that may occupy between none to 17% of a burned area (Perera et al., 2009). Fire severity is also lower at the burn periphery (Epting and Verbyla, 2005). Burn heterogeneity therefore complicates the estimation of the TSLF, but plays an important role for forest succession (Schmiegelow et al., 2006). Estimation of TSLF at a coarse spatial scale could allow circumventing these issues. There are significant relationships between fire records and vegetation composition and structure (as measured from forest inventory maps) that can be exploited to derive TSLF map (Cyr et al., 2010), but such relationships at a large regional scale have yet to be explored. The spatial variations of successional patterns are also a function of drainage (topographic features) and climatic variables (Senici et al., 2010). Therefore, at large spatial scale, existing fire history generated from dendroecological reconstruction, recent fire burns, and aerial photographs could be linked with the present species composition, age class structure (bottom-up level controls), and climatic variations (top-down controls) and then extrapolated to a larger regional landscape.

Fire alone does not account for the spatial variability of C stocks (Houghton, 2005) and there are other environmental factors (e.g., elevation, soil texture and drainage, Banfield et al., 2002). Most carbon budget models (e.g. Kurz et al., 2009, Masera et al., 2003) do not integrate forest successional dynamics with environmental factors to explain the spatial variability of carbon stocks. It is thus necessary to elaborate a model of carbon dynamics that allows estimating the domain of forest age structures and consequently of carbon stocks that can be expected under a natural disturbance regime (Cyr et al., 2009). Yet, the spatial variability of carbon stocks in relation with TSLF at regional and even local landscape levels is still poorly understood due to the limitation of spatially explicit TSLF information and needs to be better quantified (Balshi et al., 2007, 2009). There is also a lack of knowledge on the relative importance of TSLF and forest structural attributes for estimating aboveground biomass carbon (ABC) across a regional scale in the boreal forest to inform carbon budget models.

Existing methods for mapping ABC fall under two main approaches: 1) ground based and 2) remote sensing approaches. We first have focussed on ground based approaches and later on remote sensing approaches. Modelling may be empirical, process-based and hybrid. Both empirical and process-based methods have advantages and disadvantages. We chose a hybrid modelling approach which is the combination of empirical and process-based knowledge to overcome the limitations encountered with both approaches (Landsberg, 2003). Existing ground based methods utilize large scale forest inventory data to estimate biomass using allometric regression equations or biomass expansion factors or remote sensing data coupled with forest inventory data. Remote sensing techniques are based on the correlation between spectral information (intensity of electromagnetic radiation received by the sensor) and biomass estimated from field measurements and allometric equations. These methods are very useful when there is a scarcity of ground plots data. Studies have demonstrated the existence of correlation between spectral reflectance variables (e.g MODIS, Moderate Resolution Spectroradiometer, Muukkonen et al.,

2007) or radar backscatter (e.g. ASAR, Advanced Synthetic Aperture Radar, Thurner et al., 2014) with above ground biomass (AGB). However, these methods are limited in estimating biomass in regions of high biomass, especially when the canopy is closed (Turner et al., 1999). Moreover, the relationship between single date reflectance data and AGB is weak under high leaf area and complex canopy conditions (Pflumagher et al., 2014). On the other hand, LiDAR (light detection and ranging, e.g Geoscience Laser Altimeter System, GLAS) active remote sensing systems, estimate canopy height and vertical structure of the forests directly by determining distance between the sensor and target through obtaining the time between the emission pulse of laser light from the sensor and signal received back in the instrument after reflecting off from the forest canopy and ground (Lefsky et al., 2002). Factors, such as data saturation, mixed pixels, complex biophysical environments, the selection of remote sensing variables, and the modelling approaches all affect AGB accuracy (Lu, 2006). Recent studies of comparing biomass maps from GLAS and MODIS in tropical forests indicated a need to improve their accuracy (Hill et al., 2013, Mitchard et al., 2014). Comparing biomass estimates from remote sensing data with inventory based estimates may therefore allow us to find potential ancillary variables to overcome the problems of saturation signal. Here AGB was used instead of ABC, because AGB maps based on remote sensing data for the area of interest were already available (e.g. Beaudoin et al., 2014, Thurner et al., 2014).

1.06 Objectives

The three objectives of this research are:

1) To map TSLF over large areas of boreal forest at a regional scale by generalizing the empirical relationships that exist between the historical records of fire, forest inventory data, and biophysical setting of the landscape.

2) To predict the spatial variability of ABC as a function of stand and environmental variables across the landscape at a regional scale, and to determine the contribution of TSLF to the predictive model.

3) To explain the spatial variation in AGB differences derived from different remote sensing data (MODIS, GLAS and ASAR) and an AGB model based on ground-inventory data on a large area of boreal forest.

We have chosen the Quebec black spruce-moss commercial forest (area, 217,000 km^2) for its rich information on fire history maps and ground inventory plots, thus serving as a useful training area to map TSLF and further allow us to link aboveground carbon biomass in relation with TSLF. Based on these three objectives, we tailored three chapters for this research in the form of articles published in, submitted

to or in preparation for peer reviewed scientific journals. The texts follow the format required for a scientific journal (*Forest Ecology and Management*).

Chapter 1- Lengthening the historical records of fire history over large areas of boreal forest in eastern Canada using empirical relationships

Chapter 2- Cover density recovery after fire disturbance controls landscape aboveground biomass carbon in the boreal forest of eastern Canada

Chapter 3- Fire disturbance history improves the consistency of remotely sensed aboveground biomass estimates for boreal forests in eastern Canada

1.07 References

Anyomi, K. A., Raulier, F., Bergeron, Y., Mailly, D., & Girardin, M. P. (2014). Spatial and temporal heterogeneity of forest site productivity drivers: a case study within the eastern boreal forests of Canada. Landscape ecology, 29(5), 905-918.

Ali, A. A., O. Blarquez, M. P. Girardin, C. Hély, F. Tinquaut, A. El Guellab, V. Valsecchi, A. Terrier, L. Bremond, A. Genries, S. Gauthier, and Y. Bergeron. 2012. Control of the multimillennial wildfire size in boreal North America by spring climatic conditions. Proceedings of the National Academy of Sciences 109:1–5.

Armstrong, G. W. 1999. A stochastic characterisation of the natural disturbance regime of the boreal mixedwood forest with implications for sustainable forest management. Canadian Journal of Forest Research 29:424–433.

Balshi, M. S., McGuire, A. D., Duffy, P., Flannigan, M., Kicklighter, D. W., & Melillo, J. 2009. Vulnerability of carbon storage in North American boreal forests to wildfires during the 21st century. Global Change Biology, 15(6), 1491-1510.

Balshi, M. S., A. D. McGuire, Q. Zhuang, J. Melillo, D. W. Kicklighter, E. Kasischke, C. Wirth, M. Flannigan, J. Harden, and J. S. Clein. 2007. The role of historical fire disturbance in the carbon dynamics of the pan-boreal region: A process-based analysis. Journal of Geophysical Research: Biogeosciences (2005–2012) 112.

Banfield, G. E., J. S. Bhatti, H. Jiang, and M. J. Apps. 2002. Variability in regional scale estimates of carbon stocks in boreal forest ecosystems: results from West-Central Alberta. Forest Ecology and Management 169:15–27.

Beaudoin, A., Bernier, P.Y., Guindon, L., Villemaire, P., Guo, X.J., Stinson, G., Bergeron, T., Magnussen, S., Hall, R.J., 2014. Mapping attributes of Canada's forests at moderate resolution through kNN and MODIS imagery. Canadian Journal of Forest research 44, 521–532.

Bergeron, Y., and J. Brisson. 1990. Fire Regime in Red Pine Stands at the Northern Limit of the Species' Range. Ecology 71:1352–1364.

Bergeron, Y., Harvey, B., Leduc, A., Gauthier, S., 1999. Forest management guidelines based on natural disturbance dynamics : Stand- and forest-level considerations. The Forestry Chronicle. 75, 49–54.

Bergeron, Y., M. Flannigan, S. Gauthier, A. Leduc, and P. Lefort. 2004. Past, current and future fire frequency in the Canadian boreal forest: implications for sustainable forest management. Ambio: A Journal of the Human Environment 33:356–360.

Bhatti, J. S., M. J. Apps, and H. Jiang. 2002. Influence of nutrients, disturbances and site conditions on carbon stocks along a boreal forest transect in central Canada. Plant and Soil 242:1–14.

Bouchard, M., D. Pothier, and S. Gauthier. 2008. Fire return intervals and tree species succession in the North Shore region of eastern Quebec. Canadian Journal of Forest Research 38:1621–1633.

Boucher, D., S. Gauthier, Grandpré. L. De., 2006. Structural changes in coniferous stands along a chronosequence and a productivity gradient in the northeastern boreal forest of Québec. Ecoscience 13:172–180.

Boucher, D., Grandpré, L. De, Gauthier, S., 2003. Développement d'un outil de classification de la structure des peuplements et comparaison de deux territoires de la pessière à mousses du Québec. The forestry chronicle. 79, 318–328.

Bonan, G. B., H. H. Shugart. 1989. Ecological processes in boreal forests. Annual Review of Ecology and Systematics 20:1–28.

Burton, P.J., Bergeron, Y., Bogdanski, B.E.C., Juday, G.P., Carcaillet, C., Bergman, I., Delorme, S., Hornberg, G., Zackrisson, O., 2007. Long-term fire frequency not linked to prehistoric occupations in northern Swedish boreal forest. Ecology, 88(2), 465-477.

Clark, J. S. 1990. Fire and climate change curing the last 750 Yr in northwestern Minnesota. Ecological Monographs 60:135–159.

Cyr, D., S. Gauthier, Y. Bergeron, and C. Carcaillet. 2009. Forest management is driving the eastern North American boreal forest outside its natural range of variability. Frontiers in Ecology and the Environment 7:519–524.

Cyr, D., S. Gauthier, D. A. Etheridge, G. J. Kayahara, and Y. Bergeron. 2010. A simple Bayesian Belief Network for estimating the proportion of old-forest stands in the Clay Belt of Ontario using the provincial forest inventory. Canadian Journal of Forest Research 40:573–584.

De Lafontaine, G., Payette, S., 2011. Shifting zonal patterns of the southern boreal forest in eastern Canada associated with changing fire regime during the Holocene. Quaternary Science Reviews. 30, 867–87

Dixon, R. K., A. M. Solomon, S. Brown, R. A. Houghton, M. C. Trexier, and J. Wisniewski. 1994. Carbon pools and flux of global forest ecosystems. Science 263:185–190.

Eliasson, P., Svensson, M., Olsson, M., & Ågren, G. I. 2013. Forest carbon balances at the landscape scale investigated with the Q model and the CoupModel–Responses to intensified harvests. Forest ecology and management, 290, 67-78.

Elmore, W., and B. Kauffman. 1994. Riparian and watershed systems: Degradation and restoration. Society for Range Management.

Epting ,J., Verbyla, D., 2005. Landscape-level interactions of prefire vegetation, burn severity, and postfire vegetation over a 16-year period in interior Alaska. Canadian Journal of Forest Research 35:1367–1377.

Fricker, J. M., H. Y. H. Chen, and J. R. Wang. 2006. Stand age structural dynamics of North American boreal forests and implications for forest management. International Forestry Review 8:395–405.

Gauthier, S., M.-A. Vaillancourt, A. Leduc, D. De Grandpré, L. Kneeshaw, H. Morin, P. Drapeau, and Y. Bergeron. 2009. Forest Ecosystem Management Origins and Foundations. Pages 1–37 Ecosystem Management in the Boreal Forest. Presses de l' Université du Québec, Québec.

Girardin, M. P., Bergeron, Y., Tardif, J. C., Gauthier, S., Flannigan, M. D., Mudelsee, M., 2006. A 229-year dendroclimatic-inferred record of forest fire activity for the Boreal Shield of Canada. International Journal of Wildland Fire, 15(3), 375-388.

Girardin, M. P., Guo, X. J., Bernier, P. Y., Raulier, F., & Gauthier, S. 2012. Changes in growth of pristine boreal North American forests from 1950 to 2005 driven by landscape demographics and species traits. Biogeosciences, 9(7), 2523-2536.

Golden, D. M., M. A. P. Smith, and S. J. Colombo. 2011. Forest carbon management and carbon trading : A review of Canadian forest options for climate change mitigation. The forestry chronicle 87:625–635.

Grandpré, L., Morissette, J., Gauthier, S., 2000. Long-term post-fire changes in the northeastern boreal forest of Quebec. Journal of Vegetation Science. Wiley Online Library. 11, 791–800.

Hansen, M. C., Stehman, S. V., Potapov, P. V. 2010. Quantification of global gross forest cover loss. Proceedings of the National Academy of Sciences, 107(19), 8650-8655.

Harden, J. W., Trumbore, S. E., Stocks, B. J., Hirsch, A., Gower, S. T., O'neill, K. P. and Kasischke, E. S. (2000), The role of fire in the boreal carbon budget. Global Change Biology, 6: 174–184.

Harper, K.A., Bergeron, Y., Drapeau, P., Gauthier, S., DeGrandpré, L. 2005. Structural development following fire in black spruce boreal forest. Forest Ecology and Management. 206(1–3): 293–306.

Harper, K.A., Bergeron, Y., Drapeau, P., Gauthier, S., De Grandpré, L., 2006. Changes in spatial pattern of trees and snags during structural development in Picea mariana boreal forests. Journal of Vegetation Science. 17, 625–636.

Henschel, C., Gray, T. 2007. Forest carbon sequestration and avoided emissions. In *A background paper for the Canadian Boreal Initiative/Ivey Foundation Forests and Climate Change Forum, Kananaskis, Alberta. Ivey Foundation*, Toronto.

Houghton, R. A. 2003. Why are estimates of the terrestrial carbon balance so different? Global Change Biology 9:500–509.

Houghton, R. A. 2005. Aboveground forest biomass and the global carbon balance. Global Change Biology, 11(6), 945-958.

Hély, C., M. P. Girardin, A. A. Ali, C. Carcaillet, S. Brewer, and Y. Bergeron. 2010. Eastern boreal North American wildfire risk of the past 7000 years: A model-data comparison. Geophysical Research Letters 37:1–6.

Hill, T. C., Williams, M., Bloom, A. A., Mitchard, E. T., Ryan, C. M., 2013. Are inventory based and remotely sensed above-ground biomass estimates consistent? PloS one, 8(9), e74170.

Johnson, E. A., and Wagner. C. E. V., 1985. The theory and use of two fire history models. Canadian Journal of Forest Research 15:214–220.

Kasischke, E. S., Stocks, B. J. (2000). Fire, climate change and carbon cycling in the Boreal Forest. New York: Springer-verlag.

Kasischke, E. S., N. L. Christensen Jr., and B. J. Stocks. 1995. Fire, Global Warming, and the Carbon Balance of Boreal Forests. Ecological Applications 5:437–451.

Kelly, R., M. L. Chipman, P. E. Higuera, I. Stefanova, L. B. Brubaker, and F. S. Hu. 2013. Recent burning of boreal forests exceeds fire regime limits of the past 10,000 years. Proceedings of the National Academy of Sciences .

Kneeshaw, D., Gauthier, S., 2003. Old growth in the boreal forest: A dynamic perspective at the stand and landscape level. Environmental Review. 11, S99–S114.

Kurz, W. A., Apps, M. J., 1999. A 70-year retrospective analysis of carbon fluxes in the Canadian forest sector. Ecological Applications, 9(2), 526-547.

Kurz, W. A., C. C. Dymond, G. Stinson, G. J. Rampley, E. T. Neilson, A. L. Carroll, T. Ebata, and L. Safranyik. 2008a. Mountain pine beetle and forest carbon feedback to climate change. Nature 452:987–990.

Kurz, W. A., Stinson, G., Rampley, G. J., Dymond, C. C., & Neilson, E. T. 2008b. Risk of natural disturbances makes future contribution of Canada's forests to the global carbon cycle highly uncertain. Proceedings of the National Academy of Sciences, 105(5), 1551-1555

Kurz, W. A., G. Stinson, G. J. Rampley, C. C. Dymond, and E. T. Neilson. 2008c. Risk of natural disturbances makes future contribution of Canada's forests to the global carbon cycle highly uncertain. Proceedings of the National Academy of Sciences of the United States of America 105:1551–1555.

Kurz, W., C. Dymond, T. White, G. Stinson, C. Shaw, G. Rampley, C. Smyth, B. Simpson, E. Neilson, and J. Trofymow. 2009. CBM-CFS3: A model of carbon-dynamics in forestry and land-use change implementing IPCC standards. Ecological Modelling 220:480–504.

Kurz, Werner A., et al. 2013 Carbon in Canada's boreal forest—A synthesis 1. Environmental Reviews 21.4: 260-292.

Landsberg, J., 2003. Modelling forest ecosystems: State of the art, challenges, and future directions. Canadian Journal of Forest Research 33, 385–397.

Landsberg, J.J., Sands, P., 2010. Physiological Ecology of Forest Production: Principles, Processes and Models. Tree Physiology. Academic Pr, pp. 680–681.

Landres, P.B., Morgan, P., Swanson, F.J., 2007. Overview of the Use of Natural Variability Concepts in Managing Ecological. Ecological Applications. 9, 1179–1188.

Lecomte, N., Simard, M., Fenton, N., Bergeron, Y., 2006. Fire severity and long-term ecosystem biomass dynamics in coniferous boreal forests of eastern Canada. Ecosystems. Springer. 9, 1215–1230.

Lefsky, M. A., Cohen, W. B., Harding, D. J., Parker, G. G., Acker, S. A., & Gower, S. T. (2002). Lidar remote sensing of above-ground biomass in three biomes. Global Ecology and Biogeography, 11(5), 393-399.

Lesieur, D., S. Gauthier, and Y. Bergeron. 2002. Fire frequency and vegetation dynamics for the south-central boreal forest of Quebec, Canada. Canadian Journal of Forest Research 32:1996–2009.

Liu, S., Bond-Lamberty, B., Hicke, J. A., Vargas, R., Zhao, S., Chen, J., et al. (2011). Simulating the impacts of disturbances on forest carbon cycling in North America: Processes, data, models, and challenges. J. Geophys. Res., 116, G00K08.

Malhi, Y. 2012. The productivity, metabolism and carbon cycle of tropical forest vegetation. Journal of Ecology 100:65–75

Masera, O. R., J. F. Garza-Caligaris, M. Kanninen, T. Karjalainen, J. Liski, G. J. Nabuurs, A. Pussinen, B. H. J. De Jong, and G. M. J. Mohren. 2003. Modeling carbon sequestration in afforestation, agroforestry and forest management projects: the CO2FIX V.2 approach. Ecological Modelling 164:177–199.

McGuire, A. D., L. G. Anderson, T. R. Christensen, S. Dallimore, L. Guo, D. J. Hayes, M. Heimann, T. D. Lorenson, R. W. Macdonald, and N. Roulet. 2009. Sensitivity of the carbon cycle in the Arctic to climate change. Ecological Monographs 79:523–555.

Miles, L., and V. Kapos. 2008. Reducing Greenhouse Gas Emissions from Deforestation and Forest Degradation: Global Land-Use Implications. Science 320 :1454–1455.

Mitchard, E. T., Feldpausch, T. R., Brienen, R. J., Lopez-Gonzalez, G., Monteagudo, A., Baker, et al., 2014. Markedly divergent estimates of Amazon forest carbon density from ground plots and satellites. Global ecology and biogeography, 23(8), 935-946

Morgan, P., C. C. Hardy, T. W. Swetnam, M. G. Rollins, and D. G. Long. 2001. Mapping fire regimes across time and space: Understanding coarse and fine-scale fire patterns. International Journal Of Wildland Fire 10:329–342.

Muukkonen, P., Heiskanen, J. 2007. Biomass estimation over a large area based on standwise forest inventory data and ASTER and MODIS satellite data: A possibility to verify carbon inventories. Remote Sensing of Environment, 107(4), 617-624.

Natural Resources Canada, C. F. S. 2012. A Blueprint for Forest Carbon Science in Canada 2012 – 2020. Ottawa. http://cfs.nrcan.gc.ca/pubwarehouse/pdfs/34222.pdf

Natural Resources Canada, 2015. Forest carbon. http://www.nrcan.gc.ca/forests/climate-change/forest-carbon/13085

Niklasson, M., and A. Granström. 2000. Numbers and Sizes of Fires: Long-Term Spatially Explicit Fire History in a Swedish Boreal Landscape. Ecology 81:1484–1499.

North, M. P., and W. S. Keeton. 2008. Emulating Natural Disturbance Regimes : an Emerging Approach for Sustainable Forest Management. Matrix:341–372.

Payette, S., A. Delwaide, A. Schaffhauser, and G. Magnan. 2012. Calculating long-term fire frequency at the stand scale from charcoal data. Ecosphere 3:59.

Pollock, S.L., Payette, S., 2010. Stability in the patterns of long-term development and growth of the Canadian spruce-moss forest. Journal of Biogeography. 1684–1697.

Perera, A. H., Remmel, T. K., Buse, L. J., Ouellette, M. R., 2009. An assessment of residual patches in boreal fires: in relation to Ontario's policy directions for emulating natural forest disturbance. *Forest Research Report-Ontario Forest Research Institute*, (169).

Pollock, S. L., and S. Payette. 2010. Stability in the patterns of long-term development and growth of the Canadian spruce-moss forest. Journal of Biogeography 37:1684–1697.

Schimel, D. S. 1995. Terrestrial ecosystems and the carbon cycle. Global Change Biology 1:77–91.

Schmiegelow, F. K., Stepnisky, D. P., Stambaugh, C. A., & Koivula, M. (2006). Reconciling Salvage Logging of Boreal Forests with a Natural-Disturbance Management Model. Conservation Biology, 20(4), 971-983.

Senici, D., Chen, H. Y., Bergeron, Y., Cyr, D. 2010. Spatiotemporal variations of fire frequency in central boreal forest. Ecosystems, 13(8), 1227-1238.

Simard, M., N. Lecomte, Y. Bergeron, P. Y. Bernier, and D. Paré. 2007. Forest productivity decline caused by successional paludification of boreal soils. Ecological Applications 17:1619–1637.

Taylor, A. R., H. Y. H. Chen, and L. VanDamme. 2009. A Review of Forest Succession Models and Their Suitability for Forest Management Planning. Forest Science 55:23–36.

Thompson, I., Mackey, B., McNulty, S., Mosseler, A., 2009. Forest Resilience, Biodiversity, and Climate Change. A synthesis of the biodiversity/resilience/stability relationship in forest ecosystems. Diversity, S.O.T.C.O.B. (Ed.), Technical Series. Secretariat of the Convention on Biological Diversity, p. 67.

Thurner, M., Beer, C., Santoro, M., Carvalhais, N., Wutzler, T., Schepaschenko, D., Shvidenko, A., Kompter, E., Ahrens, B., Levick, S. R. Schmullius, C., 2014. Carbon stock and density of northern boreal and temperate forests. Global ecology and biogeography, 23, 297–310.

Turner, D. P., Cohen, W. B., Kennedy, R. E., Fassnacht, K. S., & Briggs, J. M. 1999. Relationships between leaf area index and Landsat TM spectral vegetation indices across three temperate zone sites. Remote sensing of environment, 70(1), 52-68.

Watson, C. (2009). Forest carbon accounting:overview and principles. Retrieved Feburary 15, 2015, from http://www.beta.undp.org/content/undp/en/home/librarypage/environment-energy/climate_change/mitigation/forest-carbon-accounting-overview---principles.html

Waring, R. H., and S. W. Running. 2007. Chapter 1 - Forest Ecosystem Analysis at Multiple Time and Space Scales. Pages 1–16 in Forest Ecosystems. (Third Edition. Running, editor. Academic Press, San Diego.

Zhang, J., Huang, S., Hogg, E. H., Lieffers, V., Qin, Y., & He, F. 2014. Estimating spatial variation in Alberta forest biomass from a combination of forest inventory and remote sensing data. Biogeosciences, 11(10), 2793-2808.

2. Chapter 1: Lengthening the historical records of fire history over large areas of boreal forest in eastern Canada using empirical relationships

Dinesh Babu Irulappa Pillai Vijayakumar, Frédéric Raulier, Pierre Y. Bernier, Sylvie Gauthier, Yves Bergeron, David Pothier

This chapter has been published and can be cited as:

Irulappa Pillai Vijayakumar, D. B., Raulier, F., Bernier, P. Y., Gauthier, S., Bergeron, Y., Pothier, D., 2015. Lengthening the historical records of fire history over large areas of boreal forest in eastern Canada using empirical relationships. Forest Ecology and Management, 347, 30-39.
http://dx.doi.org/10.1016/j.foreco.2015.03.011

2.01 Abstract

Fire plays an important role for boreal forest succession, and time since last fire (TSLF) is therefore seen as a useful covariate to devise forest management strategies, but TSLF information is currently either spatially or temporarily limited. We therefore developed a TSLF map for an extensive region in eastern Canada (217 000 km^2) by generalizing the empirical relationships that exist between regional historical records of fire (1880-2000) with forest inventory data and biophysical variables. Two random forest models were used to predict TSLF at the scale of 2-km^2 cells. These cells were first classified into TSLF ≤ 120 years and > 120 years and TSLF was then estimated by decade for cells classified as younger than 120 years. Overall, both models showed a substantial agreement at the scale of both the study area and landscape units, but the accuracy remained fairly low at the scale of individual cells. Results show that the decades between 1920 and 1940 were characterized by widespread fire activity covering approximately 28% of the study region. Studies have reported a doubling of the burn rate from 1970 to 2000, but our longer-term analysis suggests that the 1970 to 2000 burn rate (4.3% $decade^{-1}$) is lower than the one detected between 1920 and 1940 (16.4% $decade^{-1}$) and provides a relevant context for interpreting the recent increases in area burned observed since 1970. These results highlight the importance of lengthening the historical records of fire history maps in order to provide a better perspective of the actual changes of fire regime.

Key words: boreal forest; fire history; time since last fire; succession; decadal burn rate; Random forests.

2.02 Introduction

Boreal forests play a significant role in the global carbon budget (32% of global forest carbon stocks, Pan et al., 2011). In Canada, disturbances such as fire, insect outbreaks and logging influence the overall stability of the boreal forest carbon sink, but stand-replacing fires remain a key driver of carbon dynamics of the boreal forest (Wooster and Zhang, 2004; Stinson et al., 2011). It directly influences the age structure and vegetation mosaic of the landscape (Weber and Stocks, 1998) while its stochasticity in space and time (Morgan et al., 2001; McKinley et al. 2011) creates heterogeneous and complex landscapes (He and Mladenoff, 1999). Time since last fire (TSLF) is thus a primary determinant of the accumulation of stand biomass and soil organic carbon (Simard et al., 2007; Raymond and McKenzie, 2012), and is related to the abundance and diversity of animal and plant communities (Azeria et al., 2009; Bergeron and Fenton, 2012). Furthermore, TSLF can be used to characterize forest age structure when the mean lifetime of the dominant tree species is shorter than the fire return interval (Garet et al., 2012). Forest age structure is used as an indicator of economic, social and ecological sustainability (Didion et al., 2007; Cyr et al., 2009; Bouchard and Garet, 2014) and forest management strategies fundamentally manipulate the age structure to optimize trade-offs between timber supply, habitat and recreation values (Bettinger et al., 2009). Past fire activity has therefore a significant impact on how forest management and conservation plans are dimensioned to enhance sustainability.

However, forest managers usually have access to detailed archives of fires only for the last few decades, a constraint that limits their capacity to set management targets based on natural variability in forest ecosystem processes. Longer historical records help better define the range of natural variability of fire regime and thus of forest age structures (Cyr et al., 2009; Bergeron et al., 2010). Knowledge of TSLF over a large spatial extent is therefore seen as useful for the planning of timber production and the conservation of biodiversity, as both types of activities require a good understanding of natural disturbances (Nalle et al., 2004; Bergeron et al., 2004a; Hauer et al., 2010; Savage et al., 2013; Börger and Nudds, 2014).

TSLF information can be acquired through direct measurements of burned areas from aerial photographs or satellite images, or through indirect methods in which fire history is reconstructed from dendroecological information (Frelich and Reich, 1995; Heyerdahl et al., 2001). All such methods are spatially or temporally limited. For instance, archived databases of area burned (Kasischke et al., 2002; Stocks et al., 2003) provide direct information over large areas but only for the past few decades. In contrast, tree or charcoal sampling and dating provide TSLF over century-level time scales but only cover limited spatial extents (Cyr et al., 2010).

Vegetation composition, cover density and stand structure of a specific forest area are known to be related to its TSLF. Across the North American boreal forest, the mean time since the last fire (MTSLF) exceeds 500 years (Bouchard et al., 2008) in the east and shortens to 100-150 years further west

(Johnstone et al., 2010). This pattern creates an east-west gradient in within-stand age structure from uneven-aged to even-aged (Cumming et al., 2000; Bergeron et al., 2004a). In boreal forests, a shorter MTSLF promotes the dominance of fire-adapted jack pine *(Pinus banksiana* Lamb) or trembling aspen (*Populus tremuloides* Michaux) (Weir et al., 2000; De Groot et al., 2003), while a longer MTSLF promotes the dominance by black spruce (*Picea mariana* (Mill.) B.S.P.) and, in extremely long MTSLF, fire-averse balsam fir (*Abies balsamea* (L.) Mill.) (Bouchard et al., 2008). Forest composition and structure are available from regular forest properties mapping over large areas and could be used as an indirect method to enhance the current spatial coverage of TSLF information.

The objective of this study was therefore to estimate TSLF for a 217,000 km^2 region of black spruce dominated boreal forest in eastern Canada through the integration of multiple sources of direct and indirect information. The specific objectives of this study were 1) to develop a TSLF map at a regional scale through the generalization of the empirical relationship existing between historical fire records with forest inventory and climate data, 2) to determine the accuracy and the temporal variation of the decadal burn rate from derived TSLF map, and 3) to identify how the burn rate estimated for the 20^{th} century at the landscape scale with the TSLF map is related to present vegetation composition. To this effect, we first trained random forest models over specific areas of our study area with known TSLFs. Vegetation, geomorphological characteristics, and climate data were used as input data. We used bootstrap replications to build confidence intervals for the TSLF estimates, which were then extrapolated to the entire study area. Finally, MTSLF values were computed with survival analyses at the scale of landscape units (~ 100 – 3000 km^2) from the resulting TSLF map to visualize how they were related to the existing vegetation composition.

2.03 Methods

2.03.01 Study Area

The study area is located in the eastern boreal forest of Canada (Fig. 2.1) and extends approximately from 49°N to 52°N and 66°W to 79°30'W corresponding to the portion of the black spruce – feather moss bioclimatic domain actually allocated to forest management and commercial harvest in the province of Québec (Robitaille and Saucier, 1996). The total extent of the study area is 217 000 km^2. This area is particularly rich in fire history maps (Fig. 2.1) and thus serving as a useful training area for testing the applicability of our methodology. The mean annual temperature for the study area varies from 0°C to -2.5°C (Bergeron et al., 2004). Mean annual precipitation increases from 800 in the west to 1200 mm year-1 in the east (Grondin et al., 2007).

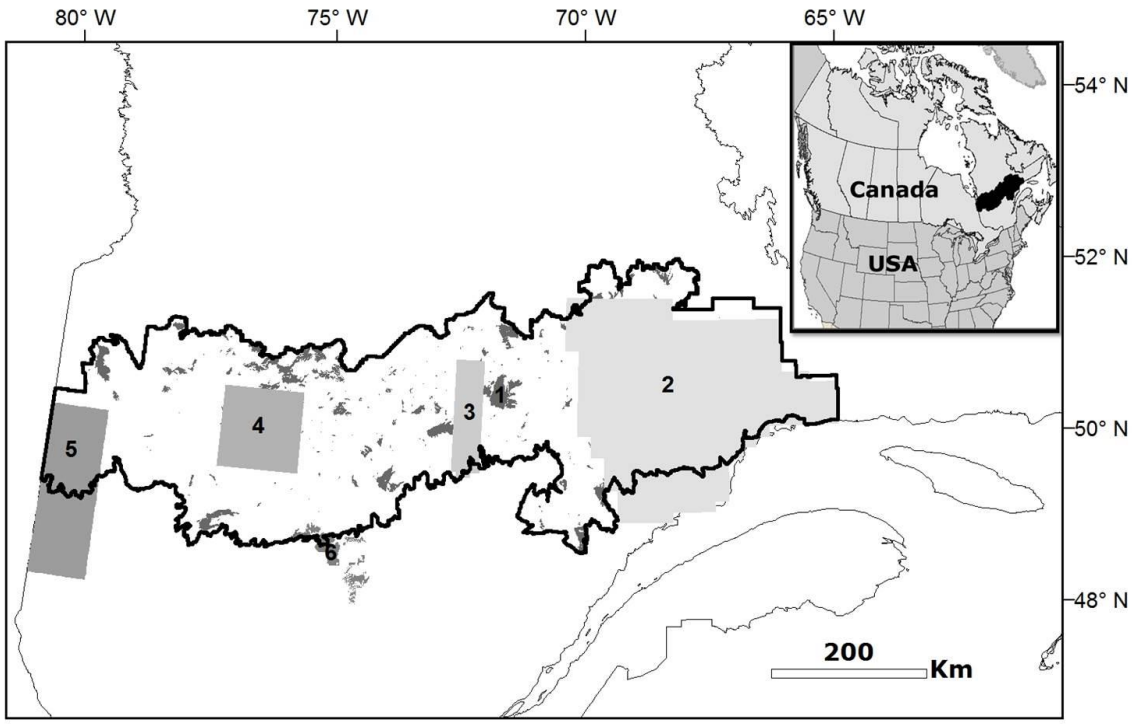

Figure 2.1. Location of study area (outlined in dark black) and fire history maps (numbered grayed areas, refer to Table 2.2). Inventory plots used for the training of the TSLF models are not shown.

Largely underlain by the Precambrian rocks of the Canadian Shield, the study area varies from organic deposits and a flat topography of the Clay Belt in the west, near James Bay (Cyr et al., 2010), to moderately hilly landscapes overlain by glacial-fluvial deposits and tills in the rest of the area. The central region has moderate elevation (339 to 535 m) with surficial deposits dominated by mesic glacial tills (Bélisle et al., 2011). The eastern section is characterized by till and rock deposits on a hilly to high hilled landscape (Bouchard et al., 2008).

The dominant forest types found in the study area vary along the precipitation gradient. Although black spruce stays dominant throughout the area, it shares its dominance with jack pine in the west, and with fire-averse balsam fir in the wetter east. Fire is the dominant disturbance across the study area, but its impact decreases in the wetter east. Spruce budworm (*Choristoneura fumiferana* Clemens) is a major periodic disturbance in the eastern half of the study area, especially in balsam fir dominated stands (Bouchard and Pothier, 2011).

2.03.02 Characterization of study units

For modeling purposes we partitioned the landscape into a square grid of 2 km^2 cells (cells of about 1414 m x 1414 m, and total of 108,477 cells). For ease of comparison with other studies and to increase our chances of past fire detection (Héon et al., 2014), we focused on the large fires (> 200 ha) that accounted

for 97% of the area burned between 1960 and 2000 in Canada (Stocks et al., 2003). Our grid corresponds to the minimum fire size of the Canadian Large Fire Database (200 ha), which provides the burned area in Canada from 1959 to 1999.

These 2-km^2 cells were characterized across the study area with a geospatial database based on forest maps produced by the Quebec Ministry of Natural Resources for its third inventory program (1992-2002), and climatic variables derived from the NCEP-NCAR Twentieth Century Reanalysis (20CR) project (Compo et al., 2011). The "Spatial information on Forest Composition based on Tessera" geospatial database – (SIFORT, Pelletier et al., 2007) is based on forest maps derived from the photointerpretation of false color infrared photos on a 1/15000 scale, for the years 1990 to 1999. The map is divided into square tiles of 15 seconds in longitude by 15 seconds in latitude, each covering a mean area of approximately 14 ha. This database provides information for each grid centroid on stand composition, age, height, cover density, surficial deposit and drainage. Surficial deposits and drainage classes were combined into seven groups defined by their rock fraction and texture and linked to the drying potential of the surficial deposits (Mansuy et al., 2010).

Meteorological stations are very sparse throughout the study region. We therefore used 1971-2000 daily minimum and maximum temperatures and precipitation obtained from the 20CR project. This climate dataset has a 2^{o} x 2^{o}spatial resolution and was specifically chosen because of its demonstrated link to tree growth in the eastern Canadian boreal forest (Girardin et al., 2012). Climatic variables (Table 2.1) were selected because of their demonstrated links to the fire regime (Le Goff et al., 2009; Mansuy et al., 2012) and downscaled with the BioSIM model (Régnière and St-Amant, 2008; Régnière, 2009). Altitude values, required to perform spatial interpolation with BioSIM, were obtained from the Shuttle Radar Topographic Mission Digital Elevation Model with 90 m resolution (van Zyl, 2001).

We aggregated the SIFORT geodatabase to our grid, with an average of 14 SIFORT tile centroids per 2-km^2 cell. Within each cell, the relative frequencies of species groups, age, height, cover density classes and surficial deposit groups were estimated with the SIFORT geodatabase and used as explanatory variables to estimate TSLF (Table 2.1). We removed cells for which more than 50% of the SIFORT tessera centroids were classified as water (7694 cells, 7.1% of total), wetlands and peatlands (8423 cells, 7.8% of total), heaths (4700, 4.3% of total), harvested land (9339 cells, 8.6% of total), insects-killed stands or wind throws (118 cells), and human infrastructure (38 cells), leaving 78,136 cells for analysis (henceforth referred to as the study dataset, corresponding to 72% of the total cell dataset and 89% of the forest area).

Table 2-1. List of explanatory variables considered for the training of the random forest models

Variables	Description
Relative frequencies of vegetation attributes ([a])	
Species composition groups	≥75% stand cover = pure, < 75% = mixed. Classified into black spruce (Pma), balsam fir (Aba), jack pine (Pba), intolerant hardwoods (Iha – aspen or birch), mixed (Mix), other conifers (Oco - conifers other than black spruce, balsam fir and jack pine) and no species composition but identified as a burned area (Brn), following Gauthier et al., (2010).
Stand age classes	0 - 20 years (age 0-20), 21 - 40 (age 21-40), 41 - 60 (age 41-60), 61 - 80 (age 61-80), 81 - 100 (age 81-100), ≥ 101 (age ≥ 101), young uneven-aged (Yua) and old uneven-aged (Oua).
Stand height classes	> 22 m (height > 22), 17 - 22 m (height 17-22), 12 - 17 m (height 12-17), 7 - 12m (height 7-12), 4 - 7 m (height 4-7), 2 - 4 m (height 2-4) and 0 - 2 m (height 0-2).
Stand cover density classes	The percentage of stands with density greater than 81% (cover > 81%), 61% - 80 % (cover 61-80%), 41% - 60% (cover 41-60%) and 25% - 40 % (cover 25-40%).
Physical variables	
Relative frequencies of surficial deposit groups ([a])	Based on a combination of soil stoniness and texture, linked to the drying potential of the surficial deposits (Mansuy et al., 2010): VAVC (very abundant, very coarse), MM (moderate, moderate), MAM (moderately abundant, moderate), MAC (moderately abundant, coarse), AC (abundant, coarse), ROC (rock) and ORG (organic) (Mansuy et al., 2010).
Elevation	The elevation for the centroid of 2 km^2 cells from SRTM DEM (90 m resolution) (van Zyl, 2001).
Slope	The slope for the centroid of 2 km^2 cells derived from elevation in ArcGIS 10.0 from the SRTM DEM.

Climate	Derived from the 20CR project (Compo et al., 2011) and BioSIM.
Temperature	The annual mean temperature (°C) for the period of 1971-2000.
Total precipitation	The mean of annual total precipitation (mm $year^{-1}$) for the period of 1971-2000.
Degree-days	The annual degree-days (above 5°C) for the period of 1971-2000 (°C $year^{-1}$).
Growing season	The mean length of growing season (days for which the mean temperature is above 5°C) for the period of 1971-2000 (days $year^{-1}$).
Potential evapotranspiration	The mean annual total Thornwaite's potential evapotranspiration (PET) (mm) for the period of 1971-2000 (Dunne and Leopold, 1978).
Aridity index	The mean annual aridity index for the period of 1971-2000 (mm), corresponding to the annual sum of the differences between monthly Thornthwaite's potential evapotranspiration and monthly precipitation.
Drought code	Fire weather index corresponding to moisture content of the deep layer of compacted organic matter, 10–20 cm deep (Amiro et al., 2005).

[a] Derived from the SIFOR geospatial database

2.03.03 Modelling TSLF

In our study region, the 200-year mean longevity of black spruce, the dominant tree species, is shorter than the reported > 500-year mean fire return interval (Bouchard et al., 2008). In the absence of fire, black spruce trees die asynchronously, thereby generating complex uneven-aged structures of near-constant mean canopy age while TSLF increases. In such cases, mean canopy age underestimates TSLF (Garet et al., 2012). We therefore based our prediction of TSLF (large spatial scale) on the relative proportions of tree species, of tree age classes, of cover densities and of heights, and on values of specific climatic variables.

We trained our TSLF model using detailed information on TSLF available for parts of the study area either from fire history maps (Fig. 2.1, Table 2.2) or from forest inventory plots. First, we discarded 9552 cells that were covered 50% or more by fires in the 1970-2000 fire maps produced operationally by the SOPFEU (the Quebec forest fire control agency, Société de protection des forêts contre le feu) (Table 2.2, Boulanger et al., 2013), since there was no need to model TSLF for that well-documented period. We

did not consider fires that burned after 2000 because the SIFORT database provides updated data on forest vegetation up to 2000. Cells covered 50% or more by a known fire polygon were attributed the TSLF value of that fire, yielding an initial training dataset of 23 289 cells, or 29.8% of the studied dataset (Table 2.2).

Inventory plots of the Quebec Ministry of Natural Resources' third inventory program (n =6,415 plots) were also used to generate additional training information for our TSLF model. According to the two plot-level rules set by Bélisle et al. (2011), tree age and TSLF are equivalent 1- if the plot is dominated by post-fire species (white birch, trembling aspen, jack pine, black spruce), and 2- if the plot is even-aged, that is with no more than 20 years of age difference among the cored dominant trees. The TSLF of cells with more than one admissible plot was set as the mean age of cored trees within the oldest plot. This procedure enabled us to assign TSLF to 2218 additional cells (2.8%), for a total of 25,507 cells with a known TSLF (32.6% of the studied dataset).

Modeling TSLF involved the successive application of two separate models in which climatic variables and forest attributes were used as explanatory variables (Table 2.1). Since our TSLF modeling relies on forest succession, climatic variables were expected to influence its dynamics. Also, two models were needed because of the censored nature of TSLF data (e.g. Johnson and Gutsell, 1994), since although all forests have burned at some point in the past, there is a cut-off value beyond which TSLF cannot be evaluated. The first model was thus used to determine that TSLF cut-off value beyond which TSLF estimates acquired a greater uncertainty. Model uncertainty was rated using the improvement of the overall classification accuracy of burned / unburned cells (TSLF ≤ or > a cut-off value) as the cut-off TSLF value was gradually reduced from a maximum of 200 years. This initial analysis yielded a cut-off TSLF value of 120 years, a value more related to the oldest age class provided by the SIFORT database (Table 2.1) than to the maximal temporal depth common to all available fire history maps (Table 2.2). Cells of the training dataset with a TSLF value greater than 120 years were thus all categorized as "unburned" (TSLF > 120 years) for further model training. A second model was then used to estimate TSLF for cells for which the first model predicted a TSLF value below 120 years.

Table 2-2. Sources used to generate the response variable for the training dataset for the random forest TSLF models

No	Fire data source	Period	Area used in the study (km^2)	Location of region
1	Quebec's Société de Protection contre les Feux (SOPFEU)	1970-2000	19104	Province of Quebec, Canada
2	Bouchard et al. (2008)	1800-2000	41472	The eastern portion of study area (70-66.5°W to 49-51.5°N)
3	Bélisle et al. (2011)	1734-2009	228	The central part of study area (71°15'W-72°45'W and 49°36'N-50°59'N)
4	Le Goff et al. (2007)	1720-2000	232	The central portion of study area (75°W-76°30'W and 49°30'N-50°30'N)
5	Bergeron et al. (2004b)	1675-2000	4192	The western part of study area (78°30'W-79°30'W and 48°N-50°N)
6	Lesieur et al. (2002)	1923-2000	454	The south-central portion of study area (74°52'55"W-73°45'15"W and 47°57'13"N-49°08'22"N)

Both models were developed using Random Forests (RF), with the *randomForest* package (Liaw and Wiener, 2002) in R (Venables and Smith, 2013). This non-parametric method makes no assumptions about the distribution of the data and can model non-linear relationships. It has the ability to handle high dimensional input variables and rank variable importance. For both models, 1000 bootstrap samples were used to draw 63% (Cutler et al., 2007) of the training dataset to build classification or regression trees

whose predictions were then combined. The remaining data (out-of-bag data) was used for cross-validation for each bootstrap iteration. The values of training parameters used in model development were: *ntree*, the number of trees to grow (1000), *mtry*, the number of the predictor variables sampled for each node (default parameters, classification: square root of the number of variables and regression: the number of variables/3), and *node size* (default parameters, classification: 1 and regression: 5). In the case of the first RF model used to form two groups based on a cut-off TSLF value, the final classification corresponded to the class most often selected by the classification trees. Accuracy was assessed with Cohen's kappa measure of agreement and the percent of correctly classified classes (PCC) through the construction of confusion matrices between the actual and predicted classes. The kappa measure corresponds to the classification accuracy adjusted for agreements that may occur due to chance alone (Cohen, 1960). A non-parametric method such as random forest is not affected by spatial autocorrelation as it does not require residuals to be independent and identically distributed, but the presence of residual autocorrelation could indicate among other things the omission of one or more important explanatory variables (e.g. Dormann et al. 2007). Furthermore, forest fire is a contagious process with potential inherent spatial autocorrelation. As a consequence we tested for the presence of residual autocorrelation with a global Moran's I index as a function of neighboring distance (Moran, 1950). To this effect, the Moran I index was computed with the cells having a value of 0 (incorrectly) or 1 (correctly classified).

For the second RF model used to estimate TSLF for cells where TSLF$\leq$ 120 years, taking the average of the bootstrap values (Cutler et al., 2007) led to biased predictions for values close to the bounds set at 30 and 120 years (i.e. corresponding to years of stand origin of 1970 and 1880). Different strategies were employed to avoid such biases, including a bias reduction technique proposed by Zhang and Lu (2012) (their model 3) or by taking the median instead of the mean as prediction. However, we found that biases were greatly reduced when bootstrap-predicted values were categorized into decades for each cell and the most frequent decade was selected as the predicted value. As a consequence of categorizing TSLF-predicted values by decades, accuracy of the second RF model was also assessed with the Cohen's kappa and the percent of correctly classified classes, instead of the coefficient of determination and root mean square error. We also tested for the presence of residual autocorrelation using the same methodology as described before (i.e. with cells being correctly or incorrectly classified). We also tested the association of the residuals (cells having a value of 0, incorrectly classified or 1, correctly classified) of both RF models with the data sources for the TSLF maps (Table 2.2) using chi-square test. Further, Cramer's V value was calculated to measure association between the two discrete variables (residuals: 0 and 1 and data sources of the TSLF maps). Cramer's V value range from 0 to 1 and the value of 0 corresponds to no association between the variables and 1 indicates perfect complete association.

The measure of the importance of a predictor variable (mean decrease in Gini coefficient when classification is used with RF and mean decrease in mean square error when regression is used instead)

is the normalized decrease in classification accuracy or mean squared error for the out-of-bag data by including the predictor variable either as originally observed or as randomly permutated in the out-of-bag data. For both models, only the six most important variables ranked by RF were used in the model building process to develop robust models (Thompson and Spies, 2009). Colinearity among selected explanatory variables was checked through correlation analyses. More details on the RF algorithm can be found elsewhere (e.g. Cutler et al., 2007; Timm and McGarigal, 2012).

2.03.04 TSLF extrapolation to the entire study area

Both models were used to impute a TSLF value (either TSLF > 120 years or a decade of stand origin between 1880 and 1970) to each 2-km^2 cell of the studied dataset, except those used in the training dataset and those covered by the fires of the SOPFEU 1970-2000 fire history map (imputed dataset, 43,077 cells). The difference between the 95th and 5th percentiles of TSLF (individual years, TSLF ≤ 120 years) generated through bootstrapping were used to provide a 90% confidence interval for each 2-km^2 cell. Half the width of these confidence intervals served to estimate margins of error of predicted values and their frequency distributions were computed by classes of predicted decade.

The three datasets (SOPFEU, training and imputed datasets) were combined to produce a TSLF map expressed in decadal classes for the entire study area. The burn rate per decade between 1880 and 2000 was then estimated for the study area from the areas belonging to each decadal TSLF and a survival analysis (Reed et al., 1998), considering that each decade might have a different burn rate (Fauria and Johnson, 2008). A survival analysis estimates the probability of an area having gone without fire for a given period of time (Johnson and Gutsell, 1994) and was required to correct for the effect of overlap in successive fires on burn rate estimates. Reed et al. (1998) have provided a recursive method to correct these past burned areas, accounting for the fact that the burn rate may change through time. The decadal burn rate was thus estimated in a recursive fashion, starting from 1980-1990 and correcting the area that had then burned by the inverse of its survival probability until the date of the 2000 TSLF map

2.03.05 Relating forest composition with past disturbances at the landscape scale

The use of a nonparametric method such as random forests makes it much more difficult to interpret the results. The results were therefore synthesized to better understand how the 20th century landscape-scale burn rate estimated with the TSLF map is related to present forest composition. To this effect, TSLF was statistically upscaled to the 625 ecological districts within our study area (size between 65 km^2 and 2975 km^2) by computing the mean time since last fire (MTSLF). Ecological districts (Robitaille and Saucier, 1996) correspond to landscape units of similar topography, surficial deposits and drainage, and have been used for characterizing vegetation (Anyomi et al., 2013; Grondin et al., 2014). MTSLF for each ecological district was computed by fitting a Weibull distribution of TSLF with PROC LIFEREG (SASv9.2, SAS Institute Inc., Cary, NC, USA). Survival analysis allows computing MTSLF by considering censored

data (TSLF > 120 years), for which an accurate estimation of TSLF was not available. Three ecological districts that completely burned between 1970 and 2000 were not considered in this analysis as a recent burn with no photointerpreted vegetation covered them.

Ecological districts were regrouped into homogeneous forest landscapes on the basis of the relative abundance of SIFORT grid cells by species composition (Table 2.1) using PROC FASTCLUS (SASv9.2, SAS Institute Inc., Cary, NC, USA). The optimum number of clusters (4) was detected with the first local maximum value of the cubic clustering criterion (CCC) by plotting its value as a function of an increasing number of clusters (Sarle, 1983). CCC is an optimization criterion that compares R^2, the proportion of the variance explained by the given number of clusters to the expected value of R^2 determined by clustering data from uniform distribution (Sarle, 1983). For each of these vegetation clusters, we computed the cell frequency with a TSLF value above or below 120 years and the variability of MTSLF values between districts of an individual cluster.

2.04 Results

2.04.01 Accuracy of TSLF models

For our first random forest model that classified 2-km^2 cells into two groups of TSLF (≤ or > 120 years), the six top-ranked predictor variables were the proportions of the four oldest stand age classes (61-80, 81-100, ≥ 101 years, old uneven-aged, Table 2.1), the relative abundance of balsam fir, and the total precipitation (Fig. 2.2a). The Cohen's kappa (0.72) indicated a substantial agreement in the classification (Landis and Koch, 1977). The model was better able to predict unburned cells (TSLF > 120 years) (classification error of 8.3%) compared to burned cells (TSLF ≤ 120 years) (error of 19.5%). Spatial autocorrelation of incorrectly classified cells was significant, which indicates clustering, and global Moran I index remained above 0.10 for distances inferior to 20 km. Clusters of incorrectly classified cells were therefore located at the boundaries or within individual fires (Supplementary material, Fig. A.1). A visual examination of the spatial distribution of these clusters did not indicate any latent spatial pattern that would have pointed to important processes not included in the RF model. The association between the residuals and data sources for the TSLF maps were significant (Chi-square value = 4934.5, $P < 0.01$). The degree of association specified by Cramér's V value was 0.43 ($P<0.001$). The percentage of errors (incorrectly classified) was significantly higher in the cells calibrated from the data of Bouchard et al. (2008) than the other data sources for the TSLF maps (Table 2.2). The results of the classification suggest that 22,196 cells (52% of the imputed dataset) burned between 1880 and 1970 (TSLF ≤ 120 years).

For our second random forest model that estimated TSLF for cells predicted as having a TSLF ≤ 120 years with the first model, the six top-ranked predictor variables (Fig. 2.2b) were the proportions of intermediate age classes 41-60, 61-80, 81-100, the total precipitation, the potential evapotranspiration,

and the percentage of stands originating from a burn. Total precipitation and potential evapotranspiration were only weakly correlated between themselves (r = -0.19, $P < 0.01$) and both variables were kept. TSLF values predicted by this second RF model and categorized by decade of stand origin, were unbiased (Fig. 2.2c) and correctly classified 85.5% of the time. This represents an "almost perfect" agreement with observed data (Cohen's kappa of 0.82, Landis and Koch, 1977). The cell-level margin of error was typically around 20 years, which is fairly high provided the time span covered (1880-2000) and no temporal trend was detected (Fig. 2.2d). The global Moran I index of incorrectly classified decades showed an approximately identical pattern with distance and values as seen in the previous model. Again, clusters of incorrectly classified decades did not show any spatial pattern over the whole study area that would have pointed to important variables missing in the RF model (Supplementary material, Fig. A.2). The residuals were significantly related to the data sources for the TSLF maps (Chi-square value = 123.6, $P < 0.01$). However, the strength of association was weak (Cramér's V value =0.15, $P<0.001$).

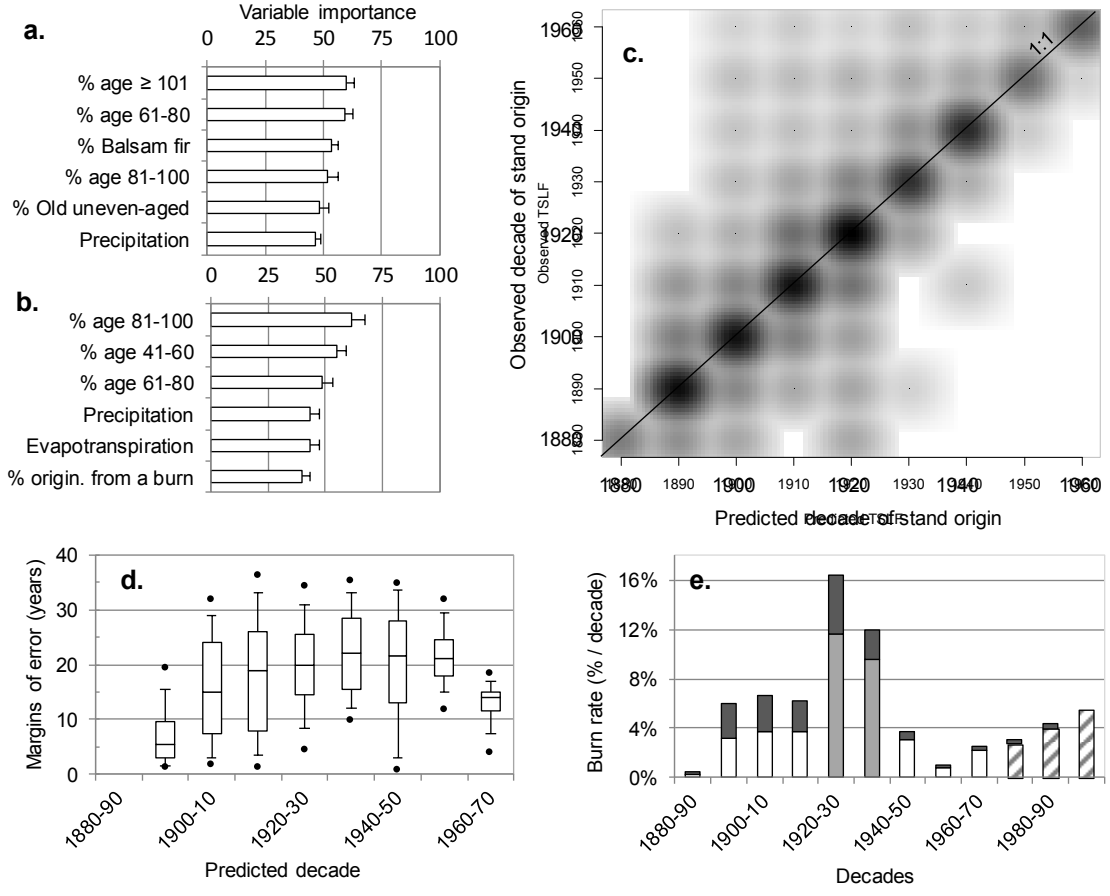

Figure 2.2. For the top six variables (Table 2.1), ranked by the random forest models for the classification of 2-km² cells into TSLF ≤ 120 years and TSLF > 120 years, (a) normalized mean decrease in Gini coefficient, and (b) normalized mean decrease in mean square error in predicted cell-level TSLF for cells in which TSLF is predicted to be less than 120 years; c) density plot of observed vs predicted year of stand origin for cells for which TSLF is predicted ≤ 120 years; d) box-and-whisker plots of margins of error for predicted TSLF values grouped by decade class; e) Decadal burn rates between 1880 and 2000 for the study region (dark grey: burn rate correction due to survival analyses, light grey: highest values of burn rate, hatching: burn rates between 1970 and 2000).

2.04.02 Temporal changes in the decadal burn rate during the 20th century

The decadal burn rate between 1880 and 2000 at the scale of the whole study area ranged from 0.5 to 16.4 % decade^{-1} (Fig. 2.2e). More importantly, decades between 1920 and 1940 seemed characterized by a widespread fire activity corresponding to 28% of the study area. This period is surrounded by two periods of moderate to low fire activity (1880-1920 and 1940-1960). Most of the fire activity between 1880 and 2000 is concentrated in a region situated between the organic plains of Abitibi, where very few fire events have occurred, and Lake Chibougamau (Fig. 2.3). Further east, the fire activity was moderate between Lake Mistassini and the White Mountains, and low on the North Shore.

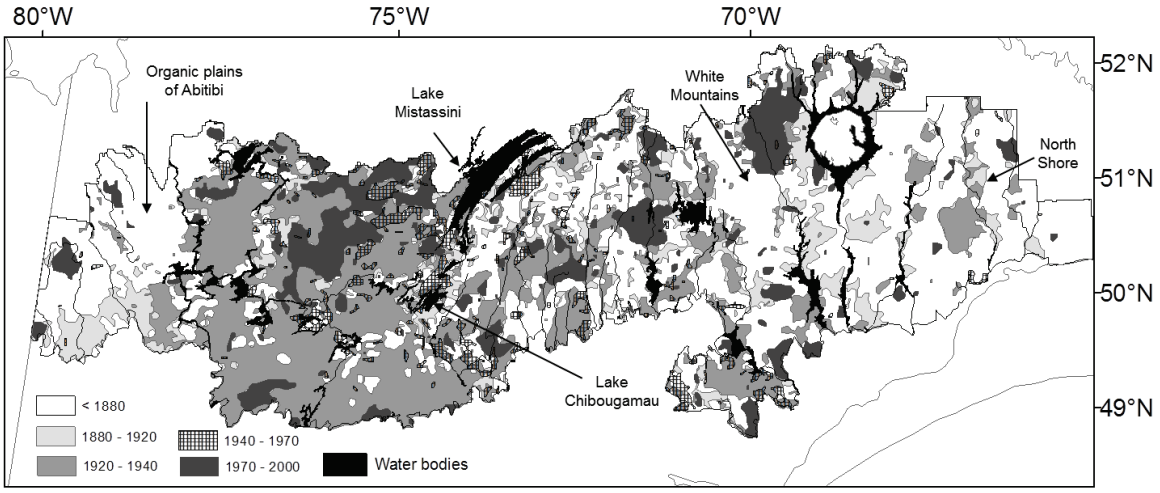

Figure 2.3. Map of predicted time since last fire by decade class (between1880 and 2000). The map was generalized by aggregating 2-km^2 cells of identical period of fire activity (1880-1920, 1920-1940, 1940-1970 and 1970-2000) and by removing any object smaller than 4 km^2.

2.04.03 Forest composition in relation to fire regime as derived from the TSLF map

At the scale of landscapes (ecological districts), cluster analysis indicated that dividing the study area into four regions or zonations based on regional vegetation composition was the optimal number to explain the heterogeneity in tree species composition. Except in one cluster, black spruce (co-)dominates in all clusters (Table 2.3). The cluster dominated by balsam fir has a median MTSLF of 217 years (Fig. 2.4b) and the highest proportion of 2-km^2 cells with a TSLF > 120 years (Fig. 2.4c) compared to the cluster dominated by black spruce and jack pine. The cluster dominated by black spruce has a closely equal proportion of cells with a TSLF ≤ 120 or > 120 years (Fig. 2.4c).

Table 2-3. Average proportions of tree species by vegetation cluster after a clustering analysis to explain the homogeneity of landscape units by vegetation composition. Species names are provided in Table 2.1. Bold numbers indicate the dominant species

		Mean of species cluster						
Cluster name	Abundance	Aba	Pma	Iha	Pba	Mix	Oco	Brn
Pma-Pba	18%	0.03	**0.42**	0.09	**0.35**	0.05	0.00	0.06
Aba-Pma	24%	**0.50**	**0.37**	0.05	0.02	0.04	0.00	0.03
Pma	47%	0.11	**0.69**	0.05	0.06	0.04	0.00	0.05
Brn-Pma	11%	0.05	**0.28**	0.03	0.11	0.02	0.00	**0.51**

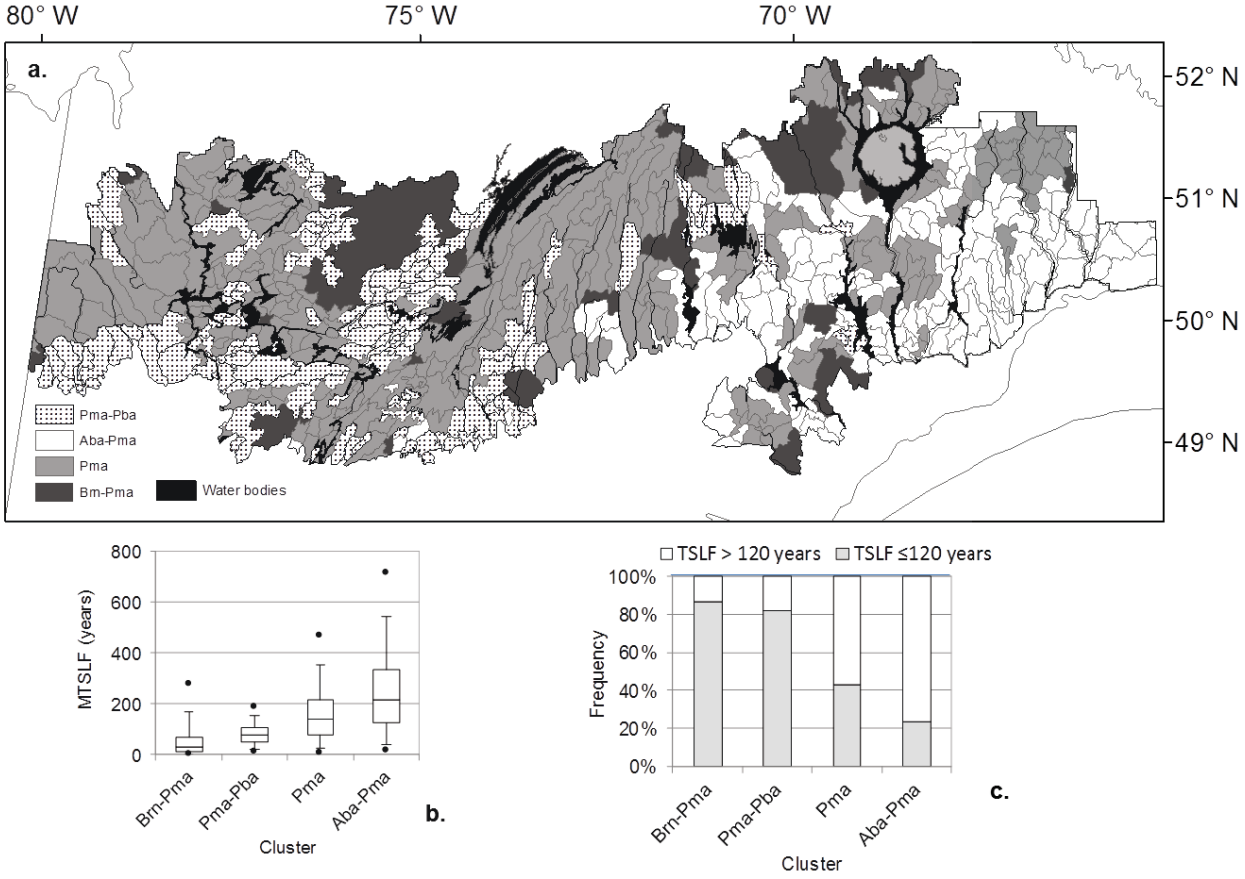

Figure 2.4. a) Vegetation map of landscape units (ecological districts) derived from a cluster analysis based on species abundance. Average proportions of species and names for each cluster are presented in Table 2.3; b) box-and-whisker plots of mean time since last fire by ecological district across the vegetation clusters; c) frequency of 2-km² cells with a TSLF value above or below 120 years by vegetation cluster.

2.05 Discussion

2.05.01 Estimation of TSLF over a large spatial extent with Random Forest models

In this study, we modeled TSLF over an area covering 217 000 km². Cyr et al. (2010) used a similar approach (Bayesian Belief network) to estimate the proportion of old-growth forest (stands older than 150 years) over 6500 km² in central Canada (Ontario), with a similar accuracy but at the scale of forest stands (areas of approximately 20 ha). Empirical methods such as random forests or Bayesian belief networks are useful to characterize the errors incurred by the extrapolation of TSLF from local observations (sample area or sample plots) that is otherwise done manually (Figs. 2.2c and 2.2d). Notably, ambiguities remain apparent when trying to spatially distinguish individual fires that have occurred between 1920 and 1940 (map provided as supplementary material, Fig. A.3).

2.05.02 Interpretation of TSLF predictors

The proportions of stand age classes per cell (Table 2.2) were strong predictors of TSLF for TSLF ≤ 120 years (Figs. 2.2a and 2.2b). Probability of predicting a TSLF > 120 years increased with an increase in the proportion of older stands, in the abundance of balsam fir and in precipitation. Such a result is in accordance with the mean longevity of black spruce in the eastern part of the study area (c. 200 years, Garet et al., 2009) and the time required for balsam fir to gradually reach the canopy (c. 200 years, Bouchard et al, 2008, their Fig. 4). Other variables that we expected to be related to the fire regime and thus to TSLF were not selected by the RF models as strong predictors. For instance, we expected the relative abundance of open spruce woodlands, a forest type that apparently results from deficient post-fire forest recovery (Lavoie and Sirois, 1998; Girard et al., 2008; Mansuy et al., 2012), to help in the estimation of TSLF. This lack of relationship may point to a relative importance of other factors such as drought events and surficial deposits that contribute to their abundance (Mansuy et al., 2012). Or alternatively, the causal relationship between fire and open spruce woodlands may operate at a finer spatial scale than that used in the present study. In fact, surficial deposits are known to be related to fire regime because of their drying potential (Mansuy et al., 2010) but the study area is dominated by only two surficial deposit groups (75%) that correspond to thick and thin undifferentiated tills with moderate to abundant stoniness with a moderate drying potential. Finally, we also expected elevation to help in the estimation of TSLF (Kasischke et al., 2002), especially in the White Mountains and the North Shore (Fig. 2.4), but at the scale of the study area, elevation is correlated with precipitation ($R^2 = 0.41$, $p < 0.001$) and precipitation was selected as strong predictor in the RF models (Figs. 2.2a and 2.2b).

2.05.03 Impacts of spatial scale on TSLF modelling

Houghton (2005) suggested as a rule of thumb that the spatial scale to be used for estimating standing biomass should be equivalent to that of fire disturbances. The spatial scale used in the present study (2 km^2) probably helped circumvent some of the problems encountered at a finer scale when relating stand age to TSLF, notably (1) the variability of fire severity linked to past fire dates (Miller et al., 2012) that affects the post-fire species composition (Barrett et al., 2011; Johnstone et al., 2011), (2) the errors linked to the photointerpretation of cartographic attributes of stand species composition, structure and age at the scale of forest stands (< 10 ha) (Waldron et al., 2012; Bernier et al., 2010), (3) the interaction between cartographic stand age and succession when TSLF exceeds the longevity of pioneering post-fire species (Garet et al., 2012; Cyr et al., 2010) and (4) local neighbourhood effects (*sensu* Frelich and Reich, 1999) observed at the scale of stands that blur the relationship existing between TSLF and species composition (e.g. Chen and Taylor, 2012). Indeed, at the coarser scale used here, it is not the exact stand age or the presence-absence of forest species that are indicators of TSLF but rather their proportional abundances within the cell (Figs. 2.2a and 2.2b).

2.05.04 Temporal changes in regional burn rate

A period of widespread fire activity over the whole study area was detected between 1920 and 1940 (Fig. 2.3) during which slightly more than 28% of the area has burned (6.1 Mha, Fig. 2.2e), corresponding to a burn rate of 16.4% decade^{-1}. This contrasts with the 4.3% decade^{-1} burn rate estimated between 1970 and 2000. The high mid-century peak in burn rate had already been observed by Grondin et al. (2014), and is apparent on account of the remarkably high proportion of stands aged between 60 and 80 years (22%). Such fire activity has also been identified by dendro-ecological studies carried out between Lake Mistassini and the organic plains of Abitibi (Lesieur et al., 2002; Le Goff et al., 2007), and to a lesser extent in other parts of the study area (Bergeron et al., 2004b; Bouchard et al., 2008; Girardin et al., 2013). This 6.1 Mha of burned area between 1920 and 1940 is not covered by the data of the Canadian forest fire statistics (e.g. Kurz and Apps, 1999, their Fig. 3 for "Boreal East") and provides a historical reference against which to compare, at least regionally, the recent increase in burn rate between 1980 and 2000 (Fig. 2.2e) that has been associated with climate change in the Canadian boreal region (e.g. Kasischke and Turetsky, 2006).

The methodology developed above to estimate regional TSLF may also help refine past estimates of fire-related carbon emissions from Canada's forests. Past assessments have been based on historical observational records. However, incomplete fire detection has been acknowledged (Podur et al., 2002; Stocks et al., 2003), especially before 1975 (Murphy et al., 2000). This situation may have led to incorrect century-long assessments of carbon budgets, at least for eastern Canada (Kurz and Apps, 1999; Chen et al., 2000; Mouillot and Field, 2005).

2.05.05 Management and conservation implications

The results discussed above show the importance of lengthening the historical records of fire history maps in order to provide a better perspective on the actual changes of fire regime and to better understand the relationship between fire activity and climate (Fauria and Johnson, 2008; Le Goff et al., 2007). The derived TSLF map has revealed the regional differences in fire regime and forest age class structures, which should be taken into account to devise region-specific forest ecosystem management strategies for maintaining regional-scale heterogeneity. In addition, the statistical model presented in this study to derive TSLF is a new tool that forest managers can use to estimate regional TSLF. Estimates of long-term fire history can also help forest ecologists forecast fire regime under future climate scenarios and understand the impacts of climate warming on the forest.

2.06 Conclusion

We have devised an approach for modelling and mapping TSLF at a relatively coarse resolution (cells of 2 km^2) over a large spatial extent (> 200 000 km^2). The training of the models used over existing fire history maps showed that at this resolution, TSLF is essentially and not surprisingly related to the

observed proportions of stand age classes. Such a relationship is modulated by the climate gradient that occurs over the study area (precipitation, evapotranspiration) and by the abundance of fire-averse tree species such as balsam fir. When TSLF is categorized into decades, the accuracy is excellent at the scale of both the study area and landscape units but remains fairly low at the scale of individual cells. At least regionally, our results suggest that the burn rates during the 20th century were characterized by widespread fire activity occurred between 1920 and 1940, more important than the recent increase observed between 1980 and 2000. This highlights the need for lengthening the historical records of fire over large spatial extents to provide a better appraisal of contemporaneous changes in the burn rate (e.g. Bergeron et al., 2010). Our approach could be adapted and transferred to the other ecological systems where there is evidence of succession trends following TSLF (Pausas et al., 2008; Baeza et al., 2011; Higuera et al., 2011).

2.07 Acknowledgements

This research was funded by the Fonds québécois de la recherche sur la nature et les technologies. We thank the Direction des inventaires forestiers, ministère de la Forêt, de la Faune et des Parcs du Québec and SOPFEU for having provided the SIFORT data and the 1970-2000 fire history map used in this study. We thank Rémi Saint-Amant for providing the normal climate database from the 20CR project ready for BioSIM simulations and Hakim Ouzennou, Guillaume Cyr and Kenneth Anyomi with data processing. We also thank Dominic Cyr, Héloïse Le Goff, Annie-Claude Bélisle and Daniel Lesieur for explaining the fire history and dendro-ecological data used in this study. We likewise thank Anne Theodorescu who worked with us as a summer intern for help with writing this manuscript. We finally thank Brendan Rogers for providing very thoughtful comments on a final draft of this manuscript and Pamela Cheers for her editorial help.

2.08 References

Amiro, B. D., Logan, K. A., Wotton, B. M., Flannigan, M. D., Todd, J. B., Stocks, B. J., Martell, D. L., 2005. Fire weather index system components for large fires in the Canadian boreal forest. Int. J. Wildland Fire 13, 391–400. doi:10.1071/WF03066.

Anyomi, K. A., Raulier, F., Bergeron, Y., Mailly, D., 2013. The predominance of stand composition and structure over direct climatic and site effects in explaining aspen (*Populus tremuloides* Michaux) site index within boreal and temperate forests of western Quebec, Canada. For. Ecol. Manage. 302, 390–403. doi:10.1016/j.foreco.2013.03.035.

Azeria, E. T., Fortin, D., Lemaître, J., Janssen, P., Hébert, C., Darveau, M., Cumming, S. G., 2009. Fine-scale structure and cross-taxon congruence of bird and beetle assemblages in an old-growth boreal forest mosaic. Glob. Ecol. Biogeogr. 18, 333–345. doi:10.1111/j.1466-8238.2009.00454.x.

Baeza, M. J., Santana, V. M., Pausas, J. G., Vallejo, V. R., 2011. Successional trends in standing dead biomass in Mediterranean basin species. J. Veg. Sci. 22, 467–474. doi:10.1111/j.1654-1103.2011.01262.x.

Barrett, K., McGuire, A. D., Hoy, E. E., Kasischke, E. S., 2011. Potential shifts in dominant forest cover in interior Alaska driven by variations in fire severity. Ecol. Appl. 21, 2380–2396. doi:10.1890/10-0896.1.

Bélisle, A. C., Gauthier, S., Cyr, D., Bergeron, Y., Morin, H., 2011. Fire Regime and Old-Growth Boreal Forests in Central Quebec, Canada: An Ecosystem Management Perspective. Silva Fenn. 45, 889–908. www.metla.fi/silvafennica/full/sf45/sf455889.pdf

Bergeron, Y., Cyr, D., Girardin, M. P., Carcaillet, C., 2010. Will climate change drive 21st century burn rates in Canadian boreal forest outside of its natural variability: collating global climate model experiments with sedimentary charcoal data. Int. J. Wildland Fire 19, 1127–1139. doi:10.1071/WF09092.

Bergeron, Y., Fenton, N. J., 2012. Boreal forests of eastern Canada revisited: old growth, nonfire disturbances, forest succession, and biodiversity. Botany 90, 509–523. doi:10.1139/b2012-034.

Bergeron, Y., Flannigan, M., Gauthier, S., Leduc, A., Lefort, P., 2004a. Past, current and future fire frequency in the Canadian boreal forest: implications for sustainable forest management. Ambio. 33, 356–360. doi:10.1579/0044-7447-33.6.356.

Bergeron, Y., Gauthier, S., Flannigan, M., Kafka, V., 2004b. Fire Regimes at the transition between mixedwood and coniferous boreal Forest in Northwestern Quebec. Ecology 85, 1916–1932. doi:10.1890/02-0716.

Bernier, P. Y., Guindon, L., Kurz, W. A., Stinson, G., 2010. Reconstructing and modelling 71 years of forest growth in a Canadian boreal landscape: a test of the CBM-CFS3 carbon accounting model. Can. J. For. Res. 40, 109–118. doi:10.1139/X09-177.

Bettinger, P., Boston, K., Siry, J.P., Grebner, D.L., 2009. Forest Management and Planning.Academic Press, Burlington, MA (331 pp.).

Börger, L., Nudds, T. D., 2014. Fire, humans, and climate: modeling distribution dynamics of boreal forest waterbirds. Ecol. Appl. 24, 121–141. doi:10.1890/12-1683.1.

Bouchard, M., Garet, J., 2014. A framework to optimize the restoration and retention of large mature forest tracts in managed boreal landscapes. Ecol. Appl. 24, 1689–1704. doi: 10.1890/12-1683.1.

Bouchard, M., Pothier, D., 2011. Long-term influence of fire and harvesting on boreal forest age structure and forest composition in eastern Québec. For. Ecol. Manage. 261, 811–820. doi:10.1016/j.foreco.2010.11.020.

Bouchard, M., Pothier, D., Gauthier, S., 2008. Fire return intervals and tree species succession in the North Shore region of eastern Quebec. Can. J. For. Res. 38, 1621–1633. doi: 10.1139/X07-201.

Boulanger, Y., Gauthier, S., Gray, D. R., Le Goff, H., Lefort, P., Morissette, J., 2013. Fire regime zonation under current and future climate over eastern Canada. Ecol. Appl. 23, 904–923. doi:10.1890/12-0698.1.

Chen, H. Y. H., Taylor, A. R., 2012. A test of ecological succession hypotheses using 55-year time-series data for 361 boreal forest stands. Glob. Ecol. Biogeogr. 21, 441–454. doi: 10.1111/j.1466-8238.2011.00689.x.

Chen, J., Chen, W., Liu, J., Cihlar, J., Gray, S., 2000. Annual carbon balance of Canada's forests during 1895–1996. Glob. Biogeochem. Cycles 14, 839–849. doi:10.1029/1999GB001207.

Cohen, J., 1960. A coefficient of agreement for nominal scales. Educ. Psychol. Meas., 20, 37–46.

Compo, G. P., Whitaker, J. S., Sardeshmukh, P. D., Matsui, N., Allan, R. J., Yin, X., Gleason, B. E., Vose, R. S., Rutledge, G., Bessemoulin, P., Brönnimann, S., Brunet, M., Crouthamel, R. I., Grant, A. N., Groisman, P. Y., Jones, P. D., Kruk, M. C., Kruger, A. C., Marshall, G. J., Maugeri, M., Mok, H. Y., Nordli, Ø., Ross, T. F., Trigo, R. M., Wang, X. L., Woodruff, S. D., Worley, S. J., 2011. The twentieth century reanalysis project. Q. J. R. Meteorol. Soc. 137, 1–28. doi:10.1002/qj.776.

Cumming, S. G., Schmiegelow, F. K. A., Burton, P. J., 2000. Gap dynamics in boreal aspen stands: Is the forest older than we think? Ecol. Appl. 10, 744–759. doi:10.1890/1051-0761(2000)010[0744:GDIBAS]2.0.CO;2.

Cutler, D. R., Edwards, T. C., Beard, K. H., Cutler, A., Hess, K. T., Gibson, J., Lawler, J. J., 2007. Random forests for classification in ecology. Ecology 88, 2783–2792. doi:10.1890/07-0539.1.

Cyr, D., Gauthier, S., Bergeron, Y., Carcaillet, C., 2009. Forest management is driving the eastern North American boreal forest outside its natural range of variability. Front. Ecol. Environ. 7, 519–524. doi:10.1890/080088.

Cyr, D., Gauthier, S., Etheridge, D. A., Kayahara, G. J., Bergeron, Y., 2010. A simple Bayesian Belief Network for estimating the proportion of old-forest stands in the Clay Belt of Ontario using the provincial forest inventory. Can. J. For. Res. 40, 573–584. doi:10.1139/X10-025.

De Groot, W. J., Bothwell, P. M., Carlsson, D. H., Logan, K. A., Lepš, J., 2003. Simulating the effects of future fire regimes on western Canadian boreal forests. J. Veg. Sci. 14, 355–364. doi:10.1111/j.1654-1103.2003.tb02161.x.

Didion, M., Fortin, M.-J., Fall, A., 2007. Forest age structure as indicator of boreal forest sustainability under alternative management and fire regimes: A landscape level sensitivity analysis. Ecol. Model. 200, 45–48. doi:10.1111/j.1654-1103.2003.tb02161.x.

Dormann, C.F., McPherson, J.M., Araújo, M.B., Bivand, R., Bolliger, J., Carl, G., Davies, R.G., Hirzel, A., Jetz, W., Kissling, W.D., Kühn, I., Ohlemüller, R., Peres-Neto, P.R., Reineking, B., Schröder, B., Schurr, F.M., Wilson, R., 2007. Methods to account for spatial autocorrelation in the analysis of species distributional data: a review. Ecography. 30, 609-628. doi: 10.1111/j.2007.0906-7590.05171.x.

Dunne, T., Leopold, L. B., 1978. Water in environmental planning. New York: 566–580.

Fauria, M. M., Johnson, E. A., 2008. Climate and wildfires in the North American boreal forest. Philos. Trans. R. Soc. B 363, 2317–2329. doi:10.1098/rstb.2007.2202.

Frelich, L. E., Reich, P. B., 1995. Spatial Patterns and Succession in a Minnesota Southern-Boreal Forest. Ecol. Monogr. 65, 325–346. doi:10.2307/2937063.

Frelich, L. E., Reich, P. B., 1999. Minireviews: neighborhood effects, disturbance severity, and community stability in forests. Ecosystems 2, 151–166. doi:10.1007/s100219900066.

Garet, J., Pothier, D., Bouchard, M., 2009. Predicting the long-term yield trajectory of black spruce stands using time since fire. For. Ecol. Manage. 257, 2189–2197. doi:10.1016/j.foreco.2009.03.001.

Garet, J., Raulier, F., Pothier, D., Cumming, S. G., 2012. Forest age class structures as indicators of sustainability in boreal forest: Are we measuring them correctly? Ecological Indicators 23, 202–210. doi:10.1016/j.ecolind.2012.03.032.

Gauthier, S., Boucher, D., Morissette, J., De Grandpré, L., 2010. Fifty-seven years of composition change in the eastern boreal forest of Canada. J. Veg. Sci. 21, 772–785. doi: 10.1111/j.1654-1103.2010.01186.x.

Girard, F., Payette, S., Gagnon, R., 2008. Rapid expansion of lichen woodlands within the closed-crown boreal forest zone over the last 50 years caused by stand disturbances in eastern Canada. J. Biogeogr. 35, 529–537. doi: 10.1111/j.1365-2699.2007.01816.x.

Girardin, M. P., Ali, A. A., Carcaillet, C., Gauthier, S., Hely, C., Le Goff, H., Terrier, A., Bergeron, Y., 2013. Fire in managed forests of eastern Canada: Risks and options. For. Ecol. Manage. 294, 238–249. doi:10.1016/j.foreco.2012.07.005.

Girardin, M. P., Guo, X. J., Bernier, P. Y., Raulier, F., Gauthier, S., 2012. Changes in growth of pristine boreal North American forests from 1950 to 2005 driven by landscape demographics and species traits. Biogeosciences 9, 2523–2536. doi: 10.5194/bgd-9-1021-2012.

Grondin, P., Gauthier, S., Borcard, D., Bergeron, Y., Noël, J., 2014. A new approach to ecological land classification for the Canadian boreal forest that integrates disturbances. Landsc. Ecol. 29, 1–16. doi:10.1007/s10980-013-9961-2.

Grondin, P., Noel, J., Hotte, D., 2007. L'intégration de la végétation et de ses variables cartographie d'unités homogènes du Québec méridional. Quebec city, Canada. bibvir2.uqac.ca/archivage/030005474.pdf (accessed on October 28, 2014)

Hauer, G., Cumming, S., Schmiegelow, F., Adamowicz, W., Weber, M., Jagodzinski, R., 2010. Tradeoffs between forestry resource and conservation values under alternate policy regimes: A spatial analysis of the western Canadian boreal plains. Ecol. Model. 221, 2590–2603. doi:10.1016/j.ecolmodel.2010.07.013.

He, H. S., Mladenoff, D. J., 1999. Spatially explicit and stochastic simulation of forest-landscape fire disturbance and succession. Ecology 80, 81–99. doi:10.1890/0012-9658(1999)080[0081:SEASSO]2.0.CO;2.

Héon, J., Arseneault, D., Parisien, M.-A., 2014. Resistance of the boreal forest to high burn rates. Proceedings of the National Academy of Sciences 111, 13888–13983. doi: 10.1073/pnas.1409316111.

Heyerdahl, E. K., Brubaker, L. B., Agee, J. K., 2001. Spatial controls of historical fire regimes: A multiscale example from the interior west, USA. Ecology 82, 660–678. doi: 10.1890/0012-9658(2001)082[0660:SCOHFR]2.0.CO;2.

Higuera, P. E., Chipman, M. L., Barnes, J. L., Urban, M. A., Hu, F. S., 2011. Variability of tundra fire regimes in Arctic Alaska: millennial-scale patterns and ecological implications. Ecol. Appl. 21, 3211–3226. doi:10.1890/11-0387.1.

Houghton, R. A., 2005. Aboveground forest biomass and the global carbon balance. Glob. Chang. Biol. 11, 945–958. doi:10.1111/j.1365-2486.2005.00955.x.

Johnson, E. A., Gutsell, S. L., 1994. Fire frequency models, methods and Interpretations. Adv. Ecol. Res. 25, 239–287.

Johnstone, J. F., Hollingsworth, T. N., Chapin, F. S., Mack, M. C., 2010. Changes in fire regime break the legacy lock on successional trajectories in Alaskan boreal forest. Glob. Chang. Biol. 16, 1281–1295. doi:10.1111/j.1365-2486.2009.02051.x.

Kasischke, E. S., Turetsky, M. R., 2006. Recent changes in the fire regime across the North American boreal region—Spatial and temporal patterns of burning across Canada and Alaska. Geophys. Res. Lett. 33, L09703. doi:10.1029/2006GL025677.

Kasischke, E. S., Williams, D., Barry, D., 2002. Analysis of the patterns of large fires in the boreal forest region of Alaska. Int. J. Wildland Fire 11, 131–144. doi:10.1071/WF02023.

Kurz, W. A., Apps, M. J., 1999. A 70-year retrospective analysis of carbon fluxes in the Canadian forest sector. Ecol. Appl. 9, 526–547. doi: 10.1890/1051-0761(1999)009[0526.AYRAOC]2.0.CO;2

Landis, J. R., Koch, G. G., 1977. The measurement of observer agreement for categorical data. Biometrics 33, 159–174. Available from http://www.jstor.org/stable/2529310.

Lavoie, L., Sirois, L., 1998. Vegetation changes caused by recent fires in the northern boreal forest of eastern Canada. J. Veg. Sci. 9, 483–492. doi: 10.2307/3237263.

Le Goff, H., Flannigan, M. D., Bergeron, Y., 2009. Potential changes in monthly fire risk in the eastern Canadian boreal forest under future climate change. Can. J. For. Res. 39, 2369–2380. doi: 10.1139/X09-153.

Le Goff, H., Flannigan, M. D., Bergeron, Y., Girardin, M., 2007. Historical fire regime shifts related to climate teleconnections in the Waswanipi area, central Quebec, Canada. Int. J. Wildland Fire 16, 607-618. doi: 10.1071/WF06151.

Lesieur, D., Gauthier, S., Bergeron, Y., 2002. Fire frequency and vegetation dynamics for the south-central boreal forest of Quebec, Canada. Can. J. For. Res. 32, 1996–2009. doi: 10.1139/x02-113.

Liaw, A., Wiener, M., 2002. Classification and Regression by randomForest. R news, 2(3), 18-22. http://cran.r-project.org/web/packages/randomForest/randomForest.pdf (accessed on October 24, 2014)

Mansuy, N., Gauthier, S., Robitaille, A., Bergeron, Y., 2010. The effects of surficial deposit–drainage combinations on spatial variations of fire cycles in the boreal forest of eastern Canada. Int. J. Wildland Fire 19, 1083–1098. doi: 10.1071/WF09144.

Mansuy, N., Gauthier, S., Robitaille, A., Bergeron, Y., 2012. Regional patterns of postfire canopy recovery in the northern boreal forest of Quebec: interactions between surficial deposit, climate, and fire cycle. Can. J. For. Res. 42, 1328–1343. doi: 10.1139/x2012-101

McKinley, D. C., Ryan, M. G., Birdsey, R. A., Giardina, C. P., Harmon, M. E., Heath, L. S., Houghton, R. A., Jackson, R. B., Morrison, J. F., Murray, B. C., Pataki, D. E., Skog, K. E., 2011. A synthesis of current knowledge on forests and carbon storage in the United States. Ecol. Appl. 21, 1902–1924. doi:10.1890/10-0697.1.

Miller, J. D., Skinner, C. N., Safford, H. D., Knapp, E. E., Ramirez, C. M., 2012. Trends and causes of severity, size, and number of fires in northwestern California, USA. Ecol. Appl. 22, 184–203. doi: 10.1890/10-2108.1.

Moran, P. A., 1950. Notes on continuous stochastic phenomena. Biometrika. 17-23.

Morgan, P., Hardy, C. C., Swetnam, T. W., Rollins, M. G., Long, D. G., 2001. Mapping fire regimes across time and space: Understanding coarse and fine-scale fire patterns. Int. J. Wildland Fire 10, 329–342. doi: 10.1071/WF01032.

Mouillot, F., Field, C. B., 2005. Fire history and the global carbon budget: a 1°× 1°fire history reconstruction for the 20th century. Glob. Chang. Biol. 11, 398–420. doi: 10.1111/j.1365-2486.2005.00920.x.

Murphy, P.J., Mudd, J.P., Stocks, B.J., Kasischke, E.S., Barry, D., Alexander, M.E., French, N.H.F., 2000. Historical fire records in the North American boreal forest. In Fire, climate change, and carbon cycling in the boreal forest. Edited by E.S. Kasischke and B.J. Stocks. Springer-Verlag, New York. pp. 274–288.

Nalle, D. J., Montgomery, C. A., Arthur, J. L., Polasky, S., Schumaker, N. H., 2004. Modeling joint production of wildlife and timber. J. Environ. Econ. Manage. 48, 997–1017. doi:10.1016/j.jeem.2004.01.001.

Pan, Y., Birdsey, R.A., Fang, J., Houghton, R., Kauppi, P.E., Kurz, W.A., Phillips, O.L., Shvidenko, A., Lewis, S.L., Canadell, J.G., Ciais, P., Jackson, R.B., Pacala, S.W., McGuire, A.D., Piao, S., Rautiainen, A., Sitch, S., Hayes, D., 2011. A large and persistent carbon sink in the World's forests. Science 333, 988–993. doi:10.1126/science.1201609.

Pausas, J. G., Llovet, J., Rodrigo, A., Vallejo, R., 2008. Are wildfires a disaster in the Mediterranean basin? – A review. Int. J. Wildland Fire 17, 713–723. doi: 10.1071/WF07151.

Pelletier, G., Dumont, Y., Bédard, M., 2007. SIFORT: Système d'Information FORestière par Tesselle, Manuel de l'usager. Ministère des Ressources naturelles et de la Faune du Québec. Québec, QC, Canada. https://www.mffp.gouv.qc.ca/publications/forets/fimaq/usager.pdf. (accessed on October 2, 2014)

Podur, J., Martell, D. L., Knight, K., 2002. Statistical quality control analysis of forest fire activity in Canada. Can. J. For. Res. 32, 195–205. doi: 10.1139/x01-183.

Raymond, C. L., McKenzie, D., 2012. Carbon dynamics of forests in Washington, USA: 21st century projections based on climate-driven changes in fire regimes. Ecol. Appl. 22, 1589–1611. doi: 10.1890/11-1851.1.

Reed, W. J., Larsen, C. P. S., Johnson, E. A., MacDonald, G. M., 1998. Estimation of temporal variations in historical fire frequency from time-since-fire map data. For. Sci. 44, 465–475.

Régnière, J., 2009. Predicting insect continental distributions from species physiology. J. Unasylva 60, 37–42.

Régnière, J., St-Amant, R., 2008. BioSIM 9 user's manual : Information Report LAU-X-134E. Natural Resources Canada, Canadian Forest Service, Laurentian Forestry Center, Quebec, QC, Canada. https://cfs.nrcan.gc.ca/publications?id=28768 (accessed on October 7, 2014)

Robitaille, A., Saucier, J.-P., 1996. Land district, ecophysiographic units and areas: The landscape mapping of the ministère des ressources naturelles du Québec. Environ. Monit. Assess. 39, 127–148. doi: 10.1007/BF00396141

Sarle, W. S., 1983. SAS Technical Report A-108, Cubic clustering criterion. 56. https://support.sas.com/documentation/onlinedoc/v82/techreport_a108.pdf (accessed on March 7, 2014)

Savage, D., Wotton, B. M., Martell, D. L., Woolford, D. G., 2013. The impact of uncertainty concerning historical burned area estimates on forest management planning. For. Sci. 59, 578–588. doi:10.5849/forsci.11-081.

Simard, M., Lecomte, N., Bergeron, Y., Bernier, P. Y., Paré, D., 2007. Forest productivity decline caused by successional paludification of boreal soils. Ecol. Appl. 17, 1619–1637. doi:10.1890/06-1795.1.

Stinson, G., Kurz, W. A., Smyth, C. E., Neilson, E. T., Dymond, C. C., Metsaranta, J. M., Boisvenue, C., Rampley, G. J., Li, Q., White, T. M., Blain, D., 2011. An inventory-based analysis of Canada's managed forest carbon dynamics, 1990 to 2008. Glob. Chang. Biol. 17, 2227–2244. doi: 10.1111/j.1365-2486.2010.02369.x.

Stocks, B. J., Mason, J. A., Todd, J. B., Bosch, E. M., Wotton, B. M., Amiro, B. D., Flannigan, M. D., Hirsch, K. G., Logan, K. A., Martell, D. L., 2003. Large forest fires in Canada, 1959-1997. J. Geophys. Res. 108(D1), 8149. doi: 10.1029/2001JD000484.

Thompson, J. R., Spies, T. A., 2009. Vegetation and weather explain variation in crown damage within a large mixed-severity wildfire. For. Ecol. Manage. 258, 1684–1694. doi:10.1016/j.foreco.2009.07.031.

Timm, B. C., McGarigal, K., 2012. Fine-scale remotely-sensed cover mapping of coastal dune and salt marsh ecosystems at Cape Cod National Seashore using Random Forests. Remote Sens. Environ. 127,106–117. doi:10.1016/j.rse.2012.08.033.

Van Zyl, J. J., 2001. The Shuttle Radar Topography Mission (SRTM): a breakthrough in remote sensing of topography. Acta Astronaut. 48, 559–565. doi: 10.1016/S0094-5765(01)00020-0.

Venables, W. N., Smith, D. M., 2013. the R Core Team. An Introduction to R. Version 2.

Waldron, K., Ruel, J.-C., Gauthier, S., 2012. The effects of site characteristics on the landscape-level windthrow regime in the North Shore region of Quebec, Canada. Forestry 86, 159–171. doi: 10.1093/forestry/cps061.

Weber, M. G., Stocks, B.J., 1998. Forest fires and sustainability in the boreal forests of Canada. Ambio. 27, 545–550.

Weir, J. M. H., Johnson, E. A., Miyanishi, K., 2000. Fire frequency and the spatial age mosaic of the mixed-wood boreal forest in western Canada. Ecol. Appl. 10, 1162–1177. doi: 10.1890/1051-0761(2000)010[1162:FFATSA]2.0.CO;2

Wooster, M. J., Zhang, Y. H., 2004. Boreal forest fires burn less intensely in Russia than in North America. Geophys. Res. Lett. 31, L20505. doi: 10.1029/2004GL020805

Zhang, G., Lu, Y., 2012. Bias-corrected random forests in regression. J. Appl. Statist. 39, 151–160. doi:10.1080/02664763.2011.578621.

2.09 Supplementary material

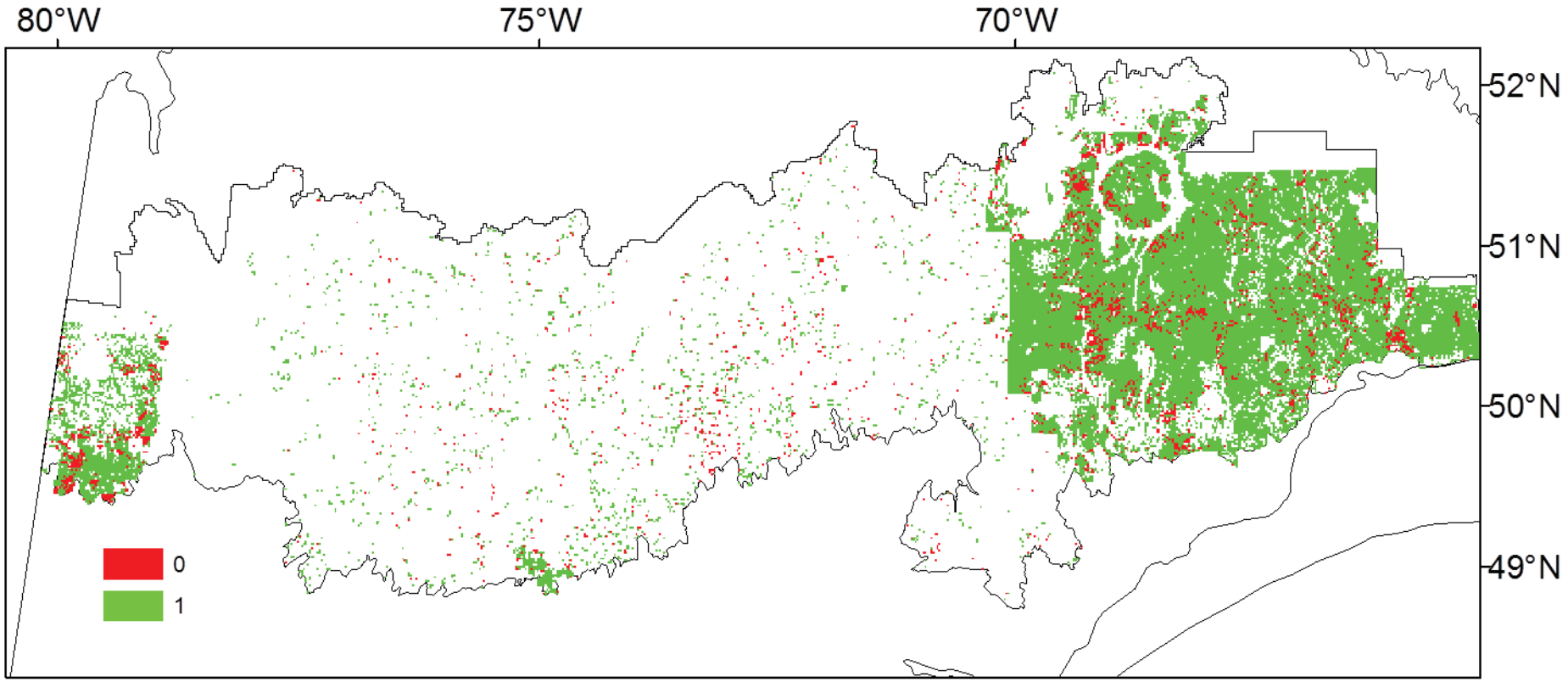

Fig. A.1. Map of residuals for classifying cells into TSLF ≤ 120 years (between 1880 and 1970) and TSLF > 120 years (< 1880) (training dataset). The value of 0 (red region) indicates incorrectly classified cell and 1 (green region) indicates a correctly classified cell

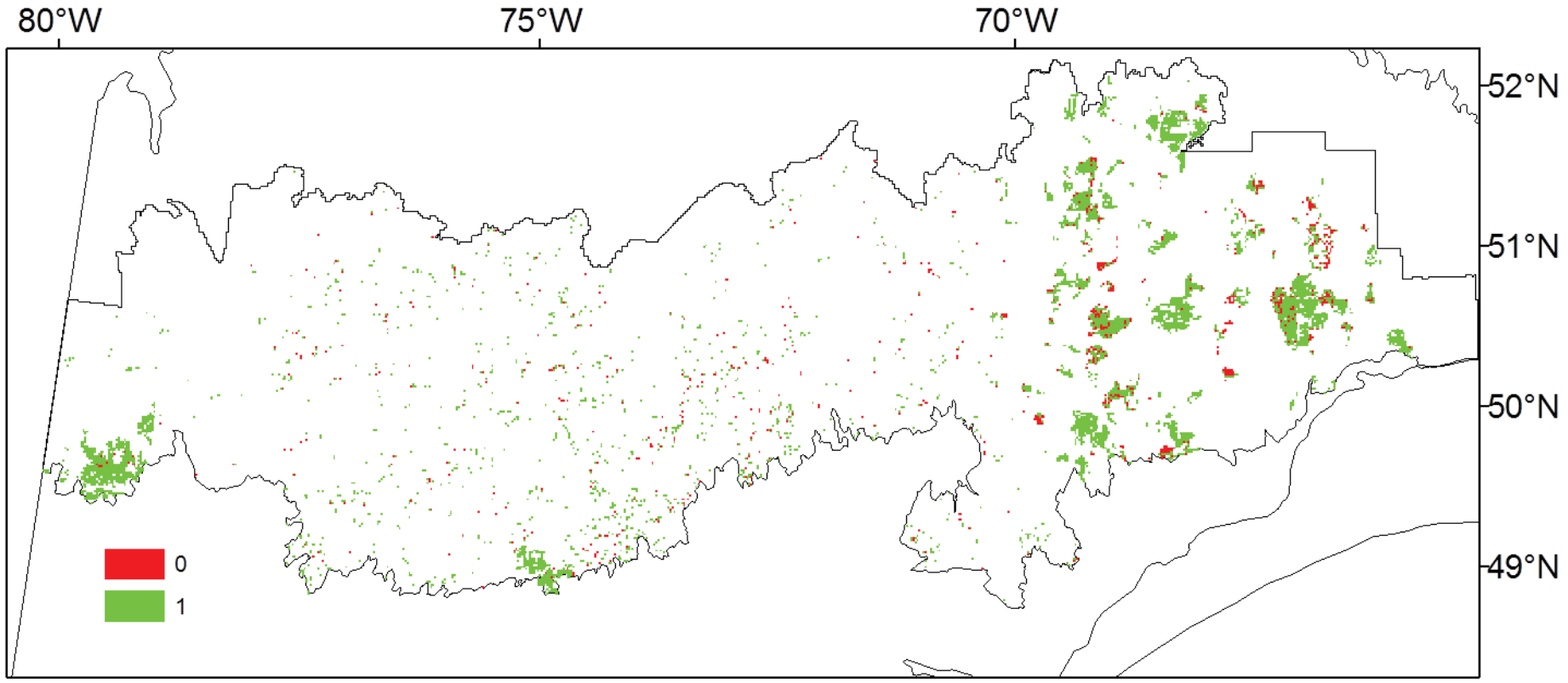

Fig. A.2. Map of residuals for predicting the decade of stand origin (between 1880 and 1970) (training dataset). The value of 0 (red) indicates cells with an incorrectly classified decade and 1 (green), cells with a correctly classified decade.

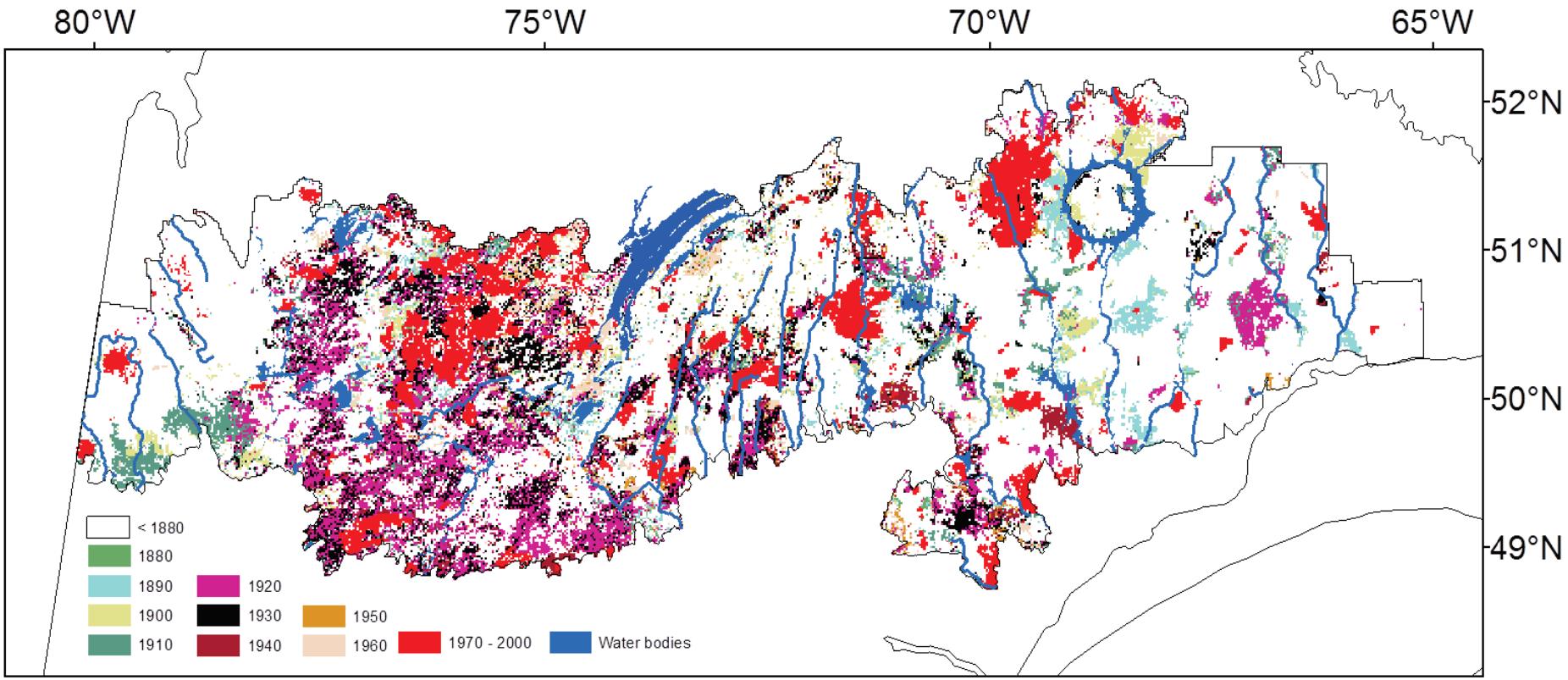

Fig. A.3. Map of predicted year of stand origin (between 1880 and 1970), predicted TSLF > 120 years (< 1880), and observed TSLF (1970-2000, SOPFEU dataset) for the study region.

3. Chapter 2: Cover density recovery after fire disturbance controls landscape aboveground biomass carbon in the boreal forest of eastern Canada

Dinesh Babu Irulappa Pillai Vijayakumar, Frédéric Raulier, Pierre Bernier, David Paré, Sylvie Gauthier, Yves Bergeron, David Pothier

This chapter has been published and can be cited as:

Irulappa Pillai Vijayakumar, D.B., Raulier, F., Bernier, P. Y., Paré, D., Gauthier, S., Bergeron, Y., Pothier, D. 2016. Cover density recovery after fire disturbance controls landscape aboveground biomass carbon in the boreal forest of eastern Canada. Forest Ecology and Management, 360, 170–180.

3.01 Abstract

In existing carbon budget models, carbon stocks are not explicitly related to forest successional dynamics and environmental factors. Yet time-since-last-fire (TSLF) is an important variable for explaining successional changes and subsequent carbon storage. The objective of this study was to predict the spatial variability of aboveground biomass carbon (ABC) as a function of TSLF and other environmental factors across the landscape at regional scales. ABC was predicted using random forest models, both at the sample-plot level and at the scale of 2-km^2 cells. This cell size was chosen to match the observed minimum fire size of the Canadian large fire database. The percentage variance explained by the empirical sample-plot level model of ABC was 50%. At that scale, TSLF was not significantly related to ABC. At the 2-km^2 scale, ABC was influenced mainly by the proportions of cover density classes, which explained 83% of the variance. Changes in cover density were related to TSLF at the same 2-km^2 scale, indicating that the increase in cover density following fire disturbance is a dominant mechanism through which TSLF acts upon ABC at the scale of landscapes.

Keywords: time-since-last-fire; boreal forest; Random Forest; aboveground biomass carbon; Successional dynamics

3.02 Introduction

The boreal forest stores 32% of global total forest (861 ± 66 Pg) carbon (C) and has a C stock density comparable to that of tropical forests (Pan et al., 2011a). Residence times of C in forest ecosystems play an important role in the global C cycle (Melillo et al., 2002; Magnani et al., 2007), and control the stability (Malhi and Grace, 2000) and productivity (Simard et al., 2007; Malhi, 2012) of forest ecosystems. Aboveground biomass carbon (ABC) is a key variable for understanding contribution of forests on global carbon budget (Houghton, 2005). Forest stand age, as determined by stand-replacing disturbances such as fire, is a key variable for estimating forest C stocks. Living C biomass peaks around the average life expectancy of the dominant tree species within the canopy of boreal forests, but undergoes further increases with stand age in tropical and temperate forests (Pregitzer and Euskirchen, 2004). Spatial variation of C stock is not solely related to forest age (Houghton, 2005) but also to other factors such as soil drainage (Wang et al., 2003), soil texture, climate (Chen et al., 2015) and topography (Grant, 2004).

Fire is a major driver that controls landscape C storage in boreal forests (Harden et al., 2000; Stinson et al., 2011). Extrapolation of C budgets from the stand- to the landscape-level must also consider forest age class structure (Kurz et al., 2009; Pan et al., 2011b). Understanding the interaction between forest age class structure, forest succession and stand-replacing disturbances can improve the spatial accuracy of C stock estimates (Houghton, 2003), particularly ABC. Existing C budget models (e.g. Chen et al., 2003; 2010; Kurz et al., 2009) use growth and yield curves as a function of stand age to explain the spatial variability of ABC stocks, but these curves do not incorporate forest succession dynamics (i.e., post-disturbance recovery, stand composition and structural changes; Taylor et al., 2009). These elements of forest succession dynamics are related to TSLF (time-since-last fire). Further, stand age is only related to TSLF until the canopy trees of the first cohort begin to die off, which occurs when the time that has elapsed since the last stand-initiating disturbance exceeds the mean longevity of the dominant canopy tree species (Garet et al., 2012). The use of forest age alone as a surrogate variable for TSLF may thus lead to inaccuracies in subsequent carbon budget analyses.

Post-fire forest successional dynamics vary according to the disturbance frequency and the physical environment of the landscape (Johnstone et al., 2010). Given the large longitudinal gradient in fire cycle length across the North American boreal forest (Bergeron et al., 2004), the use of mean tree age alone in empirical yield tables will therefore not provide accurate landscape-level values of ABC estimates (Banfield et al., 2002). In such cases, a better way to infer landscape-level ABC estimates could be provided through the use of probability distribution functions of ABC as a function of TSLF and environmental factors. Yet variability of boreal forest

carbon, including ABC, at regional scales in relation with TSLF is still poorly understood due to the general lack of spatially explicit fire history data (Balshi et al., 2007).

The objective of this study was thus to predict the spatial variability of ABC as a function of stand and environmental variables across the landscape at a regional scale, and to determine the contribution of TSLF to the predictive model. To this effect, a hybrid modelling approach was selected to overcome the limitations that are encountered with both theoretical ecological models and statistical relationships (Mäkelä et al., 2000; Landsberg, 2003). We developed two ABC models with a hierarchical scaling approach, one at the fine scale of 400-m^2 forest inventory plots, and one at the coarse scale of 2-km^2 square cells, for the black spruce-feather moss forest of eastern Canada (area: 217,000 km^2). The 2-km^2 cell size was selected to match the minimum fire size that was used in the Canadian large fire database (1950-1999). Fires that were 200 ha and more in areas accounted for 97% of the forest area that had been burned in Canada between 1950 and 1999 (Stocks et al., 2003). The experimental region was specifically selected for its richness in terms of fire history maps as a means of serving as a training area for studying variation in ABC over the landscape in relation to TSLF. We compared the predictive accuracy of the fine and coarse-scale models, and evaluated the contribution of TSLF to both models. Our overall modelling approach aimed at testing the hypothesis that TSLF is the main factor explaining spatial variation in ABC.

3.03 Material and Methods

3.03.01 Study region

The study was conducted in a 217,000 km^2 region of the boreal forest roughly bounded between 49° N and 52° N, and from 66° W to 79°30' W (Fig. 3.1). This region is influenced by both continental and maritime climates with a mean annual temperature between 0 °C and -2.5 °C, increasing from north to south, and mean annual precipitation between 800 mm and 1400 mm, increasing from west to east. The length of the growing season (i.e., the number of days with a mean daily temperature above 5 ^oC) varies between 120 and 160 days y^{-1} (Robitaille and Saucier, 1998).

The region is located on the Canadian Shield, composed mostly of Precambrian rocks. In the western portion of the study, the area adjacent to James Bay is dominated by organic deposits with flat topography (Clay Belt). The central region is a landscape of moderate elevation (300-500 m) covered by mesic glacial tills. In the east, the landscape becomes hillier with elevations ranging from 700 to 1000 m and is covered by glacial tills of varying thickness.

The forest canopy is dominated by black spruce (*Picea mariana* (Mill.) BSP) in conjunction with jack pine (*Pinus banksiana* Lamb.) in the west and fire-averse balsam fir (*Abies balsamea* [L.]

Miller) in the eastern portion of the study region. Other tree species that are present in small numbers are trembling aspen (*Populus tremuloides* Michx.), paper or white birch (*Betula papyrifera* Marsh.), white spruce (*Picea glauca* [Moench] Voss), and eastern larch or tamarack (*Larix laricina* [Du Roi] K.Koch). The understory vegetation consists mainly of hypnaceous mosses and ericaceous shrubs.

Fire in the region is a major driver of succession (Lecomte et al., 2006; Cyr et al., 2007). The fire cycle is shorter (100 to 300 years) in the west (Bergeron et al., 2004) than in the east (> 500 years) (Bouchard et al., 2008). The western region is characterized by continental and warm climate that favours more frequent fires. On contrary, the eastern region is characterized by a maritime climate with high precipitation that promotes long fire free periods. Spruce budworm (*Choristoneura fumiferana* [Clemens]) outbreaks occurred in the southeastern part of the study region, especially where balsam fir stands dominate the landscape (Bouchard and Pothier, 2011).

3.03.02 Datasets and study units

We used temporary sample plot (TSP) data (Fig. 3.1b), forest stand maps, fire history maps (Fig. 3.1a), and climate data derived from the NCEP-NCAR Twentieth Century Reanalysis (20CR) project (Compo et al., 2011). These datasets were produced at various spatial scales. Therefore, we adopted a spatially explicit hierarchical approach (Wu and David, 2002) to scale data up or down to the scale of our study units (i.e., plot, stand, and 2-km^2 square cells).

The TSP third inventory database (1992–2003) contains measurements that were taken across the whole region (Fig. 3.1b) by the Ministry of Natural Resources of Quebec (MRNQ). The 400-m^2 field plots within that database were established in transects of from 2 to 7 plots. In each plot, species and diameter at 1.3 m (diameter at breast height, DBH) were recorded for all the trees with a DBH > 9.0 cm. Age was estimated for three to five dominant or co-dominant trees from growth ring counts on cores taken at 1 m height. Organic layer depth, drainage class, surficial deposit type, soil texture and humus type were also recorded for 8739 plots. Values of plot-level aboveground biomass were computed by summing the aboveground biomasses of individual trees (foliage, branches, stem wood and stem bark), which were estimated through the application of species-specific DBH-based biomass allometric equations (Buech and Rugg, 1989; Ter-Mikaelian and Korzukhin, 1997; Jenkins et al., 2004; Lambert et al., 2005; Ung et al., 2008). Biomass estimates were then transformed to carbon using a conversion factor of 0.5 g of C per gram of oven-dry biomass (Gower et al., 1997).

A TSLF value was attributed to each plot that was located within the fire history maps. If more than one TSLF value was available because of overlapping fire polygons, the most recent TSLF

value was attributed to each plot. A TSLF value was also assigned to the plots lying outside of the fire history maps when post-fire species (paper birch, trembling aspen, jack pine, black spruce) dominated their cover and the age difference among their cored dominant trees is less than 20 years (Bélisle et al., 2011). In total, 7509 plots had a TSLF value; this was the ABC training dataset.

Forest stand maps were based on photo-interpretation of 1:15000 aerial photographs that were acquired by MRNQ between 1990 and 1999, and used to delineate stands (average size, ~8 ha) and classify their vegetation. Given the extent of the study area, we used the SIFORT spatial geodatabase (Spatial information on Forest Composition, based on Tessera; Pelletier et al., 2007) rather than entire forest maps. This database is derived from forest maps and systematically divides the area into tiles of 15 seconds longitude by 15 seconds latitude, with each tile covering about 14 ha at the latitude of the study region. Information on species type, stand structure, surficial deposit and drainage was extracted from these maps for each tile centroid. Surficial deposits refer to quaternary sediments (clay, gravel, sand, and silt) that occur on the surface of overlying bedrock that were deposited or accumulated by ice, wind, or gravity (Fullerton et al., 2003). Surficial deposits were grouped into seven classes that explained soil drying potential based on a combination of soil stoniness and texture: very abundant, very coarse (VAVC); moderate, moderate (MM); moderately abundant, moderate (MAM); moderately abundant, coarse (MAC); abundant, coarse (AC); rock (ROC); and organic (ORG) (Mansuy et al., 2010).

The region of interest has very few weather stations. Therefore, values of climate variables that were required for our analysis were extracted from downscaled 20CR climate reanalysis data (Compo et al., 2011). Downscaling from a 2° x 2° spatial resolution to plot, SIFORT tile centroid, and 2-km^2 cell levels was conducted using BioSIM (Régnière and St-Amant, 2008) and the 90-m resolution grid of Shuttle Radar Topographic Mission (SRTM) digital elevation model (DEM) (Van Zyl, 2001). Daily minimum and maximum temperatures, and precipitation for the period 1971-2000 were extracted from the 20CR data and entered into BioSIM to compute climate variables that were known to relate to tree growth in eastern Canadian boreal forests (Girardin et al., 2012): annual mean temperature; annual total precipitation; annual degree-days (above 5 ^{o}C); growing season length, i.e., cumulative days where mean temperature is > 5 ^{o}C (days y^{-1}); an aridity index (mm y^{-1}), which was computed as the annual summed differences between monthly Thornthwaite potential evapotranspiration (PET) and monthly precipitation (Dunne and Leopold, 1978); potential evapotranspiration (Dunne and Leopold, 1978); and drought code, which is a fire weather index indicating moisture content of the deep compacted organic matter layer (10-20 cm; Amiro et al., 2005).

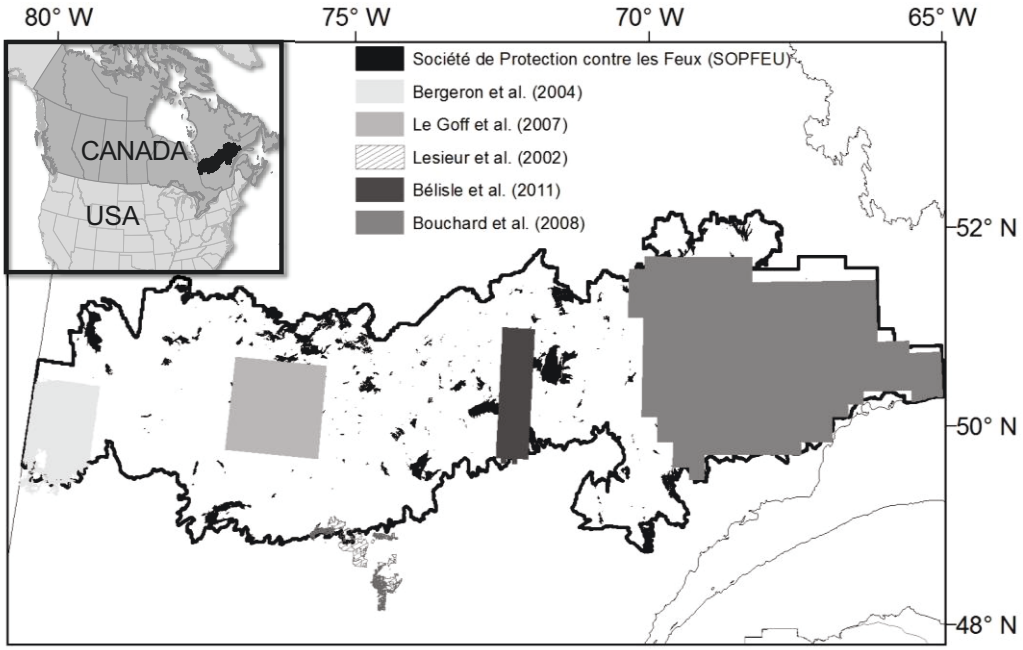

(a)

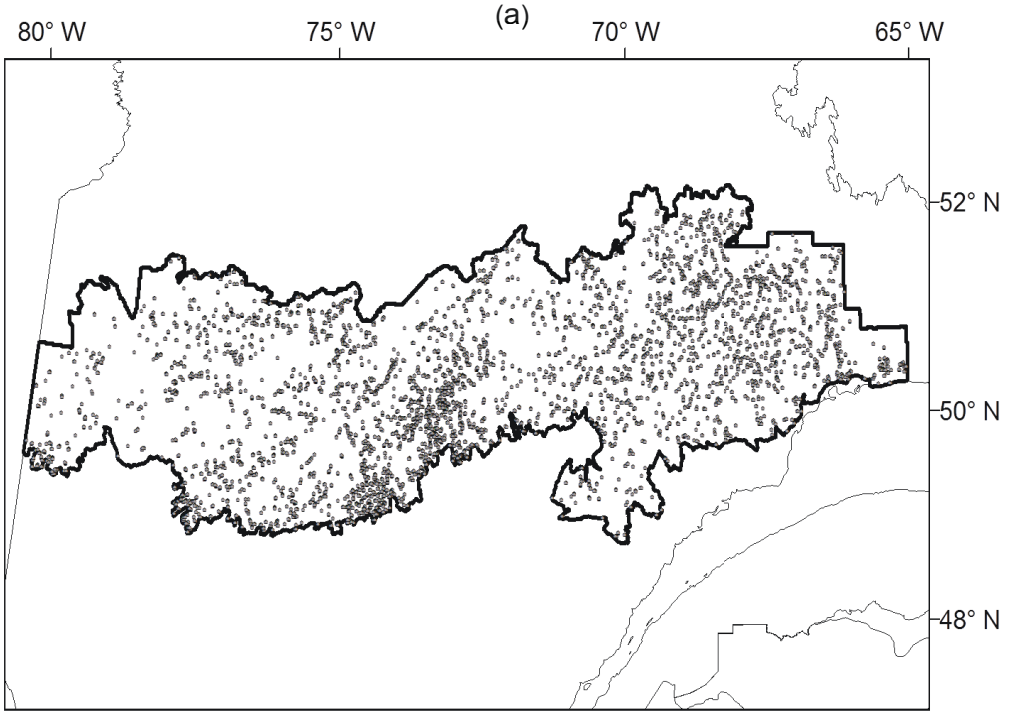

(b)

Figure 3.1. Panel a) Location of the study area (dark outline) with training areas for which time- since-last-fire was available from published studies. Panel b) Distribution of forest inventory plots used in the analysis.

For estimating ABC in relation with TSLF, we chose a scale of 2-km^2, which corresponds to the minimum fire size of the Canadian large fire database (1950-1999), as fires larger than 2 km^2 in size account for most of the burned area (Stocks et al., 2003). We consequently partitioned our study area into a square grid of 2-km^2 cells (1414 m x 1414 m, 108,477 cells). We overlaid the 2-km^2 square cells onto the SIFORT geospatial database, with an average of 14 SIFORT tile centroids per 2-km^2 cell, and estimated the within-cell relative frequencies of all SIFORT

attributes. Cells in which more than 50% of the SIFORT tile centroids were classified as water (7694 cells, 7.1% of total), wetlands and peatlands (8423 cells, 7.8% of total), heaths (4700, 4.3% of total), harvested land (9339 cells, 8.6% of total), insect-killed stands or windthrows (118 cells), and human infrastructure (38 cells) were removed, leaving 78,136 cells for the analysis of ABC (89% of forest area).

We assigned a TSLF value to each 2-km^2 cell when 50% or more of its area was covered by the fire polygon maps that were produced by SOPFEU (Société de protection des forêts contre le feu, the Quebec forest fire control agency; 9552 cells). We used fire polygons between 1970 and 2000 because the cartographic attributes of the SIFORT database correspond to the years 1990-1999. For the remaining cells, a TSLF value was assigned to cells when 50% or more of the area was covered by a known fire polygon of existing fire history maps (Fig. 3.1a, 23,289 cells). For remaining cells that lacked a TSLF value, we selected cells that had more than one forest inventory plot meeting the rules set by Bélisle et al. (2011). This process provided a TSLF value for 1393 additional cells. Overall, 34,234 cells had a TSLF value (training dataset, 43.8% of the studied dataset). For the remaining 43,092 cells (imputed dataset), predicted TSLF values (1880 to 2000, by decadal classes) were available from Irulappa Pillai Vijayakumar et al. (2015), based on the training of existing fire history information with forest maps and climate data.

3.03.03 Scaling framework

We scaled ABC estimates that were derived from plots to SIFORT tiles and, subsequently, to 2-km^2 cells along a "hierarchical scaling ladder" (Wu and David 2002) using successive models. We first trained a random forest (RF) model on plot-level ABC estimates using cartographic stand structural attributes (species composition groups, stand age classes, stand height classes, and stand cover density classes) as predictors, together with observed TSLF values that were classified into decadal classes, climatic and physical variables (surficial deposit classes, elevation and slope). This model was used to estimate ABC values at all SIFORT tile centroids that were included in the training dataset, which were then averaged within each 2-km^2 cell included in the same dataset. Using these 2-km^2 cell-level estimates of ABC, we then trained another predictive RF model, which used the within-cell relative frequencies of SIFORT attributes, a set of climate variables, and the observed TSLF values that had been classed in decadal classes as predictor variables. The resulting model was used to evaluate the importance of TSLF for predicting ABC at the scale of 2-km^2, and to estimate values of ABC within all 2-km^2 cells across the entire study region.

The RF procedure builds a multitude of classification or regression trees using a bootstrap approach that randomly selects 63% (Cutler et al., 2007) of the training dataset for each individual tree. The remaining OOB data (out-of-bag data) were used for cross-validation at each

bootstrap iteration. Tree-level predictions are combined by taking their mean, median or modal values. We found that frequency distributions (1000 trees) of predicted values were strongly skewed, on account of the tendency of estimated ABC frequency distribution being significantly skewed at the plot level. Therefore, we used the median value as the final predictor to control potential bias problems.

For this modelling exercise, predictor variables were pre-selected (initial variable selection) using the *Boruta* package (adapted from Kursa and Rudnicki, 2010) in R (Venables and Smith, 2013) with imax = 1000 (maximum number of iterations) and ntree = 1000 (number of trees). Predictor variables were also assessed for multicollinearity using Pearson product-moment (*r*) correlation coefficients with a 0.70 threshold (Dormann et al., 2013), and their ecological relevance with respect to the processes of interest (Austin, 2002). For each RF model, only six variables were retained to maintain model parsimony (Thompson and Spies, 2009). The RF procedure in R was run using the following parameter settings: ntree, the number of trees that were to be grown (1000); mtry, the number of predictor variables that were sampled for each node (the number of variables/3, i.e., 6/3); and node size, the minimum number of cases within terminal nodes (5). Further details regarding the RF procedure can be found in Cutler et al. (2007) and Timm and McGarigal (2012).

We evaluated model accuracy by computing the coefficient of determination (r^2) between predicted and observed ABC values, and the root-mean-square error (RMSE). The differences between the 95th and 5th percentiles (1000 iterations) of bootstrap-generated ABC values were divided by the predicted median value to obtain a coefficient of variation (CV,%) for each cell. Although it is not an absolute assessment of accuracy, the CV provides a relative measure of uncertainty (Saatchi et al., 2007). The difference between the 95th and 5th percentiles of ABC at each 2-km^2 cell also served as a confidence interval.

Random Forest is a non-parametric, non-spatially explicit model that does not account for spatial autocorrelation among predictors. However, residual spatial autocorrelation may point to the absence of important processes that are relevant to predictions (e.g., Dormann et al., 2007; Bahn et al., 2013). We computed Moran's I, an index of spatial autocorrelation (Moran, 1950), as a model diagnostic, calculated over a range of from 2 to 30 km in ArcGIS 10.0 (ESRI, Redlands, CA, USA). We applied a threshold criterion that the absolute index values were > 0.3 as an indicator of autocorrelation (e.g., Oliver and Webster, 1990; Hitziger et al., 2014). We checked if the mean residuals of ABC at the scale of 2-km^2 differ among data sources for the TSLF maps (Fig. 3.1a) using Analysis of variance (ANOVA) test. The R^2 value was calculated from the ANOVA table to measure the strength of relationship between the mean residuals of ABC and data sources for the TSLF maps.

3.03.04 Quantifying information loss due to scaling-up

A strategy of scaling-up that was based on predicted values from models artificially reduces data variability at coarser scales. Therefore we checked whether ignoring the prediction error of ABC values at the scale of SIFORT tiles influenced the results of model training at the 2-km^2 scale. These ABC values correspond to the median value of 1000 regression tree predictions. Instead of using these median values, we randomly sampled (with replacement) one of these predictions for each SIFORT tile within each 2-km^2 cell one thousand times to compute 1000 ABC values for each 2-km^2 cell. These values were then randomly picked for training the 2-km^2 scale RF models. The number of RF models to train at that scale was fixed to constrain the coefficient of variation (CV) of residual variance at the scale of individual 2-km^2 cells below 10%. This procedure allowed us to rate the loss of residual variation at the 2-km^2 scale by not accounting for the prediction error of predicted values at SIFORT-tile level.

3.03.05 Result synthesis and visualization

Analyzing variation in ABC as a function of TSLF is equivalent to producing ABC yield curves. The quantity of aboveground biomass that is found in a forest site is related to its productivity (Skovsgaard and Vanclay, 2008). For this reason, we regrouped ecological districts into homogeneous regions using biophysical factors that were related to forest productivity and compared ABC yield curves between these homogeneous regions. Ecological districts are landscape units (65 km^2 to 2975 km^2) of similar topography, dominant surficial deposits, drainage and climate (Robitaille and Saucier, 1996). Gauthier et al. (2015) have shown for a study area that encompassed our own that forest productivity at our regional scale is related mainly to growing season degree-days and a combination of surficial deposits and drainage.

Ecological districts were regrouped with disjoint cluster analysis (PROC FASTCLUS, SAS v9.4, SAS Institute Inc., Cary, NC, USA) as a function of their centroid degree-days and their relative abundances of marginal surficial deposit groups that are least abundant within study region (organic, stony and coarse textured and rock surficial deposits; provided by Mansuy et al., 2010). We only used marginal surficial deposit groups, because the study area was dominated (75%) by undifferentiated tills with moderate to abundant stoniness. Clustering should identify one zone with biophysical factors that are typical of the study area and marginal zones, which differ in terms of their climate or their abundance of growth-limiting surficial deposits. The optimum number of clusters was chosen with the first local maximum value of the cubic clustering criterion when plotted against the number of clusters. For each cluster, we computed frequency distributions of ABC values at the 2-km^2 scale by TSLF decade within the training dataset.

3.04 Results

3.04.01 Estimation of aboveground biomass carbon

Plot-level estimates of ABC ranged between 0.1 Mg ha^{-1} and 188.3 Mg ha^{-1} (mean, 44.5 Mg ha^{-1}). The six top-ranked variables predicting plot-level ABC were stand cover density, height classes, cover type, dominant tree age, total precipitation, and surficial deposits (Fig. 3.2a). Correlation between ABC and TSLF at the plot scale was significant, but weak (r = - 0.03, P < 0.01). The plot-level RF model explained 50% of the observed variance, while its RMSE was of 13.9 Mg ha^{-1} (Fig. 3.2b). Moran's I for the residuals of ABC indicated weak spatial autocorrelation (I = 0.05 at distances less than 20 km).

The six top-ranked variables predicting ABC at the 2-km^2 scale were relative abundance of three cover density classes (25-40%, 41-60%, 61-80%), potential evapotranspiration, growing season length, and total precipitation (Fig. 3.2d). The relative abundances of cover density classes were the most important variables explaining ABC at the 2-km^2 scale (Fig. 3.2d). Correlation between ABC and TSLF at the scale of 2-km^2 was much stronger than at the plot-level (r^2 = 0.67, r = 0.82, P < 0.01), yet TSLF was not included among the most important predictor variables. Total precipitation, potential evapotranspiration and growing season length were only weakly inter-correlated. The percentage of variance explained when predicting ABC was 83% (Fig. 3.2e), which was greater than the value of 50% that was calculated at the plot-level. Predicted values of ABC at the scale of 2-km^2 ranged from 1.2 Gg km^{-2} to 7.8 Gg km^{-2} (Fig. 3.2c). RMSE in the prediction of ABC was 0.28 Gg km^{-2}. Residuals for ABC at the scale of 2-km^2 also indicated minor spatial autocorrelation (Moran's I = 0.09 at distances less than 20 km. The mean residuals of ABC at 2-km^2 scale differ significantly among data sources for the TSLF maps (ANOVA test F value = 38.6, P < 0.001). However, the strength of relationship between them was negligible (R^2 = 0.007).

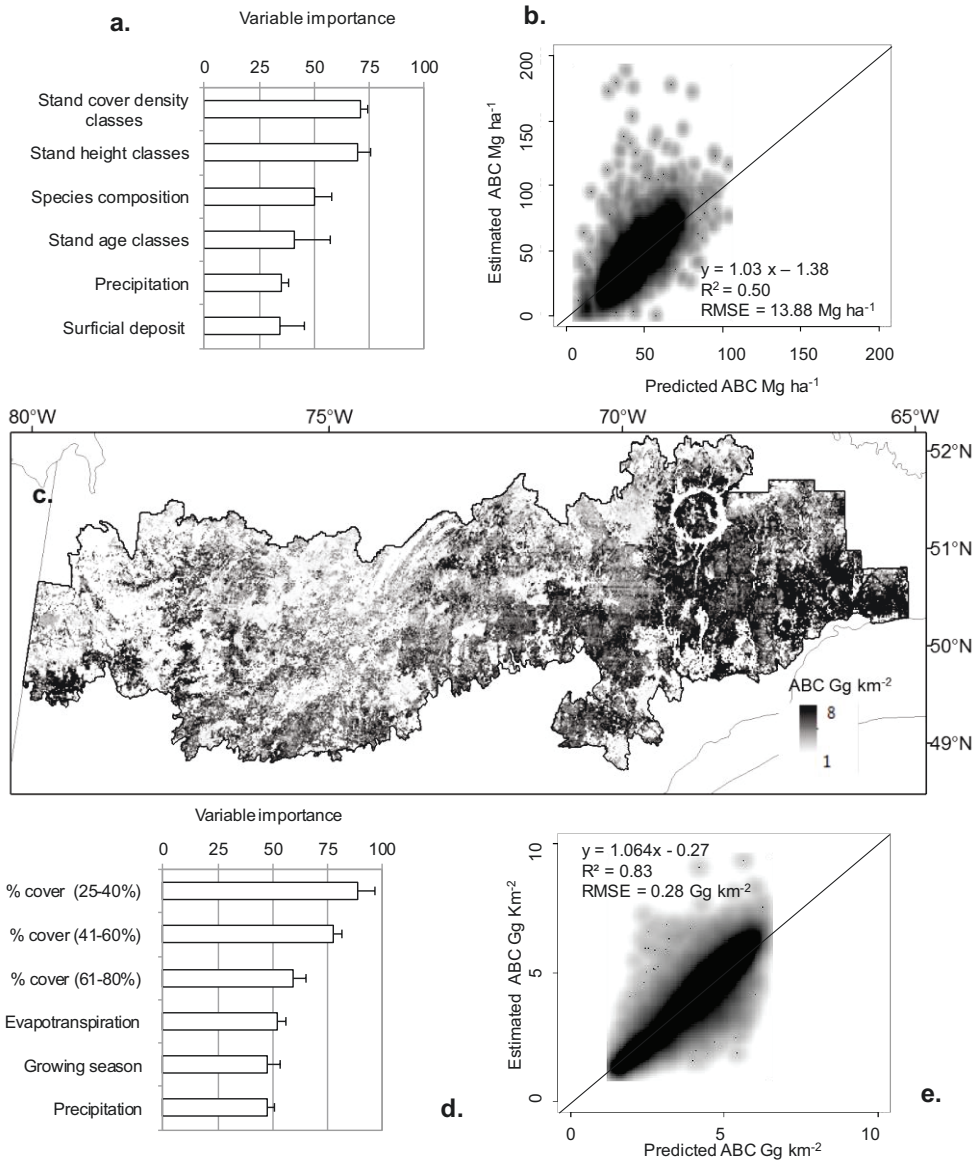

Figure 3.2. Top six variables ranked by the random forest models for the prediction of ABC at plot level (a) and at scale of 2-km^2 cells (d). Density plot of estimated ABC vs predicted ABC at plot level (b) and at 2-km^2 scale (e). c) Map of ABC predicted with RF modelling at the scale of 2 km^2.

A minimum 300 repetitions of 2-km^2 scale RF model training with randomly selected prediction values at SIFORT-tile level was necessary to achieve a CV of ABC residual variance at 2-km^2 cell scale that was below 10% (Fig. 3.3a). With this method, the percentage of variance that was explained for ABC was 82% (Fig. 3.3b), a value very close to that obtained initially (83%, Fig. 3.2e). The coefficient of determination between predictions of ABC at the 2-km^2 scale, which included or excluded the variability of predictions at the SIFORT-tile level, was 95% (Fig. 3.3c).

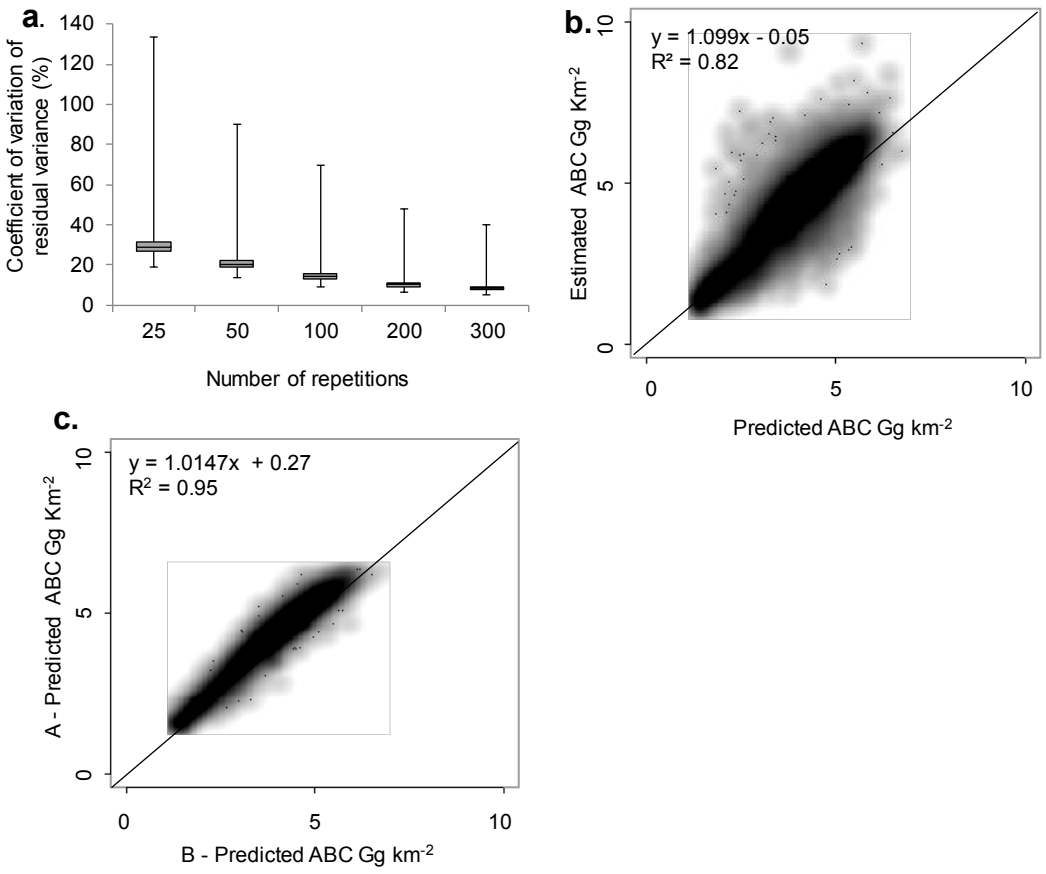

Figure 3.3. (a) Box-and-whisker plots of the coefficient of variation of residual variance for individual 2-km^2 cells as a function of the number of repetitions of RF model training for ABC prediction. (b) Density plot of estimated vs predicted ABC values at 2-km^2 scale when variability of predicted values at SIFORT tile centroid level is considered for ABC predictions. (c) Density plot of predicted values of ABC at 2-km^2 scale when variability of predicted values at SIFORT tile centroid level is considered (B) or not (A).

3.04.02 Variation of cover density and ABC yield curves at a regional scale

Important variables for explaining forest productivity at the regional scale (growing season degree-days, abundances of marginal surficial deposits) were used for a clustering analysis of landscapes (ecological districts). Partitioning the study area into three (Fig. 3.4) was optimal for creating homogenous forest productivity zones or regions that were based on the local maximum value of the cubic clustering criterion. The first zone was characterized by surficial organic deposits (> 40 cm thickness, i.e., the "organic" zone); the second zone was dominated by stony and coarse-textured deposits (the "coarse" zone). The third zone corresponded to the rest of the study area (the "typical" zone) (Table 3.1). RF models at the 2-km^2 scale indicated that the relative abundance of cover density classes are more important predictors of ABC than TSLF. We computed variation in the abundance of closed-cover stands (sum of three cover density

classes: > 81%, 61-80%, and 41-60%) as a function of TSLF for 2-km^2 scale cells in the organic, coarse and typical zones (Fig. 3.5).

ABC of 2-km^2 cells generally increases as a function of TSLF (60 to 90 years, maximum biomass stage) and later on stabilizes (coarse and typical zones, Figs. 3.5b and 3.5c) or declines in the later years (organic zone, Fig. 3.5a). Important differences in ABC values appeared to occur between the typical and the two other zones in the 30-60 year TSLF class, in relation to the abundance of closed-cover densities. Furthermore, maximum values of closed-cover density abundances were lower and achieved earlier in the organic zone when compared with the typical zone (Fig. 3.5d vs 3.5f).

Table 3-1. Mean proportions of the relative abundances of surficial deposits classes: very abundant, very coarse (VAVC); abundant, coarse (AC); rock (ROC); and organic (ORG) (Mansuy et al., 2010), and the means of degree-days by each cluster, which were used to explain homogeneity of the landscape units. Bold numbers indicate the maximum value of variables that were used for clustering (values are normalized).

Cluster name	Degree-days	AC	ROC	ORG	VAVC
Organic	**0.90**	-0.13	-0.52	**1.60**	-0.46
Coarse	-0.31	**0.14**	-0.51	-0.10	**1.70**
Typical	-0.16	-0.11	**0.29**	-0.42	-0.34

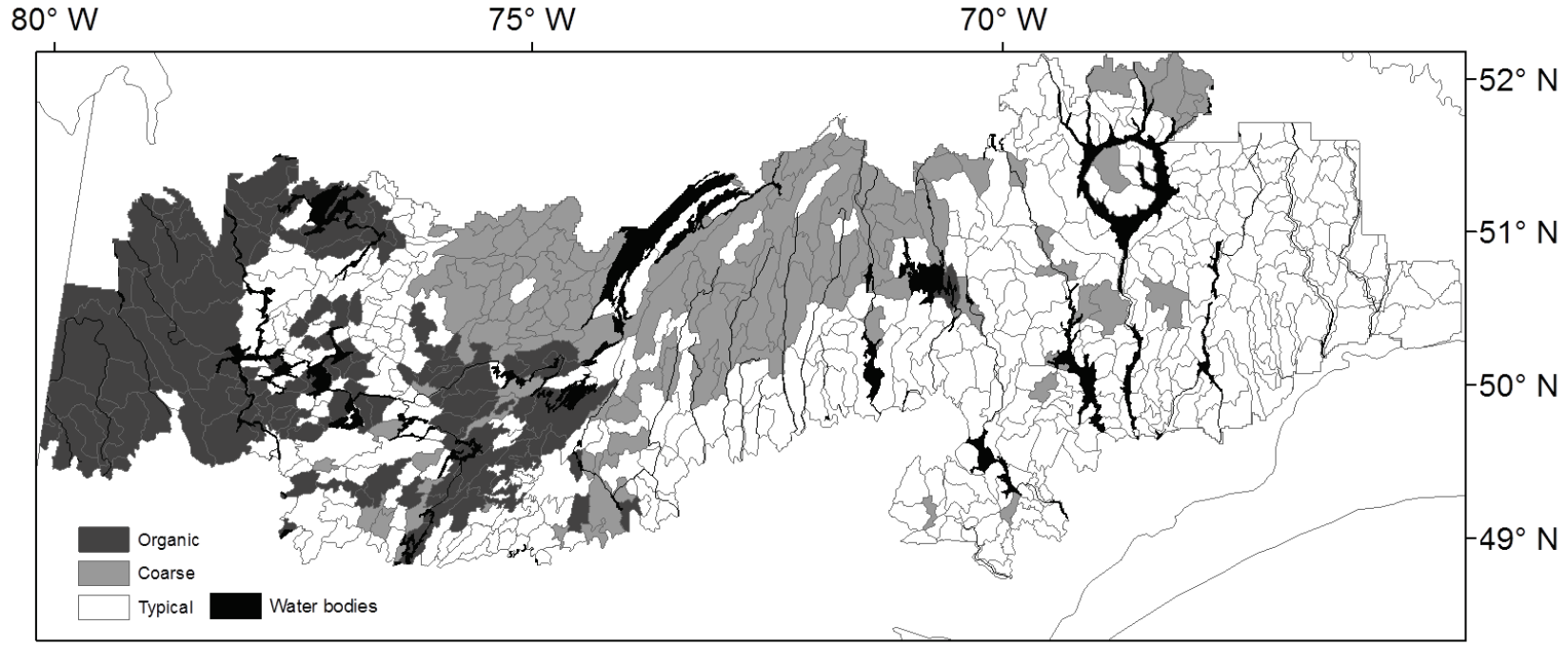

Figure 3.4. Cluster map ("organic," "coarse," and "typical" zones) of ecological districts based on centroid degree-days and their relative abundances of marginal surficial deposit groups (organic, stony and coarse-textured, and rock surficial deposits).

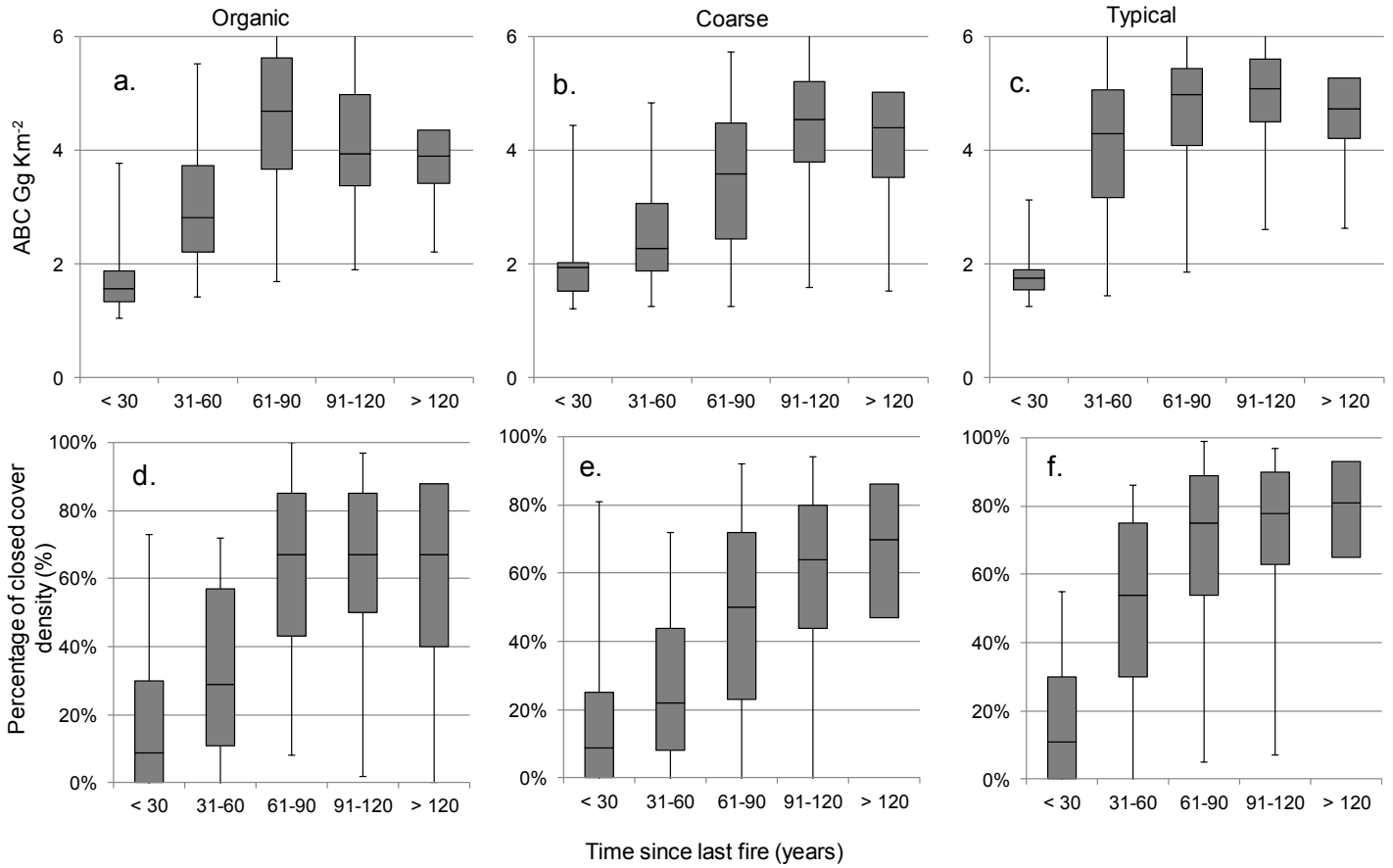

Figure 3.5. Box-and-whisker plots of ABC as a function of time-since-last-fire at 2-km^2 scale cells in "organic" (a), "coarse" (b), and "typical" (c) zones; box-and-whisker plots of the abundance of closed-density cover (> 81%, 61-80%, and 41-60%) as a function of time-since-last-fire for 2-km^2 scale cells "organic" (d), "coarse" (e), and "typical" (f) zones.

3.05 Discussion

3.05.01 Interpretation of ABC predictors at plot level

Our analysis found that cover density, stand height, species composition, tree age, total precipitation, and surficial deposits are the six best predictors of ABC at the plot level. Except for surficial deposits and precipitation, these variables are all standard inputs of growth and yield models (Weiskittel et al., 2011; Burkhart and Tomé, 2012). As forests grow over time, age should be a relatively good predictor of ABC; if height and cover density were used, they would be better predictors than age because the former normally covary with ABC, as they also account for site conditions. Surficial deposits are also an important predictor of ABC, in that they determine site drainage (e.g., Wang et al., 2003) and drying potential conditions. In contrast, TSLF was poorly correlated with ABC at the plot level ($r = -0.03$, $P < 0.01$), possibly because of a scale mismatch between plot size (400 m^2) at which scale ABC was determined, and minimum fire size (> 200 ha - Stocks et al., 2003) at which scale TSLF was estimated. Fire polygons were initially drawn at a scale that may be too coarse to accurately capture boundary features or internal zones of unburned forests in which the plots may fall. For boreal black spruce stands in the western portion of our study area, Lecomte et al. (2006) have shown that aboveground biomass at the plot level is better explained by past fire burn severity and its interaction with TSLF than by TSLF alone. Chaieb et al. (2015) similarly found that TSLF alone is not a good predictor of stand successional stages because of the interaction between succession, fire burn severity and paludification in the western part of our study region. Past fire burn severity information that is linked with fire dates is related to post-fire canopy recovery (Johnstone et al., 2010; Jin et al., 2012). Post-fire canopy recovery at the plot level is influenced, in turn, by local neighbourhood effects (Frelich and Reich, 1999). These effects may further blur the relationship between plot-level ABC and TSLF (Taylor and Chen, 2011). TSLF can be a good predictor of biomass in even-aged stands, but partial disturbances other than fire dominate when their canopy structure becomes irregular or uneven, and fluctuation in biomass might be less predictable (e.g., Bergeron and Fenton, 2012).

Alexander et al. (2012) had explained 33% of the variability in plot-level aboveground biomass with TSLF across upland boreal forests of Alaska, but their TSLF timespan was relatively short (20–59 years after fire) compared to the expected lifespan of black spruce. Wang et al. (2003) and Mack et al. (2008) also reported significant relationships between TSLF and plot-level carbon pools in the black spruce forests of western Canada and Alaska. All of these models included TSLF as the sole explanatory variable, and the significant relationships were based on a few sample plots ($n < 10$).

3.05.02 Relationship between ABC and TSLF at the 2-km^2 scale

At the 2-km^2 scale, we found a much stronger correlation between TSLF and ABC ($r^2 = 0.67$ $r = 0.82$). Nevertheless, TSLF was not selected as a strong predictor of ABC and the relative proportions of cover

density classes were the most influential variables of ABC at that scale. TSLF appears to have a significant effect on ABC values during the first decades following fire (Alexander et al., 2012), i.e., up to 60 to 90 years (Figs 3.5d-e, and also Mansuy et al., 2012: Fig. 3.6b). The effect of TSLF in the time following fire becomes much less important after 60 years at the 2-km^2 scale (Figs. 3.5a-c). These results agreed with those of Fourrier et al. (2013), who found that merchantable volume yield dynamics were controlled mainly by stand density during the first few decades following disturbance in the southeastern part of our study area.

The relative abundance of the 25-40% cover density class (open stands) was the most important predictor. Open stands or woodlands may be created when post-fire recovery is insufficient, and their presence is only partly linked to TSLF (Girard et al., 2008; Mansuy et al., 2012). Deficient post-fire canopy recovery may prevail anywhere within the black spruce forest landscape (Girard et al., 2008), but more often in pure black spruce stands (Jasinski and Payette, 2005), where it interacts with fire regime, climate and drying potential of surficial deposits (Figs. 3.2d, 3.5d-e; Simard et al., 2007; Mansuy et al., 2012).

3.05.03 Comparing accuracy with previous studies

The model r^2 (0.83) value for predicting ABC at the scale of 2-km^2 accords with those of previously published studies from remote sensing data, because of the selected spatial scale of 2 km^2. Beaudoin et al. (2014) reported an r^2 of 0.62 (vs 0.50 at plot- and 0.83 at 2-km^2 scales) for predicting aboveground biomass at a 250 x 250 m pixel size (0.06 km^2; number of training pixels, 21,037) across the forests of Canada (area, 4.0 x 10^6 km^2). Margolis et al. (2015) reported an r^2 values between 0.50 and 0.84 at plot scale (n = 565) to predict aboveground biomass across the North American boreal forest (area: 3.3 x 10^6 km^2) from the study of Neigh et al. (2013). Boudreau et al. (2008) obtained an r^2 of 0.65 at plot scale (400 m^2 plot size, n = 207) for timber-productive forests in the province of Quebec (area: 1.3 x 10^6 km^2), within which our study region is located.

Our ABC data at the 2-km^2 scale is a product of models and, therefore, may have been stripped of much of its uncontrolled randomness, reducing the range of estimates and increasing the value of r^2. With the strategy of scaling-up that we used in the present study, only 5% of variability was lost when extrapolating ABC from the plot-level to the 2-km^2 scale. Considering this additional 5% of variability in the plot-level model predictions would not have changed to any great degree the coefficient of determination between estimated and predicted values at the 2-km^2 scale.

3.05.04 Implications for C budget modelling

Studies analyzing the interaction between ABC and both TSLF (long temporal scale) and forest structure attributes at coarse scales are rare. Existing C budget models (e.g., Chen et al., 2003; 2010; Kurz et al., 2009) drive carbon dynamics with yield curves as a function of stand age, which is exact at the plot level. However, ABC at a coarser scale is not directly related to stand age and, therefore, TSLF; rather, it is

related to the speed of post-fire canopy recovery, through which TSLF exerts indirect control on ABC (Mansuy et al., 2012). ABC is related to canopy recovery (and therefore succession dynamics) at the plot level as well (e.g. Lecomte et al. 2006), but at scales coarser than the plot level, forest succession dynamics seems to be the most important ecological process dictating ABC contents.

The rate of landscape carbon accumulation over time depends upon the potential of forests to regenerate following fire, which in turn depends upon pre-fire forest conditions, TSLF, and fire severity coupled with climate (Epting et al., 2005; Johnstone and Chapin, 2006a; 2006b). The importance of post-fire vegetation recovery for estimating forest biomass is not only applicable to the eastern Canadian boreal forest, but also to the western boreal forest (Jones et al., 2013), Siberian larch forest (Berner et al., 2012), temperate forests (Pflugmacher et al., 2014), and tropical forests (Chazdon et al., 2003; Read et al., 2003), for example. Houghton (2009) and Frolking (2009) have likewise highlighted the importance of information on post-fire vegetation recovery for the assessment of global carbon dynamics. In this context, global terrestrial C budget models (e.g., Ruimy et al., 1996) should consider global monitoring of post-fire vegetation response and recovery that can be measured from satellite remote sensing data (Goetz et al., 2010). In our study region, C budget models that are currently in use (e.g., Kurz et al., 2009) should incorporate post-fire canopy recovery information, along with ABC yield curves.

3.06 Conclusion

Our objective was to test the hypothesis that TSLF is the variable controlling landscape aboveground carbon biomass. We used large datasets including fire history maps, forest maps, and forest inventory plots to quantify spatial variation of ABC in the eastern Canadian black spruce-moss forest over a large spatial extent (> 200,000 km^2) at 2-km^2 spatial resolution. We devised a modelling approach to link different spatial scales for scaling-up from inventory plots to landscapes, which provided an avenue for understanding the relative contributions of TSLF and forest structural attributes on ABC at a coarse scale. Not surprisingly, plot-level ABC is related to observed stand characteristics (height and density) and species composition. At the scale of 2-km^2, the relative abundances of cover density classes maintain control over ABC. In the eastern Canadian boreal forest, cover density increases over time through which TSLF indirectly acts upon ABC at the scale of landscapes. Our results thus illustrated the importance of post-fire canopy recovery information for assessing carbon dynamics in boreal forest ecosystems. A further study would be necessary to gain knowledge regarding the interactions of TSLF, fire severity, environmental factors and regional climate with canopy recovery after fire disturbances over large forest areas and at a coarse scale (~ 2 km^2). That scale may help address the challenge due to the variation of trajectories of post-fire forest recovery within fire perimeters that depend upon pre-fire and post-fire site conditions and the local severity of fire. Such a type of study would further serve for carbon budget models on how to incorporate post-fire canopy recovery information with ABC yield curves. Our study also

points to the importance of monitoring post-fire vegetation response and recovery to inform global carbon budget analyses.

3.07 Acknowledgements

This work was funded by the Fonds québécois de la recherche sur la nature et les technologies. We thank the Direction des inventaires forestiers, Ministère de la Forêt, de la Faune et des Parcs du Québec (MFFP), for providing access to forest inventory plots, forest maps and the SOPFEU fire history map. We thank Rémi Saint-Amant for providing the normal climate database from the 20CR project ready for BioSIM simulations and Hakim Ouzennou for help with data processing. We finally thank William (Bill) F.J. Parsons for his editorial help.

3.08 References

Alexander, H.D., Mack, M.C., Goetz, S., Beck, P.S.A., Belshe. E.F., 2012. Implications of increased deciduous cover on plot structure and aboveground carbon pools of Alaskan boreal forests. Ecosphere 3, 45. http://dx.doi.org/10.1890/ES11-00364.1.

Amiro, B.D., Logan, K.A., Wotton, B.M., Flannigan, M.D., Todd, J.B., Stocks, B.J., Martell, D.L., 2005. Fire weather index system components for large fires in the Canadian boreal forest. Int. J. Wildland Fire 13, 391–400. http://dx.doi.org/10.1071/WF03066.

Andersen, H.-E., Strunk, J., Temesgen, H., Atwood, D., Winterberger, K., 2012. Using multilevel remote sensing and ground data to estimate forest biomass resources in remote regions: a case study in the boreal forests of interior Alaska. Can. J. Remote Sens. 37, 596–611. http://dx.doi.org/10.5589/m12-003.

Austin, M.P., 2002. Spatial prediction of species distribution: an interface between ecological theory and statistical modelling. Ecol. Model. 157, 101–118. http://dx.doi.org/10.1016/S0304-3800(02)00205-3.

Bahn, V., McGill, B.J., 2013. Testing the predictive performance of distribution models. Oikos 122, 321–331. http://dx.doi.org/ 10.1111/j.1600-0706.2012.00299.x.

Balshi, M. S., McGuire, A. D., Zhuang, Q., Melillo, J., Kicklighter, D. W., Kasischke, E., Wirth, C., Flannigan, M., Harden, J., Clein. J. S., Burnside, T.J., McAllister, J., Kurz, W.A., Apps, M., Shvidenko, A., 2007. The role of historical fire disturbance in the carbon dynamics of the pan-boreal region: A process-based analysis. J. Geophys. Res.-Biogeo. 112, G02029. http://dx.doi.org/10.1029/2006JG000380.

Banfield, G.E., Bhatti, J.S., Jiang, H., Apps, M.J., 2002. Variability in regional scale estimates of carbon stocks in boreal forest ecosystems: results from West-Central Alberta. For. Ecol. Manage. 169, 15–27. http://dx.doi.org/10.1016/S0378-1127(02)00292-X.

Bélisle, A.C., Gauthier, S., Cyr, D., Bergeron, Y., Morin, H., 2011. Fire regime and old-growth boreal forests in central Québec, Canada: an ecosystem management perspective. Silva Fenn. 45, 77. http://dx.doi.org/10.14214/sf.77

Beaudoin, A., Bernier, P.Y., Guindon, L., Villemaire, P., Guo, X.J., Stinson, G., Bergeron, T., Magnussen, S., Hall, R.J., 2014. Mapping attributes of Canada's forests at moderate resolution through *k*NN and MODIS imagery. Can. J. For. Res. 44, 521–532. http://dx.doi.org/10.1139/cjfr-2013-0401.

Bergeron, Y., Gauthier, S., Flannigan, M., Kafka, V.G., 2004. Fire regimes at the transition between mixedwood and coniferous boreal Forest in Northwestern Quebec. Ecology 85, 1916–1932. http://dx.doi.org/10.1890/02-0716.

Bergeron, Y., Fenton, N.J., 2012. Boreal forests of eastern Canada revisited: old growth, nonfire disturbances, forest succession, and biodiversity. Botany 90, 509–523. http://dx.doi.org/10.1139/b2012-034.

Berner, L.T., Beck, P.S.A., Loranty, M.M., Alexander, H.D., Mack, M.C., Goetz, S.J., 2012. Cajander larch (*Larix cajanderi*) biomass distribution, fire regime and post-fire recovery in northeastern Siberia. Biogeosciences 9, 3943–3959. http://dx.doi.org/10.5194/bg-9-3943-2012.

Bouchard, M., Pothier, D., 2011. Long-term influence of fire and harvesting on boreal forest age structure and forest composition in eastern Québec. For. Ecol. Manage. 261, 811–820. http://dx.doi.org/10.1016/j.foreco.2010.11.020.

Bouchard, M., Pothier, D., Gauthier, S., 2008. Fire return intervals and tree species succession in the North Shore region of eastern Quebec. Can. J. For. Res. 38, 1621–1633. http://dx.doi.org/10.1139/X07-201.

Boudreau, J., Nelson, R.F., Margolis, H.A., Beaudoin, A., Guindon, L., Kimes, D.S., 2008. Regional aboveground forest biomass using airborne and spaceborne LiDAR in Québec. Remote Sens. Environ. 112, 3876–3890. http://dx.doi.org/10.1016/j.rse.2008.06.003

Buech, R.R., Rugg, D.J., 1989. Biomass relations of shrub components and their generality. For. Ecol. Manage. 26, 257–264. http://dx.doi.org/10.1016/0378-1127(89)90086-8

Burkhart, H.E., Tomé, M., 2012. Modeling Forest Trees and Stands. Springer Science & Business Media.

Chaieb, C., Fenton, N.J., Lafleur, B., Bergeron, Y., 2015. Can we use forest inventory mapping as a coarse filter in ecosystem based management in the black spruce boreal forest? Forests 6, 1195–1207. http://dx.doi.org/10.3390/f6041195.

Chazdon, R.L., 2003. Tropical forest recovery: legacies of human impact and natural disturbances. Perspect. Plant Ecol. Evol. Syst. 6, 51–71. http://dx.doi.org/10.1078/1433-8319-00042.

Chen, H.Y.H., Luo, Y., 2015. Net aboveground biomass declines of four major forest types with forest ageing and climate change in western Canada's boreal forests. Glob. Change Biol., in press. http://dx.doi.org/10.1111/gcb.12994.

Chen, J., Colombo, S.J., Ter-Mikaelian, M.T., Heath. L.S., 2010. Carbon budget of Ontario's managed forests and harvested wood products, 2001–2100. For. Ecol. Manage. 259, 1385–1398. http://dx.doi.org/10.1016/j.foreco.2010.01.007.

Chen, J.M., Ju, W., Cihlar, J., Price, D.T, Liu, J., Chen, W., Pan, J., Black, T.A., Barr, A.G., 2003. Spatial distribution of carbon sources and sinks in Canada's forests. Tellus Ser. B 55, 622–641. http://dx.doi.org/10.1034/j.1600-0889.2003.00036.x

Compo, G.P., Whitaker, J.S., Sardeshmukh, P.D., Matsui, N., Allan, R.J., Yin, X., Gleason, B.E., Vose, R.S., Rutledge, G., Bessemoulin, P., Brönnimann, S., Brunet, M., Crouthamel, R.I., Grant, A.N., Groisman, P.Y., Jones, P.D., Kruk, M.C., Kruger, A.C., Marshall, G.J., Maugeri, M., Mok, H.Y., Nordli, Ø., Ross, T.F., Trigo, R.M., Wang, X.L., Woodruff, S.D., Worley, S.J., 2011. The twentieth century reanalysis project. Q. J. Roy. Meteorol. Soc. 137, 1–28. http://dx.doi.org/10.1002/qj.776.

Cutler, D.R., Edwards Jr., T.C., Beard, K.H., Cutler, A., Hess, K.T., Gibson, J., Lawler, J.J., 2007. Random forests for classification in ecology. Ecology 88, 2783–2792. http://dx.doi.org/10.1890/07-0539.1.

Cyr, D., Gauthier, S., Bergeron. Y., 2007. Scale-dependent determinants of heterogeneity in fire frequency in a coniferous boreal forest of eastern Canada, Landscape Ecol. 22, 1325–1339. http://dx.doi.org/10.1007/s10980-007-9109-3.

Dormann, C.F., Elith, J., Bacher, S., Buchmann, C., Carl, G., Carré, G., Garcia Marquéz, J.R., Gruber, B., Lafourcade, B., Leitão, P.J., Münkemüller, T., McClean, C., Osborne, P.E., Reineking, B., Schröder, B., Skidmore, A.K., Zurell, D., Lautenbach, S., 2013. Collinearity: a review of methods to deal with it and a simulation study evaluating their performance. Ecography, 36, 27–46.

Dormann, C.F., McPherson, J.M., Araújo, M.B., Bivand, R., Bolliger, J., Carl, G., Davies, R.G., Hirzel, A., Jetz, W., Kissling, W.D., Kühn, I., Ohlemüller, R., Peres-Neto, P.R., Reineking, B., Schröder, B., Schurr, F.M., Wilson, R., 2007. Methods to account for spatial autocorrelation in the analysis of species distributional data: a review. Ecography 30, 609–628. http://dx.doi.org/10.1111/j.2007.0906-7590.05171.x.

Dunne, T., Leopold, L. B., 1978. Water in Environmental Planning. 1st ed. W.H. Freeman & Company, New York. pp. 566–580.

Epting, J., Verbyla, D., 2005. Landscape-level interactions of prefire vegetation, burn severity, and postfire vegetation over a 16-year period in interior Alaska. Can. J. For. Res. 35, 1367–1377. http://dx.doi.org/10.1139/x05-060.

Fourrier, A., Pothier, D., Bouchard, M., 2013. A comparative study of long-term stand growth in eastern Canadian boreal forest: Fire versus clear-cut. For. Ecol. Manage. 310, 10–18. http://dx.doi.org/10.1016/j.foreco.2013.08.011.

Frelich, L.E., Reich, P.B., 1999. Neighborhood effects, disturbance severity, and community stability in forests. Ecosystems 2, 151–166. http://dx.doi.org/10.1007/s100219900066.

Frolking, S., Palace, M.W., Clark, D.B., Chambers, J Q., Shugart, H.H., Hurtt, G.C., 2009. Forest disturbance and recovery: A general review in the context of spaceborne remote sensing of impacts on aboveground biomass and canopy structure. J. Geophys. Res.-Biogeo. 114, G2. http://dx.doi.org/10.1029/2008JG000911.

Fullerton, D.S., Bush, C.A., Pennell, J.N., 2003. Map of surficial deposits and materials in the eastern and central United States (east of 102 degrees west longitude). US Department of the Interior and US Geological Survey, Washington, D.C. <http://pubs.usgs.gov/imap/i-2789/i-2789_p.pdf> (accessed 07.10.2015).

Garet, J., Raulier, F., Pothier, D., Cumming. S.G., 2012. Forest age class structures as indicators of sustainability in boreal forest: Are we measuring them correctly? Ecol. Indic. 23, 202–210. http://dx.doi.org/10.1016/j.ecolind.2012.03.032.

Gauthier, S., Raulier, F., Ouzennou, H., Saucier, J.P., 2015.Strategic analysis of forest vulnerability to risk related to fire: an example from the coniferous boreal forest of Quebec. Can. J. For. Res. 45, 553–565. http://dx.doi.org/10.1139/cjfr-2014-0125.

Girard, F., Payette, S., Gagnon, R., 2008. Rapid expansion of lichen woodlands within the closed-crown boreal forest zone over the last 50 years caused by stand disturbances in eastern Canada. J. Biogeogr. 35, 529–537. http://dx.doi.org/10.1111/j.1365-2699.2007.01816.x.

Girardin, M.P., Guo, X J., Bernier, P.Y., Raulier, F., Gauthier, S., 2012. Changes in growth of pristine boreal North American forests from 1950 to 2005 driven by landscape demographics and species traits. Biogeosci. Discuss. 9, 1021–1053. http://dx.doi.org/10.5194/bg-9-2523-2012.

Goetz, S. J., Sun, M., Baccini, A., Beck, P. S. A., 2010. Synergistic use of spaceborne lidar and optical imagery for assessing forest disturbance: An Alaska case study. J. Geophys. Res.-Biogeo. 115, G2. http://dx.doi.org/10.1029/2008JG000898.

Gower, S.T., Vogel, J.G., Norman, J.M., Kucharik, C.J., Steele, S.J., Stow, T.K., 1997. Carbon distribution and aboveground net primary production in aspen, jack pine, and black spruce stands in Saskatchewan and Manitoba, Canada. J. Geophys. Res. 102(D24), 29029–29041. http://dx.doi.org/10.1029/97JD02317.

Grant, R.F., 2004. Modeling topographic effects on net ecosystem productivity of boreal black spruce forests. Tree Physiol. 24, 1–18. http://dx.doi.org/10.1093/treephys/24.1.1.

Harden, J.W., Trumbore, S.E., Stocks, B.J., Hirsch, A., Gower, S.T., O'neill, K.P., Kasischke, E.S., 2000. The role of fire in the boreal carbon budget. Glob. Change Biol. 6, 174–184. http://dx.doi.org/10.1046/j.1365-2486.2000.06019.x.

Hitziger, M., Ließ, M., 2014. Comparison of three supervised learning methods for digital soil mapping: Application to a complex terrain in the Ecuadorian Andes. Applied and Environmental Soil Science 2014, Article ID 809495. http://dx.doi.org/10.1155/2014/809495.

Houghton, R.A., 2003. Why are estimates of the terrestrial carbon balance so different? Glob. Change Biol. 9, 500–509. http://dx.doi.org/10.1046/j.1365-2486.2003.00620.x.

Houghton, R.A., 2005. Aboveground forest biomass and the global carbon balance. Glob. Change Biol. 11, 945–958. http://dx.doi.org/10.1111/j.1365-2486.2005.00955.x.

Houghton, R.A., Hall, F., Goetz, S.J., 2009. Importance of biomass in the global carbon cycle. J. Geophys. Res.-Biogeo. 114, G00E03. http://dx.doi.org/10.1029/2009JG000935.

Irulappa Pillai Vijayakumar, D. B., Raulier, F., Bernier, P. Y., Gauthier, S., Bergeron, Y., Pothier, D., 2015. Lengthening the historical records of fire history over large areas of boreal forest in eastern Canada using empirical relationships. For. Ecol. Manage. 347, 30–39. http://dx.doi.org/10.1016/j.foreco.2015.03.011

Jasinski, J.P., Payette, S., 2005. The creation of alternative stable states in the southern boreal forest, Quebec, Canada. Ecol. Monogr. 75, 561–583. http://dx.doi.org/10.1890/04-1621.

Jenkins, J.C., Chojnacky, D.C., Heath, L.S., Birdsey, R.A., 2004. Comprehensive database of diameter-based biomass regressions for North American tree species. USDA Forest Service, Northeastern Research Station, Newton Square, PA. General Technical Report NE-319. 45 pp. http://svinet2.fs.fed.us/ne/durham/4104/ papers/ne_gtr319_jenkins_and_others.pdf (accessed 19 August 2014)

Jin, Y., Randerson, J.T., Goetz, S.J., Beck, P.S., Loranty, M.M., Goulden, M.L., 2012. The influence of burn severity on postfire vegetation recovery and albedo change during early succession in North American boreal forests. J. Geophys. Res.-Biogeo. 117, G01036. http://dx.doi.org/10.1029/2011JG001886.

Johnstone, J.F., Chapin III, F.S., 2006a. Effects of soil burn severity on post-fire tree recruitment in boreal forest. Ecosystems 9, 14–31. http://dx.doi.org/10.1007/s10021-004-0042-x.

Johnstone, J.F., Chapin III, F.S., 2006b. Fire interval effects on successional trajectory in boreal forests of northwest Canada. Ecosystems 9, 268–277, http://dx.doi.org/10.1007/s10021-005-0061-2.

Johnstone, J.F., Hollingsworth, T.N., Chapin III, F.S., Mack, M.C., 2010. Changes in fire regime break the legacy lock on successional trajectories in Alaskan boreal forest. Glob. Change Biol. 16, 1281–1295. http://dx.doi.org/10.1111/j.1365-2486.2009.02051.x.

Jones, M. O., Kimball, J. S., Jones, L. A., 2013. Satellite microwave detection of boreal forest recovery from the extreme 2004 wildfires in Alaska and Canada. Glob. Change Biol. 19, 3111–3122. http://dx.doi.org/10.1111/gcb.12288.

Kursa, M.B, Rudnicki, W.R., 2010. Feature selection with the Boruta package. J. Stat. Softw. 36, 1–13. <http://www.jstatsoft.org/v36/i11>

Kurz, W.A., Dymond, C.C., White, T.M., Stinson, G., Shaw, C.H., Rampley, G.J., Smyth, C.E., Simpson, B.N., Neilson, E.T., Trofymow, J.A., Metsatanta, J.M., Apps, M.J., 2009. CBM-CFS3: A model of carbon-dynamics in forestry and land-use change implementing IPCC standards. Ecol. Model. 220, 480–504. http://dx.doi.org/10.1016/j.ecolmodel.2008.10.018.

Lambert, M.C., Ung, C.-H., Raulier. F., 2005. Canadian national tree aboveground biomass equations. Can. J. For. Res. 35, 1996–2018. http://dx.doi.org/10.1139/x05-112.

Landsberg, J., 2003. Modelling forest ecosystems: State of the art, challenges, and future directions. Can. J. For. Res. 33, 385–397. http://dx.doi.org/10.1139/x02-129.

Lecomte, N., Simard, M., Fenton, N., Bergeron, Y., 2006. Fire severity and long-term ecosystem biomass dynamics in coniferous boreal forests of eastern Canada. Ecosystems 9, 1215–1230. http://dx.doi.org/10.1007/s10021-004-0168-x.

Le Goff, H., Flannigan, M.D., Bergeron, Y., Girardin, M.P., 2007. Historical fire regime shifts related to climate teleconnections in the Waswanipi area, central Quebec, Canada. Int. J. Wildland Fire 16, 607–618. http://dx.doi.org/10.1071/WF06151.

Lesieur, D., Gauthier, S., Bergeron, Y., 2002. Fire frequency and vegetation dynamics for the south-central boreal forest of Quebec, Canada. Can. J. For. Res. 32, 1996–2009. http://dx.doi.org/10.1139/x02-113.

Mack, M.C., Treseder, K.K., Manies, K.L., Harden, J.W., Schuur, E.A., Vogel, J.G., Randerson, J.T., Chapin III, F.S., 2008. Recovery of aboveground plant biomass and productivity after fire in mesic and dry black spruce forests of interior Alaska. Ecosystems 11, 209–225. http://dx.doi.org/10.1007/s10021-007-9117-9.

Magnani, F., Mencuccini, M., Borghetti, M., Berbigier, P., Berninger, F., Delzon, S., Grelle, A., Hari, P., Jarvis, P.G., Kolari, P., Kowalski, A.S., Lankreijer, H., Law, B.E., Lindroth, A., Loustau, D., Manca, G., Moncrieff, J.B., Rayment, M., Tedeschi, V., Valentini, R., Grace, J., 2007. The human footprint in the carbon cycle of temperate and boreal forests. Nature 447, 849–851. http://dx.doi.org/10.1038/nature05847.

Mäkelä, A., Landsberg, J., Ek, A.R., Burk, T.E., Ter-Mikaelian, M., Ågren, G.I., Oliver, C.D., Puttonen, P., 2000. Process-based models for forest ecosystem management: current state of the art and challenges for practical implementation. Tree Physiol. 20, 289–298. http://dx.doi.org/10.1093/treephys/20.5-6.289.

Malhi, Y., 2012. The productivity, metabolism and carbon cycle of tropical forest vegetation. J. Ecol. 100, 65–75. http://dx.doi.org/10.1111/j.1365-2745.2011.01916.x.

Malhi, Y., Grace. J., 2000. Tropical forests and atmospheric carbon dioxide. Trends Ecol. Evol. 15, 332–337. http://dx.doi.org/10.1016/S0169-5347(00)01906-6.

Mansuy, N., Gauthier, S., Robitaille, A., Bergeron, Y., 2010. The effects of surficial deposit–drainage combinations on spatial variations of fire cycles in the boreal forest of eastern Canada. Int. J. Wildland Fire 19, 1083–1098. http://dx.doi.org/10.1071/WF09144.

Mansuy, N., Gauthier, S., Robitaille, A., Bergeron, Y., 2012. Regional patterns of postfire canopy recovery in the northern boreal forest of Quebec: interactions between surficial deposit, climate, and fire cycle. Can. J. For. Res. 42, 1328–1343. http://dx.doi.org/10.1139/x2012-101.

Margolis, H. A., Nelson, R. F., Montesano, P. M., Beaudoin, A., Sun, G., Andersen, H. E., Wulder, M., 2015. Combining satellite lidar, airborne lidar and ground plots to estimate the amount and distribution of aboveground biomass in the boreal forest of North America. Can. J. For. Res. 45, 838–855. http://dx.doi.org/10.1139/cjfr-2015-0006.

Melillo, J.M., Steudler, P.A., Aber, J.D., Newkirk, K., Lux, H., Bowles, F.P., Catricala, C., Magill, A., Ahrens, T., Morrisseau. S., 2002. Soil warming and carbon-cycle feedbacks to the climate system. Science 298, 2173–2176. http://dx.doi.org/10.1126/science.1074153.

Moran, P.A.P., 1950. Notes on continuous stochastic phenomena. Biometrika, 37, 17–23.

Neigh, C.S.R., Nelson, R.F., Ranson, K.J., Margolis, H.A., Montesano, P.M., Sun, G., Kharuk,V., Naesset, E., Wulder, M., Andersen, H.-E., 2013. Taking stock of circumboreal forest carbon with ground measurements, airborne and spaceborne LiDAR. Remote Sens. Environ. 137, 274–287. http://dx.doi.org/10.1016/j.rse.2013.06.019.

Oliver, M.A., Webster, R., 1990. Kriging: a method of interpolation for geographical information systems. Int. J. Geogr. Inf. Syst. 4, 313–332. http://dx.doi.org/10.1080/02693799008941549.

Pan, Y., Birdsey, R.A., Fang, J., Houghton, R., Kauppi, P.E., Kurz, W.A., Phillips, O.L., Shvidenko, A., Lewis, S.L., Canadell, J.G., Ciais, P., Jackson, R.B., Pacala, S.W., McGuire, A.D., Piao, S., Rautiainen, A., Sitch, S., Hayes, D., 2011a. A large and persistent carbon sink in the world's forests. Science333, 988–993. http://dx.doi.org/10.1126/science.1201609.

Pan, Y., Chen, J.M., Birdsey, R., McCullough, K., He, L., Deng, F., 2011b. Age structure and disturbance legacy of North American forests. Biogeosciences 8, 715–732. http://dx.doi.org/10.5194/bg-8-715-2011.

Pelletier, G., Dumont, Y., Bédard, M., 2007. SIFORT: Système d'Information FORestière par Tesselle, Manuel de l'usager. Ministère des Ressources naturelles et de la Faune du Québec. Québec, QC, Canada. https://www.mffp.gouv.qc.ca/ publications/forets/fimaq/usager.pdf. (accessed on 2 October 2014)

Pflugmacher, D., Cohen, W.B., Kennedy, R.E., Yang, Z., 2014. Using Landsat-derived disturbance and recovery history and lidar to map forest biomass dynamics. Remote Sens. Environ. 151, 124–137. http://dx.doi.org/10.1016/j.rse.2013.05.033.

Pregitzer, K.S., Euskirchen. E.S., 2004. Carbon cycling and storage in world forests: biome patterns related to forest age. Glob. Change Biol. 10, 2052–2077. http://dx.doi.org/10.1111/j.1365-2486.2004.00866.x

Régnière, J., St-Amant, R., 2008. BioSIM 9 user's manual. Natural Resources Canada, Canadian Forest Service, Laurentian Forestry Centre, Quebec, QC, Canada. Information Report LAU-X-134E. <https://cfs.nrcan.gc.ca/ publications?id=28768>(accessed 7 October 2014)

Read, L., Lawrence, D., 2003. Recovery of biomass following shifting cultivation in dry tropical forests of the Yucatan. Ecol. Appl. 13, 85–97. http://dx.doi.org/10.1890/1051-0761(2003)013[0085:ROBFSC]2.0.CO;2.

Robitaille, A., Saucier, J.-P., 1996. Land district, ecophysiographic units and areas: The landscape mapping of the Ministère des Ressources Naturelles du Québec. Environ. Monit. Assess. 39, 127–148. http://dx.doi.org/10.1007/BF00396141.

Robitaille, A., Saucier, J.-P., 1998. Paysages régionaux du Québec méridional. Direction de la gestion des stocks forestiers et Direction des relations publiques, ministère des Ressources naturelles du Québec. Les publications du Québec, Québec.

Ruimy, A., Kergoat, L., Field, C.B., Saugier, B., 1996. The use of CO_2 flux measurements in models of the global terrestrial carbon budget. Glob. Change Biol. 2, 287–296. http://dx.doi.org/10.1111/j.1365-2486.1996.tb00080.x.

Saatchi, S.S., Houghton, R.A., Dos Santos Alvala, R.C., Soares, J.V., Yu, Y., 2007. Distribution of aboveground live biomass in the Amazon basin. Glob. Change Biol. 13, 816-837. http://dx.doi.org/10.1111/j.1365-2486.2007.01323.x.

Simard, M., Lecomte, N., Bergeron, Y., Bernier, P.Y., Paré, D., 2007. Forest productivity decline caused by successional paludification of boreal soils. Ecol. Appl. 17, 1619–1637. http://dx.doi.org/10.1890/06-1795.1.

Stinson, G., Kurz, W.A., Smyth, C.E., Neilson, E.T., Dymond, C.C., Metsaranta, J.M., Boisvenue, C., Rampley, G.J., Li, Q., White, T.M., Blain, D., 2011. An inventory-based analysis of Canada's managed forest carbon dynamics, 1990 to 2008. Glob. Change Biol. 17, 2227–2244. http://dx.doi.org/10.1111/j.1365-2486.2010.02369.x.

Stocks, B. J., Mason, J. A., Todd, J. B., Bosch, E. M., Wotton, B. M., Amiro, B. D., Flannigan, M. D., Hirsch, K. G., Logan, K. A., Martell, D. L., 2003. Large forest fires in Canada, 1959-1997. J. Geophys. Res. 108 (D1), 8149. http://dx.doi.org/10.1029/2001JD000484.

Skovsgaard, J.P., Vanclay, J.K., 2008. Forest site productivity: a review of the evolution of dendrometric concepts for even-aged stands. Forestry81, 13–31. http://dx.doi.org/10.1093/forestry/cpm041.

Taylor, A.R., Chen, H.Y.H., 2011. Multiple successional pathways of boreal forest plots in central Canada. Ecography34, 208–219. http://dx.doi.org/10.1111/j.1600-0587.2010.06455.x.

Taylor, A.R., Chen, H.Y.H., VanDamme, L., 2009. A review of forest succession models and their suitability for forest management planning. For. Sci. 55, 23–36.

Ter-Mikaelian, M.T., Korzukhin, M.D., 1997. Biomass equations for sixty-five North American tree species. For. Ecol. Manage. 97, 1–24. http://dx.doi.org/10.1016/S0378-1127(97)00019-4.

Thompson, J.R., Spies, T.A., 2009. Vegetation and weather explain variation in crown damage within a large mixed-severity wildfire. For. Ecol. Manage. 258, 1684–1694. http://dx.doi.org/10.1016/j.foreco.2009.07.031.

Timm, B.C., McGarigal, K., 2012. Fine-scale remotely-sensed cover mapping of coastal dune and salt marsh ecosystems at Cape Cod National Seashore using Random Forests. Remote Sens. Environ. 127, 106–117. http://dx.doi.org/10.1016/j.rse.2012.08.033.

Ung, C.H., Bernier, P., Guo, X.-J., 2008. Canadian national biomass equations: new parameter estimates that include British Columbia data. Can. J. For. Res. 38, 1123–1132. http://dx.doi.org/10.1139/X07-224.

Van Zyl, J.J., 2001. The Shuttle Radar Topography Mission (SRTM): a breakthrough in remote sensing of topography. Acta Astronaut. 48, 559–565. http://dx.doi.org/10.1016/S0094-5765(01)00020-0.

Venables, W. N., Smith, D. M., 2013. the R Core Team. An Introduction to R. Version 2.

Wang, C., Bond-Lamberty, B., Gower. S.T., 2003. Carbon distribution of a well- and poorly-drained black spruce fire chronosequence. Glob. Change Biol. 9, 1066–1079. http://dx.doi.org/10.1046/j.1365-2486.2003.00645.x.

Weiskittel, A.R., Hann, D.W., Kershaw Jr., J.A., Vanclay, J.K., 2011. Forest Growth and Yield Modeling. John Wiley & Sons.

Wu, J., David, J.L., 2002. A spatially explicit hierarchical approach to modeling complex ecological systems: theory and applications. Ecol. Model. 153, 7–26. http://dx.doi.org/10.1016/S0304-3800(01)00499-9.

4. Chapter 3: Fire disturbance history improves the consistency of remotely sensed aboveground biomass estimates for boreal forests in eastern Canada

Dinesh Babu Irulappa Pillai Vijayakumar, Frédéric Raulier, Pierre Bernier, Sylvie Gauthier, Yves Bergeron, David Pothier

Manuscript under preparation

4.01 Abstract

Fire is an important driver of boreal forest succession dynamics in North America and time since last fire (TSLF) is seen as a useful variable to explain successional change and subsequently aboveground biomass (AGB). Accurate estimation of AGB using remote sensing data is still challenging and an approach based on an understanding of forest disturbance and succession could help improve AGB estimation. Within a large study area (> 200 000 km^2) located in the northeastern American boreal forest, we compared remotely sensed biomass estimates of MODIS (Moderate Resolution Imaging Spectroradiometer), GLAS (Geoscience Laser Altimeter System) and ASAR (Advanced Synthetic Aperture Radar) with inventory-based estimates derived from ground plots, and forest maps. This comparison was made at a spatial scale of 2-km^2, which corresponds to the minimum size for fires to be considered important enough and included in the Canadian large fire database. Large fires play a determinant role on the landscape mosaic in these forests. We identified that TSLF could explain the differences between MODIS (45%), GLAS (47%) or ASAR (23%) and inventory based estimates, when associated with surficial geological substrate information at that scale. Our results therefore showed the importance of generating maps of TSLF to serve as a potential ancillary variable for improving the accuracy of remotely sensed AGB estimates in North American boreal forests. We also demonstrated the effectiveness of scaling up remotely sensed data to a scale at which disturbances tend to occur for integrating fire history information.

Keywords: Aboveground biomass; boreal forests; remote sensing; successional dynamics; MODIS; GLAS; ASAR

4.02 Introduction

Forested biomes cover approximately 3.7 billion ha (FAO, 2015), and accordingly play a major role in the global carbon (C) cycle. Tropical forests store about 55% of total (861 ± 66 Pg, including in soil (to 1-m depth) and in live biomass: above and below ground) C stocks in comparison to 32 % and 14% for boreal and temperate forests, respectively (Pan et al., 2011). In a recent study, Bradshaw et al. (2015) reported total carbon stocks of 367.3 to 1715.8 Pg (mid-point = 1095 Pg), which are about 3.8 times those estimated by Pan et al. (2011) for boreal forests. These considerable differences indicate that improvements are still required to improve the accuracy of C stock estimates. In tropical forests, deforestation is the main cause for changes in C stocks, but natural disturbances remain the main driver in temperate and boreal forests (Houghton 2005). It follows that trajectories of forest recovery patterns after disturbance play a key role in both regional and global C budgets (Frolking et al., 2009) and may adequately help for C stocks estimations (Irulappa Pillai Vijayakumar et al., 2016). Information on aboveground biomass (AGB) is used for assessing the contribution of forest ecosystems to the global C budget (McGuire, 2002), for assessing forest ecosystem productivity (Malhi, 2012), or for supporting bioenergy production (Mansuy et al., 2015).

The remotely sensed spatial distribution of AGB is estimated through the correlation that exists between remote-sensing reflectance data at the pixel scale with field measurements of biomass using allometric equations or biomass expansion factors. For example, Thurner et al. (2014) applied a biomass retrieval algorithm called BIOMASAR (Santoro et al., 2011) to ENVISAT (Environment Satellite) Advanced Synthetic Aperture Radar (ASAR) data to obtain a carbon density map for northern boreal and temperate forests across the Northern Hemisphere. Beaudoin et al. (2014) used the Moderate Resolution Imaging Spectroradiometer (MODIS) to map forest attributes, including AGB, across Canada's forests with a non-parametric model that had been calibrated from a systematic grid of photo-plots that were established and maintained by Canada's National Forest Inventory (Gillis et al., 2005). Optical multispectral remote sensing data (e.g. MODIS) are not physically related to AGB because canopy reflectance is more related to leaf area index and canopy cover (Le Toan et al., 2011). Radar measurements are physically related to AGB for their ability to penetrate forest canopy (Kasischke et al., 1997), but their penetration capability depends on the radar wavelength. Radar measurements are acquired in K, X, C, L and P bands (different wavelengths) and their penetration capability increases with wavelength (Dobson et al., 1992). Short-wavelength X- or C-band cannot penetrate into canopy and interacts principally with canopy cover elements. In contrast, long-wavelength P-band has stronger penetration capability capturing vertical structure information and is accordingly highly sensitive to AGB estimation (Saatchi et al., 2011a). Ongoing planning is underway for the launch of European Space Agency P-band BIOMASS radar satellite that appears to be the only sensor capable of providing both AGB and height measurements (Le Toan et al., 2011). Optical multispectral imagery and short-wavelength radar data (e.g. C-band ENVISAT ASAR) are limited by saturation when estimating biomass in regions of high biomass and complex canopy

structures (Turner et al., 1999; Pflugmacher et al., 2012). In contrast, LiDAR (Light Detection and Ranging)-based active remote sensing technologies can measure canopy height and crown dimensions directly, through measurements of distance between the sensor and target, thereby overcoming data saturation in biomass estimation (Drake et al., 2003).

Global empirical relationships have been established between LiDAR-derived forest canopy height and AGB (Lefsky et al., 2002; Drake et al., 2003; Lefsky et al., 2005; Asner et al., 2012). Airborne LiDAR methods represent an effective alternative to optical and short-wavelength radar sensors to provide accurate information on AGB (Zolkas et al., 2013). Their use is however only possible at local to small-regional scales (Zhao and Popescu, 2009), as they become prohibitive at larger scales for their high cost of data acquisition (Popescu et al., 2011). Spaceborne LiDAR (Light Detection and Ranging) sensors also exist, and the Geoscience Laser Altimeter System (GLAS) onboard the Ice, Cloud and land Elevation Satellite (ICESat), which was launched by NASA in 2003, was the first spaceborne LiDAR sensor to potentially provide global estimates of forest canopy height. . However, GLAS data are limited for wall-to-wall AGB mapping due to their spatially discrete coverage, with 60-70 m footprints spaced by 170 m along the satellite track and 2.5 to 15 km between tracks (Sun et al., 2011). To overcome these limitations, Simard et al. (2011) used the relationship between GLAS footprint level LiDAR-derived canopy height and spatially continuous ancillary variables from MODIS data for generating a wall to wall map of canopy height at the global scale. Zhang et al. (2014b) demonstrated that those GLAS canopy height estimates were promising data for calculating biomass in the forest regions of Alberta, Canada (r^2 = 0.62, root mean square error (RMSE) = 47.03 Mg ha^{-1}). Chi et al. (2015) also used MODIS data for extrapolating AGB estimates from GLAS footprint level at a nation-wide scale in China. Nevertheless, the use of global relationships between canopy height and biomass across large forest areas at regional scales may fail to incorporate spatial gradients that exist across the landscape and, thus, may produce large spatially correlated errors (Mitchard et al., 2014). Each set of satellite remote sensing product has limitations, therefore, with respect to its spatial resolution, spatial coverage and temporal resolution (Frolking et al., 2009). An accurate model of spatial variability of AGB depends upon the choice of remote sensing variables, scale and modelling methodologies (Houghton, 2005; Lu, 2006; Zhao et al., 2010).

The comparisons of biomass maps from different sources of remote sensing data may provide useful information from which more accurate AGB estimates can be derived (e.g., Mitchard et al., 2013). Hill et al. (2013) compared biomass estimates from nine different studies (e.g., Saatchi et al., 2011b; Baccini et al., 2012) based on MODIS and GLAS data that were acquired across tropical forests at the extent of continental Africa. They found only low correlations between the various estimates, suggesting a need to improve assessment of their accuracy. In particular, the lack of sufficient spatially exhaustive ground-based data tends to underestimate errors in remotely sensed estimates (Hill et al., 2013; Mitchard et al., 2014).

The addition of prior vegetation recovery trends, disturbance histories (e.g., Pflugmacher et al., 2014), and known forest structural attributes (e.g., Main-Knorn et al., 2011) to remote sensing data could subsequently improve the accuracy of biomass estimation. In North American boreal ecosystems, changes in C storage over time are related to fire events (Harden et al., 2000), which are highly stochastic in both time and space (Girardin et al., 2013). A disturbance regime may be characterized by disturbance frequency, size and severity (Bergeron et al., 2002). Small fires are most frequent, but infrequent large fires predominantly shape the boreal landscape mosaic (Johnson et al., 1998; Bergeron et al., 2004). Burn severity varies inside fire perimeters (Johnstone et al., 2010; Jin et al., 2012), which blurs the relationship existing between disturbance history, post-fire canopy recovery and AGB (Lecomte et al., 2006; Chaieb et al., 2015). Time since last fire (TSLF) is the most significant predictor of postfire canopy recovery (Mansuy et al., 2012), which is related to changes associated with forest structural attributes over time (e.g. canopy cover) that control AGB at the scale of landscapes (Irulappa Pillai Vijayakumar et al., 2016). Postfire canopy recovery process is also influenced by edaphic factors (surficial deposits, parent material, organic matter accumulation), topography and regional climate (Mansuy et al., 2012). Studies based on remote sensing data to estimate AGB seldom consider the spatial knowledge of recorded forest disturbances and recovery patterns of the study system (Chu and Guo, 2014). Fire disturbances and their distribution over the landscape are inherently spatial and therefore, the choice of the spatial scale for an analysis relating AGB with vegetation recovery and disturbance histories is important. Frolking et al. (2009) recommended matching the scale of biomass estimation with that of fire disturbance, namely large fires in this case.

The goal of this study was to explain the spatial variation in AGB differences between estimates that were derived from different remote sensing data (MODIS, GLAS and ASAR) and those that were obtained from an AGB model based on ground-inventory data amassed over a large area of the boreal forest. AGB estimates generated from different remote sensing sensors, namely passive optical (MODIS), active microwave (ASAR) and active optical (GLAS) should be expected to differ. Therefore, our purpose was not to find the best remote sensing data product, to validate existing modelling approaches, or to compare different remote sensing products. But we intended to determine how much each satellite-derived AGB estimates diverge from inventory estimates over large forest areas, and possibly identify factors that would help to improve their accuracy, especially information on past disturbance history. We have selected Quebec's black spruce-feather moss forest in eastern Canada (area: 217 000 km^2) as a study region, given its richness in terms of fire history maps and forest inventory data. Thus this study region served as a useful training area to derive relatively accurate biomass values and to analyze biomass estimation differences over a very large area. AGB estimates that are based on MODIS spectral data, and ASAR data collected for the study area were already available from Beaudoin et al. (2014) and Thurner et al. (2014), respectively. We also estimated AGB using ICESat/GLAS data following the methodology successfully developed by Zhang et al. (2014b). We compared these estimates, with an inventory based

AGB map (Irulappa Pillai Vijayakumar et al., 2016) based on a large number of forest inventory plots and spatial explicit aerial photo-interpreted stand maps. Our comparison analysis aimed at identifying the important predictors, especially TSLF (time-since-last fire), that could be used as ancillary input variables for more accurate remotely sensed biomass estimates.

4.03 Methods

A general flow diagram of the data and methods used for AGB estimation and comparison is displayed in Fig.4.1.

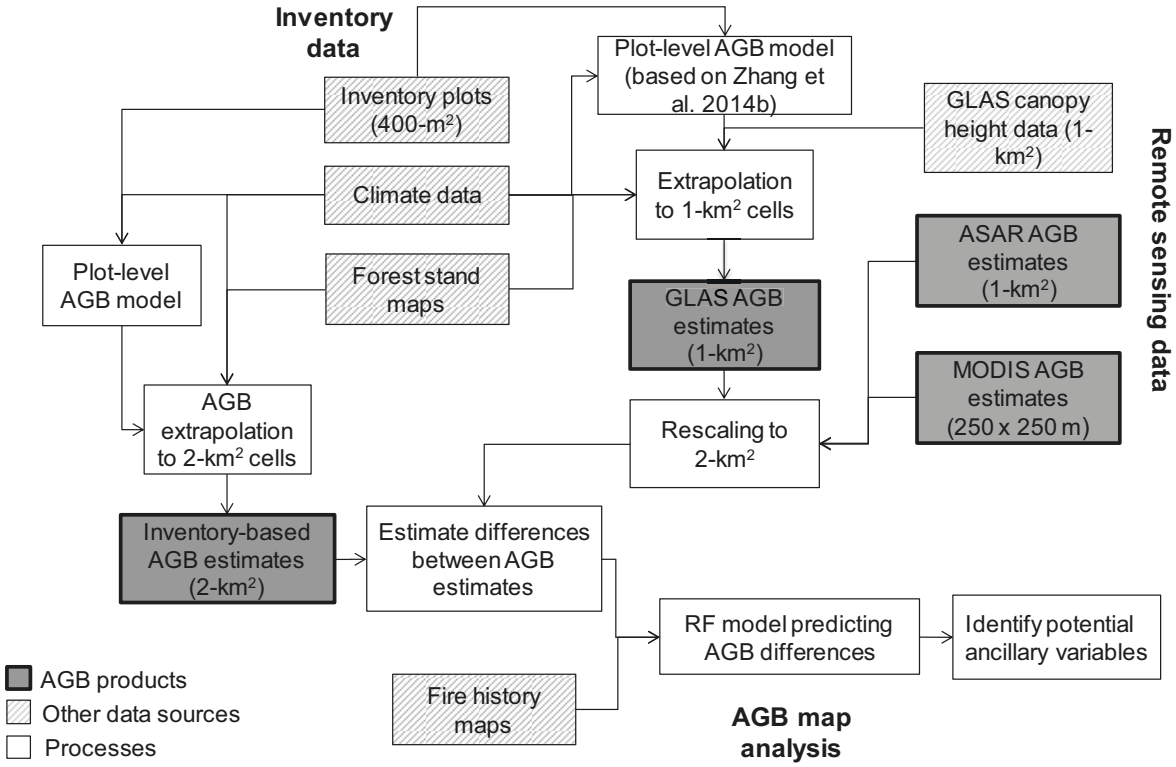

Figure 4.1. General flow diagram

4.03.01 Study area

Our study region (Fig. 4.2) is the black spruce (*Picea mariana* (Mill.) BSP) -moss bioclimatic domain (Robitaille and Saucier, 1998) within the province of Quebec, Canada (49°N to 52°N and 66°W to 79° 30'W, area : 217,000 km^2). It is divided along a longitudinal climate gradient into eastern and western subdomains, which differ from one another in biophysical environments and consequently in fire regime and vegetation. The western continental climate favors more frequent forest fires, unlike the east, which is characterized by a maritime climate that is due to the influence of the Atlantic Ocean and the Gulf of St. Lawrence. Fuel moisture conditions are rarely conducive to fire spread.

Current vegetation composition is particularly related to this gradient in climate and fire activity. In the west (near James Bay), relief is generally flat. Annual precipitation and mean annual temperature are 700 mm and -0.65 °C, respectively, with an average growing season of 165 days (Robitaille and Saucier, 1998). This western region is thus characterized by relatively short fire return intervals (270 years; Bergeron et al., 2004), leading to the establishment of landscapes that are dominated by post-fire tree species such as black spruce, jack pine (*Pinus banksiana* Lamb.) and, to a lesser extent, by white or paper birch (*Betula papyrifera* Marsh.) and trembling aspen (*Populus tremuloides* Michx.). In the east, annual precipitation varies between 1000 and 2000 mm and mean annual temperature is -1.5 °C, with a growing season of 150 days (Saucier et al., 2009). Fire return intervals are thus longer (> 500 years; Bouchard et al., 2008) which generate abundant fire-averse balsam fir (*Abies balsamea* [L.] Mill.), mixed with black spruce.

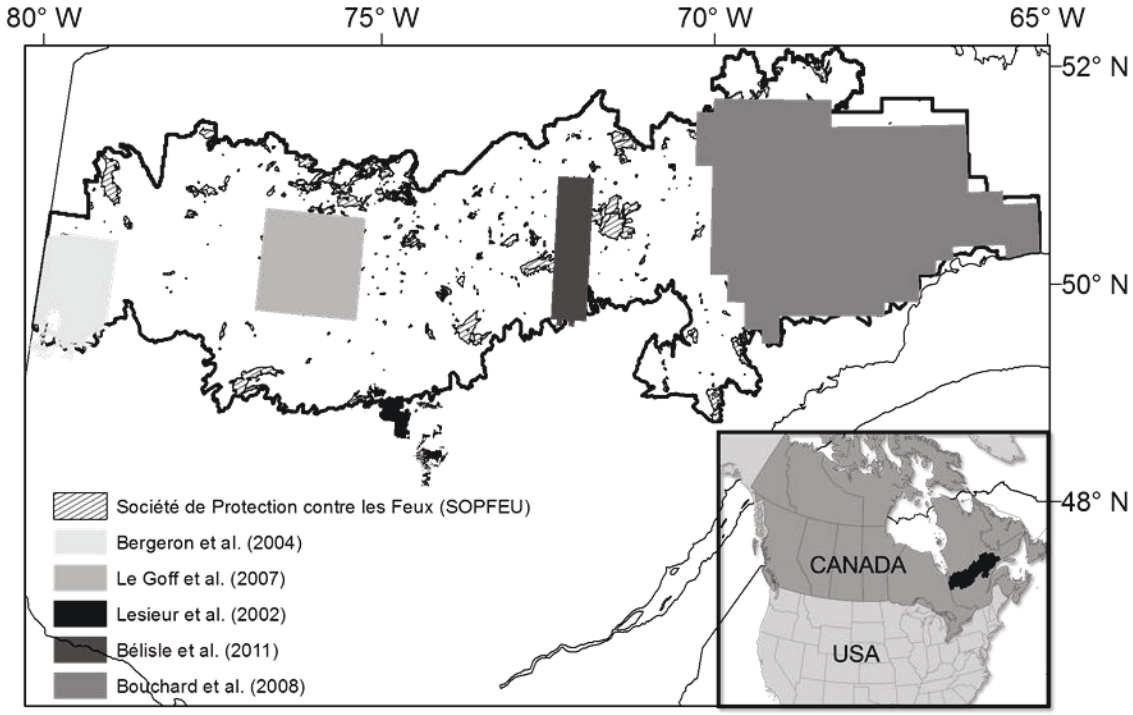

Figure 4.2. Locations of the study area (dark outline) and training datasets (grey areas) from the published studies.

4.03.02 Estimation of AGB based on inventory data

We used the inventory-based AGB estimates of Irulappa Pillai Vijayakumar et al. (2016). AGB values were estimated at a spatial scale of 2-km^2 in line with a process-based understanding of fire disturbance in our study area. This cell-size corresponds to the minimum size for large fires included in the Canadian large fire database and large fires account for 97% of the total area burned between 1959 and 1999 (Stocks et al., 2003). Such scale also seemed adequate to circumvent confounding issues typically found with finer scales, such as the variation of post-fire forest recovery patterns within burned areas due to the

variability of fire severity (Jin et al., 2012) and neighboring effects (Frelich and Reich, 1999). A spatial explicit hierarchical modelling (Wu and David, 2002) approach was developed by Irulappa Pillai Vijayakumar et al. (2016) to sequentially scale-up aboveground biomass carbon (ABC) from inventory plots (temporary sample plot database; 400-m^2, 1992-2003) to forest stands map (size: 14 ha) and then to the scale of 2-km^2 cells. Spatial explicit forest stand properties across the study area were obtained from the SIFORT geospatial database (Spatial Information on Forest Composition based on Tesserae, Pelletier et al., 2007) originating from forest maps (1:15,000 scale) and elaborated by the Quebec Ministry of Natural Resources between 1990 and 1999 for its third inventory program (1992-2002). This database consists of a mosaic of square tiles, divided into slices of 15 s of latitude by 15 s of longitude and covering an average area of 14 hectares. Eighty-nine percent of the study area was considered for AGB estimation, leaving wetlands and peatlands, water, heaths, harvested land, insect-killed stands or windthrows and human infrastructure.

First, a non-parametric RF plot-level model (r^2 = 0.50, RMSE = 13.88 Mg ha^{-1}) was trained relating ABC estimates using observed forest attributes and climate variables. This model was then extrapolated to all SIFORT tile centroids in a training dataset, and then averaged within each 2-km^2 cell to obtain spatially continuous estimates. The training dataset covered 43.8% of the present study area (Fig. 4.2) and included all areas for which a TSLF value could be provided from contemporaneous and historical fire maps. More details on this training area are provided below. Another non-parametric RF model was then calibrated at 2-km^2 scale (r^2 = 0.83, RMSE = 0.28 Gg km^{-2}) to impute ABC across the whole study area. Abundances of canopy cover density classes were the main variables influencing ABC estimates at the 2-km^2 scale. ABC represents 50% of AGB (Gower et al., 1997). More detailed information can be found in Irulappa Pillai Vijayakumar et al. (2016).

4.03.03 Estimations of AGB from remote sensing data

We have used three remote sensing data products (MODIS, GLAS and ASAR) to estimate biomass at the 2-km^2 scale. We have selected these three data products to consider the most common types of sensors (passive [optical multi-spectral] and active [radar and laser scanner]) used for AGB estimation (Lu et al., 2014). We first calibrated an AGB model with spaceborne GLAS LiDAR canopy height data by adapting the methodology developed by Zhang et al. (2014b). In a 450 000 km^2 study area in Alberta (western Canada), they showed that observed canopy height, elevation and climate variables were significantly related to AGB at the plot level (n = 1968) using random forest model. They then used this relationship to predict AGB values for the entire area at a 1-km^2 scale using GLAS canopy height data. Accordingly, we used a combination of plot inventory data, GLAS data, climate data (from the NCEP-NCAR Twentieth Century Reanalysis project; Compo et al., 2011), and elevation to predict AGB. GLAS canopy height data at the 1-km^2 scale for our study region were obtained from Simard et al. (2011). They established a relationship between spatially discrete GLAS footprint level LiDAR-derived canopy height estimates and

spatially continuous ancillary variables such as the MOD44B percent tree cover product (Hansen et al., 2003) from MODIS, the elevation information from the Shuttle Radar Topography Mission (Farr et al., 2007), global climate data from the Tropical Rainfall Measuring Mission (Kummerow et al., 1998), and the Worldclim database (Hijmans et al., 2005) to generate global canopy height map. Plot-level AGB values (n = 8739, from the third regular forest inventory [1992-2003], Ministry of Natural Resources of Quebec) were estimated by converting diameter at breast height (DBH, 1.3 m) into biomass using species-specific allometric equations for commercial tree species (Lambert et al., 2005; Ung et al., 2008), non-commercial tree species (Ter-Mikaelian and Korzukhin, 1997), and shrubs (Buech and Rugg, 1989). These estimates were summed at the plot level. A random forest (RF) model was then developed to estimate plot-level AGB with observed canopy height (dominant height of the canopy, i.e., mean height of the dominant trees; Burkhart and Tomé, 2012), elevation and climate variables (Table 4.1). This model was then used to interpolate AGB across the study region using GLAS canopy height data at 1 km resolution.

We developed RF models in the R package *randomForest* (Liaw and Wiener, 2002). A random forest model is non-parametric and insensitive to non-normal and skewed data, has the ability to model non-linear relationships, and can provide the measurements of relative strength of predictor variables. The selection of predictors for fitting RF models was performed using the *Boruta* package (iterations = 1000; number of trees = 1000) for R (adapted from Kursa and Rudnicki, 2010). We selected the six most important variables assessed by *Boruta* to fit parsimonious and robust models (Thompson and Spies, 2009). Correlation analyses were performed to detect collinearity between the selected predictors (threshold: $r > 0.70$, e.g., Dormann et al., 2013) to avoid problems of multicollinearity. We tested for spatial autocorrelation in model residuals to detect potential omission of important variables (Dormann et al., 2007). To this end, we computed Global Moran's *I*, an index of spatial autocorrelation, as a function of neighbouring distance (Moran, 1950). We further analyzed residuals using Anselin's Local Moran *I* statistic (Anselin et al., 1995) to characterize local patterns of spatial association by identifying clusters with values similar in magnitude, and to identify spatial outliers.

An AGB map that was based on MODIS data for our study region was provided by Beaudoin et al. (2014). They mapped AGB at 250 x 250 m pixel resolution as a function of MODIS spectral reflectance, climatic and topographic variables using Canada's National Forest inventory photo- plots (2 km x 2 km) and the *k* nearest-neighbour (*k*NN) method. Each 2 km x 2 km photo-plot consisted of forest polygons that were characterized by cartographic attributes of vegetation composition, stand structure, and AGB information based on the models of Boudewyn et al. (2007). They rasterized AGB information from photo-plots to the 250 m x 250 m MODIS grid and used these photo-plot pixels as references to impute AGB values to the rest of the study area.

We also obtained an AGB map that was based on ASAR data from Thurner et al. (2014). This AGB map covers the Northern Hemisphere between 30° N and 80° N for boreal and temperate forests of North

America, Europe and Asia. It is based on estimates of growing stock volume (volume of tree stems per unit area, m^3 ha^{-1}) that was obtained with the BIOMASAR retrieval algorithm developed for Envisat/ASAR satellite data at a spatial resolution of 0.01° (Santoro et al., 2011). BIOMASAR is an automated approach for modelling growing stock volume as a function of radar backscatter. This technique is based on how forest structural properties affect the response of a radar signal. Volume estimates were then converted to biomass. A more detailed explanation of these products is given by Thurner et al. (2014).

We reprojected these biomass products of different resolution (1 km, GLAS biomass map; 250 m x 250 m, MODIS biomass estimates, Beaudoin et al., 2014; and 0.01° (approximately 1 km) resolution, ASAR biomass estimates, Thurner et al., 2014) to the same projection (North American Datum 1983; Lambert conformal conic projection). We then rescaled them to a resolution of 2 km^2 to match the spatial resolution of inventory-based estimates produced by Irulappa Pillai Vijayakumar et al. (2016) using a nearest-neighbour resampling method (Langner et al., 2014). Pixel values remain unchanged with this method, thereby avoiding the mixing of unsaturated and saturated pixels and the introduction of artefacts (Mitchard et al., 2013, 2014).

4.03.04 Comparison of biomass maps

The comparison results are to be inferred taking into consideration that AGB generated from different remote sensing sensors, passive optical (MODIS), active microwave (ASAR) and active optical (GLAS) were expected to differ. Therefore, comparisons are affected by the physical principles of data acquisition used in sensors and also by the spatial resolution used for the comparisons. We could not estimate the accuracy of remotely sensed biomass estimates at the scale of 2 km^2 due to the lack of observed AGB values at that scale. Comparisons of these products at a finer scale resolution were also not considered so as to match the scale from which large fire disturbances start to impact forest landscape structure on a regional scale (e.g. Johnson and Gutsell, 1994: Fig. 5; Frolking et al., 2009). The inventory-based AGB map of Irulappa Pillai Vijayakumar et al. (2016) was therefore of limited use to validate remote sensing products, but was useful to show agreement or disagreement in the spatial trends observed between remote sensing and inventory-based estimates over a large area and to search for ancillary variables related to past disturbance history.

Accuracy denotes the agreement of model-predicted values with the true values, whereas precision measures how closely the model-predicted values agree with one another (Tedeschi, 2006). Still, estimation accuracy cannot exceed precision and, therefore, precise estimates should be close to one another (Hill et al., 2013). We first explored covariations between the each of the GLAS, MODIS, ASAR and inventory based estimates in the training dataset using the Pearson correlation coefficient accounting for spatial autocorrelation in the *SpatialPack* package for R. We calculated the difference between each of the GLAS, MODIS and ASAR-based AGB estimates, and the up-scaled inventory-based estimates of AGB for each cell in the training dataset to identify potential ancillary variables. To this end, we used the

training dataset created by Irulappa Pillai Vijayakumar et al. (2015). This training dataset consists of 34,234 cells of 2-km^2 size. In this dataset, 50 % or more of the area of each 2-km^2 cell is covered by fire polygons of SOPFEU (the Quebec forest fire control agency, Société de protection des forêts contre le feu, 1970-2000) or fire history maps (1880-2000) (Fig. 4.2). In addition, cells that included at least more than one inventory plot (third inventory program [1992-2003], Ministry of Natural Resources of Quebec) indicated that forest stands were dominated by post-fire tree species (paper birch, trembling aspen, jack pine, black spruce) and were even-aged (oldest plot age was used as TSLF) (Bélisle et al., 2011).

We developed RF models relating these differences to covariates for cell-level inventory attributes (relative cell frequencies of SIFORT attributes, Table 4.1) and observed TSLF at the 2-km^2 scale. At that scale, inventory-based AGB estimates are related to the relative proportions of canopy cover density classes (Irulappa Pillai Vijayakumar et al., 2016), while canopy cover density is linked with signal saturation in remotely sensed estimates (Zhang et al., 2014a). Irulappa Pillai Vijayakumar et al. (2016) have further shown that changes in canopy cover density at that scale are related to TSLF. Therefore, TSLF that was associated with biophysical variables could serve as a surrogate of canopy density to overcome saturation effects. Furthermore, Asner et al. (2010) have shown for the Peruvian Amazon forests that surficial geological substrate and forest type information should be incorporated with satellite remote sensing data for more accurate biomass mapping. We therefore included indices of surficial deposits in the models. Results of these non-parametric models are difficult to interpret and synthesize. For this reason, we also analyzed the variation in remotely sensed AGB estimates as a function of observed TSLF at the 2-km^2 scale, which is equivalent to producing AGB yield curves. This was intended to provide insights on the relationship existing between remotely sensed biomass estimates and TSLF at the scale of 2-km^2.

Table 4-1. List of explanatory variables used in estimating AGB

Relative frequencies of vegetation variables (a)	Physical site variables	Climate variables (b)
Species composition groups - Black spruce, balsam fir, jack pine, intolerant hardwoods, mixed, other conifers and no species composition but identified as a burned area, following Gauthier et al., (2010).	Surficial deposit groups (a) –VAVC (very abundant, very coarse), MM (moderate, moderate), MAM (moderately abundant, moderate), MAC (moderately abundant, coarse), AC (abundant, coarse), ROC (rock) and ORG (organic) (Mansuy et al. 2010).	Temperature (^{o}C) – annual mean temperature Total precipitation (mm year^{-1}) – the mean of annual total precipitation Degree-days (°C year^{-1}) – Annual growing degree-days summation (above 5°C)

Stand age classes - between 0 and 20 years, 21 to 40, 41 to 60, 61 to 80, 81 to 100, ≥ 101, young uneven-aged, and old uneven-aged. Stand height classes - > 22 m, 17 to 22 m, 12 to 17 m, 7 to 12m, 4 to 7 m, 2 to 4 m, and 0 to 2 m. Stand cover density classes - > 81%, 61 to 80 %, 41 to 60%, and 25 to 40 %.	Elevation (m) - Derived for study units from SRTM DEM (90 m resolution) (van Zyl, 2001). Slope (^{o}) - derived from elevation data in ArcGIS 10.0	Growing season length (days year^{-1}) –Duration of days for which the mean temperature is above 5°C Potential evapotranspiration (mm) – Annual total potential evapotranspiration (Dunne and Leopold 1978) Aridity index (mm year^{-1}) – Aridity is accumulation of monthly water deficit (monthly Thornthwaite potential evapotranspiration - monthly precipitation) Canadian drought code – Moisture content of the deep layer of compacted organic matter, 10–20 cm deep (Amiro et al., 2005)

4.04 Results

4.04.01 Estimation of AGB using GLAS canopy height data

Ground-measured canopy height was moderately correlated with AGB at the plot level (r = 0.43, P < 0.01). With this relationship, we extrapolated AGB to the entire landscape using GLAS canopy height data at 1-km resolution. However, ground-measured canopy height and GLAS-measured canopy height were not correlated at the plot level (r = 0.014, P > 0.05). Variable importance rating with the *Boruta* procedure and the set of explanatory variables that were used by Zhang et al. (2014b) indicated that observed canopy height had the greatest influence on AGB, followed by potential evapotranspiration (PET), precipitation, elevation, drought code, and growing season (Table 4.1, Fig. 4.3a). Elevation was not included in subsequent RF model training, given its strong correlation with growing season length (r = -0.82, P < 0.01). Overall, the prediction accuracy of AGB was very weak at the plot level (r^2 = 0.29, RMSE

= 33.21 Mg ha^{-1}; Fig. 4.3b). Residuals were weakly spatially autocorrelated (Global Moran's I statistic = -0.05, for distances < 20 km).

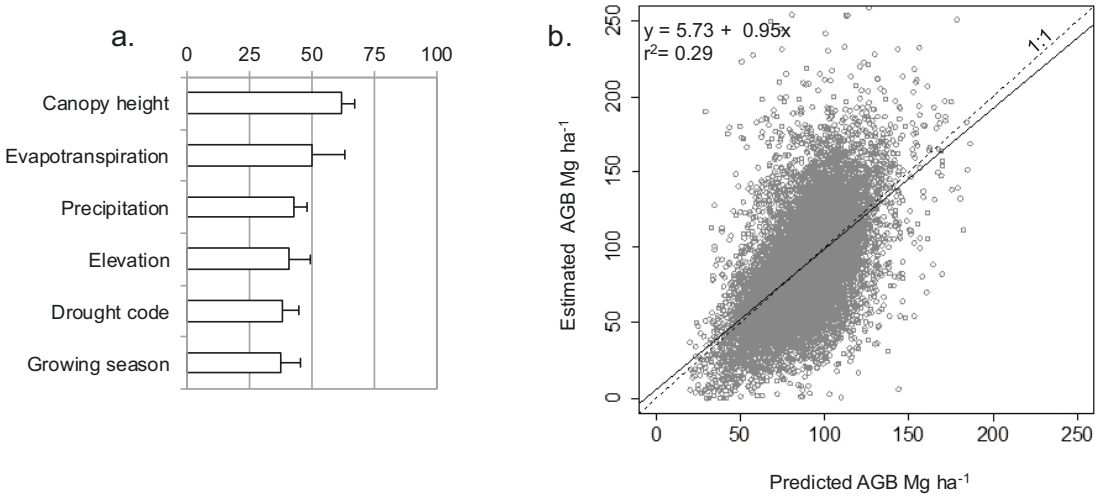

Figure 4.3. Top six variables ranked by a random forest model for the estimation of AGB based on observed canopy height at plot level (a); (b) density plot of estimated vs predicted AGB by the model based on observed canopy height at plot level

4.04.02 Spatial distribution and covariation of remotely sensed and inventory based biomass estimates

At the scale of the study area, maximum and minimum AGB values that had been calculated from remote sensing data and inventory data were in close agreement, except for ASAR estimates (MODIS estimates: 0.1 to 19.8 Gg km^{-2}; GLAS estimates: 3.9 to 18 Gg km^{-2}; ASAR estimates: 0.1 to 12 Gg km^{-2}; and inventory-based estimates: 2.1 to 18.6 Gg km^{-2}). AGB maps from MODIS and ASAR showed an expected pattern of high and low values along an east-west gradient (Figs. 4.4b, 4.4d), relative to the fire regime gradient that was observed over the study area. Spatial distributions of AGB that were estimated from MODIS and inventory data also agreed with one another. When the maps were compared visually with fire disturbance history, both maps showed low biomass values in regions of recently burned areas (Figs. 4.4a, 4.4b). The spatial gradient of AGB estimates from ASAR also showed similar degree of agreement in depicting low values in regions with recently burned areas, but these low values were more noticeable in this map (Fig. 4.4d). The GLAS biomass map exhibited a very different spatial pattern of low and high values along a north-south gradient (Fig. 4.4c), which is not associated with fire disturbance history.

When comparing remotely sensed estimates with inventory-based estimates, MODIS estimates exhibited the greatest correlation with inventory-based estimates (r = 0.54, P < 0.01; Table 4.2), when compared to GLAS (r = 0. 50, P < 0.01; Table 4.2) or ASAR estimates (r = 0.26, P < 0.01; Table 4.2). At the scale of 2 km^2, correlations among remotely sensed AGB estimates of MODIS, GLAS and ASAR were weak to

moderate: ASAR vs GLAS, $r = 0.37$, $P < 0.01$; ASAR vs MODIS, $r = 0.55$, $P < 0.01$; GLAS vs MODIS, $r = 0.38$, $P < 0.01$ (Table 4.2).

Table 4-2. Pearson correlations between each of MODIS, GLAS, ASAR and inventory based AGB estimates after accounting for spatial autocorrelation*.

	MODIS	GLAS	ASAR
Inventory based	0.54	0.50	0.26
MODIS		0.36	0.55
GLAS			0.37

*P < 0.01

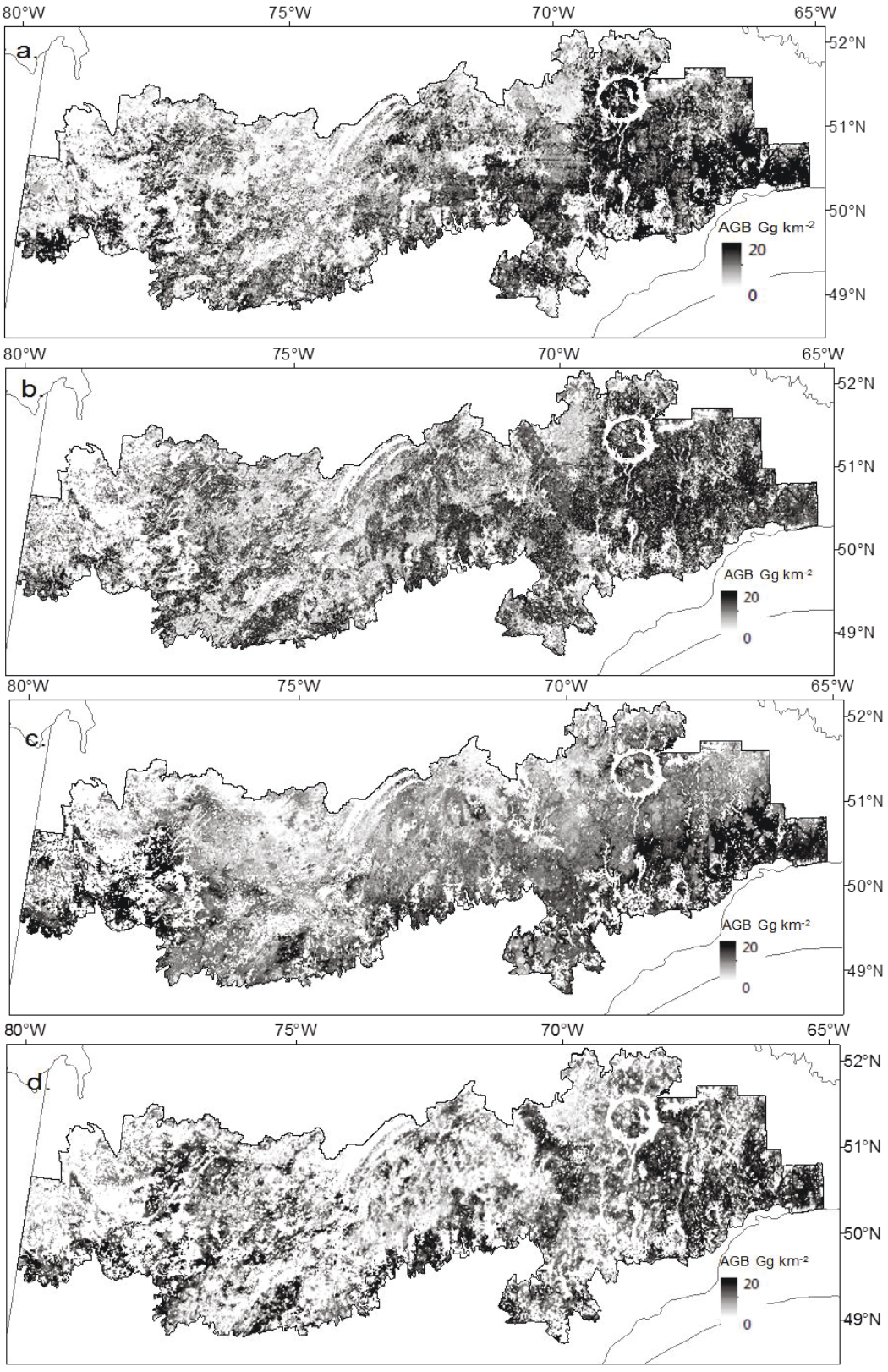

Figure 4.4. Maps of AGB at the scale of 2 km^2 based on: inventory data (a); MODIS data obtained from Beaudoin et al. (2014) (b); GLAS data (c); ASAR data obtained from Thurner et al. (2014) (d)

4.04.03 Spatial analysis of differences between inventory and remotely sensed biomass estimates

We detected significant positive spatial autocorrelations, when spatially analyzing differences between inventory and remotely sensed biomass estimates (Global Moran's *I*, distances < 20 km: MODIS estimates, $I = 0.26$, $P < 0.01$; GLAS estimates, $I = 0.31$, $P < 0.01$; ASAR estimates, $I = 0.27$, $P < 0.01$). Further analysis of differences between inventory and remotely sensed biomass estimates using Anselin's local Moran *I* (Anselin et al., 1995) indicated significant spatial clusters that were spatially linked to TSLF (Supplementary material, Figs. A.1c, A.2c, A.3c).

When we compared differences between inventory and MODIS estimates (inventory minus MODIS estimates) in recently disturbed cells (TSLF < 30 years), differences were between -2 to 2 Gg km^{-2}, matching low-similarity clusters (low values in a low-value neighborhood) (Supplementary material Figs. A.1a, A.1b). Differences increased (between 2 and 6 Gg km^{-2}) with increasing TSLF, especially in the eastern part of the study region, linked to high-similarity spatial-clusters (high values in a high-value neighborhood) (Supplementary material Fig. A.1c). High-dissimilarity spatial clusters (high values in a low value neighborhood) were mixed with low-similarity clusters (low values in a low value neighborhood).

When analyzing differences between inventory and GLAS estimates (inventory minus GLAS estimates), cells with TSLF < 30 years exhibited values between -6 and 0 Gg km^{-2}, indicating GLAS biomass values that were higher than inventory-based ones in recently burned areas and linked to low-similarity clusters (Supplementary material Figs. A.2a, A.2b). With increasing TSLF, however, positive differences were observed (0-4 Gg km^{-2}), indicating lower GLAS biomass values than inventory-based ones, corresponding to high-similarity clusters (Supplementary material Fig. A.2c).

Mapped differences between inventory based and ASAR biomass estimates (inventory minus ASAR estimates) showed that most cells had values ranging from 0 to 8 Gg km^{-2}, indicating lower ASAR biomass values. These were associated with two types of clusters, i.e., high-similarity clusters and high-dissimilarity clusters (Supplementary material Figs. A.3b, A.3c). Differences also tended to increase with increasing TSLF. Low-dissimilarity and low-similarity clusters were infrequent at the scale of the training area.

4.04.04 Detecting potential ancillary variables for remotely sensed AGB estimation

The relative proportions of cover density classes at the 2-km^2 scale were revealed as the most important potential ancillary variables when training RF models with differences between remotely sensed (MODIS, GLAS, ASAR) and inventory-based estimates (Figs. 4.5a-c). Other important variables were the relative proportions of both dominant surficial deposits (undifferentiated tills with moderate to abundant stoniness, i.e., MAM, MM; Table 1), and stony surficial deposits (ROC, Table 1). The RF models explained from 50

to 28% of variation differences observed between remotely sensed and inventory-based estimates (MODIS, r^2 = 0.50, RMSE = 1.36 Gg km^{-2}; GLAS, r^2 = 0.48, RMSE = 1.56 Gg km^{-2}; ASAR, r^2 = 0.28, RMSE = 1.97 Gg km^{-2}; Figs. 4.5d-f).

Differences between inventory-based and remotely sensed estimates generally increased as a function of the percentage of closed cover (summed frequency of three cover density classes: > 81 %, 61-80 %, 41-60 %) (Figs. 4.6a-c). We also identified TSLF as a potential alternative variable for canopy cover density (Figs. 4.7a-c) to reduce the discrepancy between remotely sensed and inventory-based estimates. Indeed, the percentages of variation that was explained by models including TSLF (MODIS, r^2 = 0.47, RMSE = 1.47 Gg km^{-2}; GLAS, r^2 = 0.47, RMSE = 1.57 Gg km^{-2}; ASAR, r^2 = 0.23, RMSE = 2.02 Gg km^{-2}; Figs. 4.7d-f) were similar to those of models relying upon the abundances of cover density classes.

4.04.05 AGB yield curves with remotely sensed products

Correlations were moderate between TSLF and remotely sensed AGB estimates at the scale of 2-km^2 (MODIS: r = 0.54, P < 0.01; GLAS: r = 0.32, P < 0.01; ASAR: r = 0.47, P < 0.01). These correlations were lower than the correlation between inventory-based estimates and TSLF (r = 0.82, P < 0.01). AGB yield curves that were based on MODIS estimates exhibited an expected trend of biomass increase as a function of TSLF until 60 to 90 years had elapsed, and a decrease thereafter, which consistent with curves that were based on inventory data, but with lower median values (Figs. 4.8a-b). AGB estimates that were based on GLAS data showed unexpectedly high values in recently disturbed 2-km^2 cells (TSLF < 30 years) (Fig. 4.8c). AGB yield curves from ASAR data exhibited a comparable trend of biomass increase as a function of TSLF (Fig. 4.8d), but their median values were consistently lower than GLAS, MODIS and inventory-based estimates.

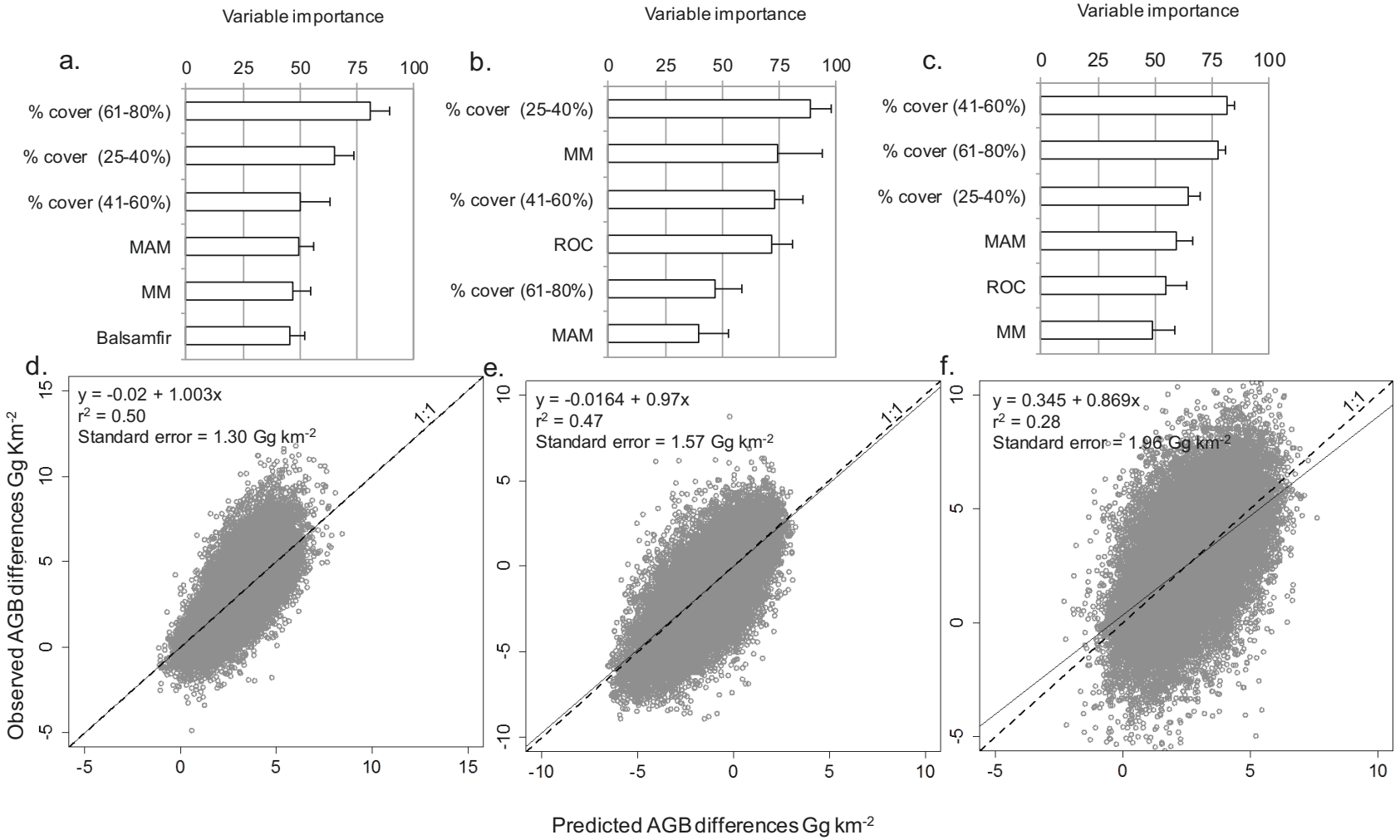

Figure 4.5 Top-six variables ranked by RF models used to explain the differences observed between remotely sensed and inventory based AGB estimates with relative frequencies of SIFORT attributes (Table 4.1) and observed TSLF: MODIS (a); GLAS (b); and ASAR (c); density plots of observed vs predicted AGB differences between inventories based and remotely sensed AGB estimates: MODIS (d), GLAS (e), and ASAR data (f).

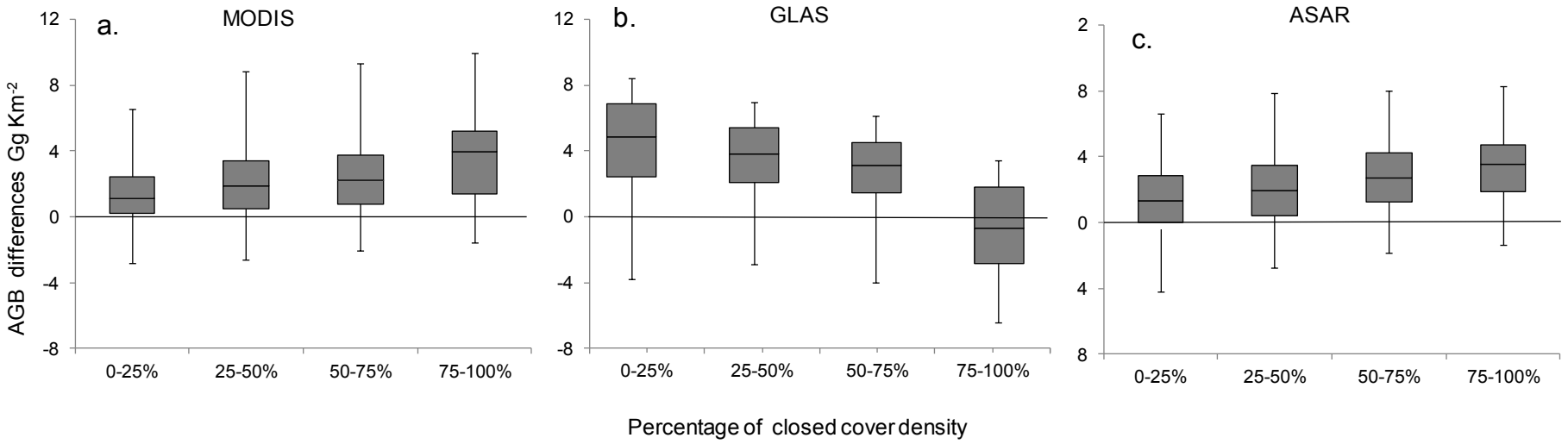

Figure 4.6. Box-and-whisker plots of differences observed between inventory based AGB estimates and biomass estimates of MODIS (a), GLAS (b), and ASAR (c), regrouped by abundance classes of canopy closed cover density.

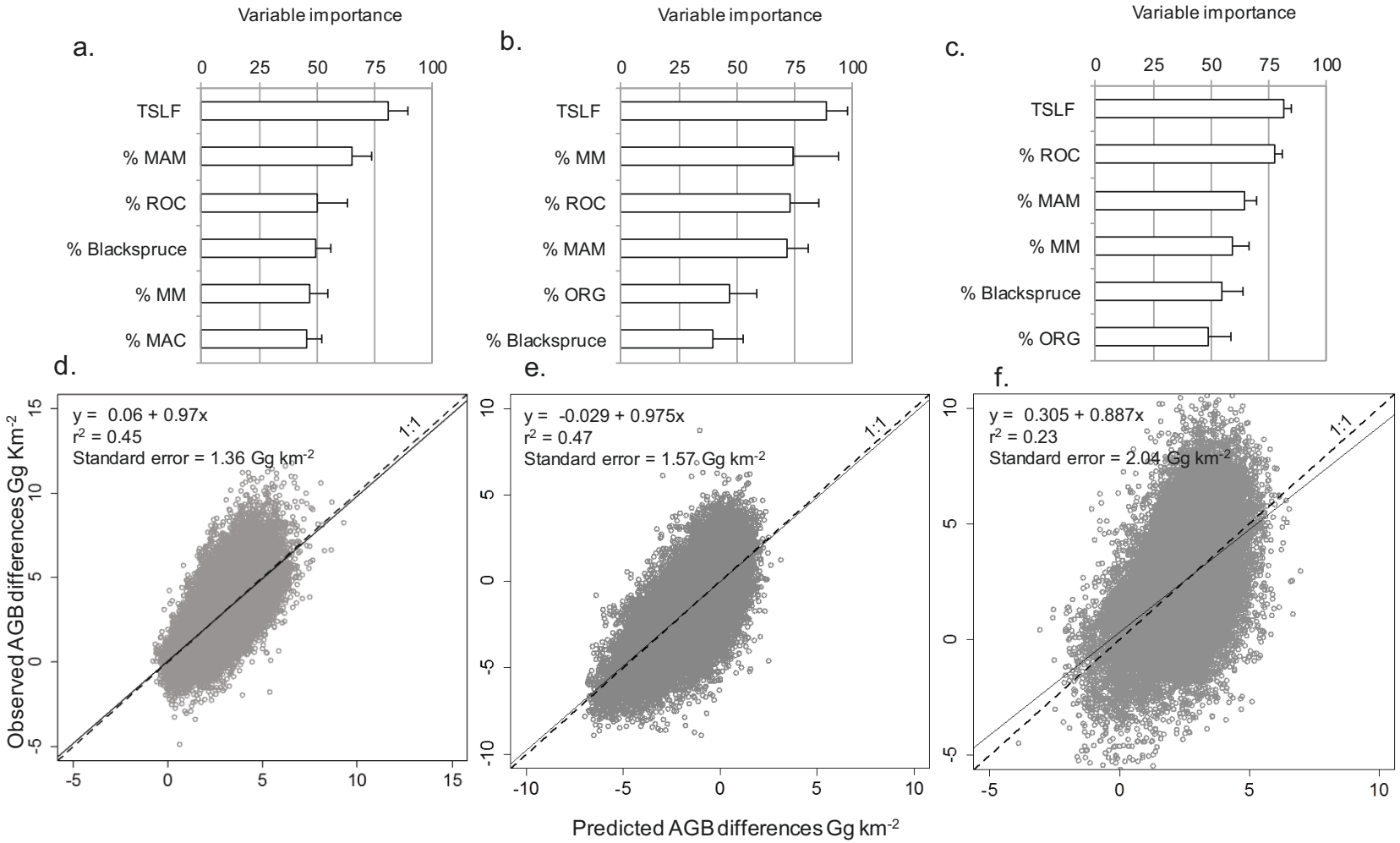

Figure 4.7. Top-six variables ranked by RF models used to explain the differences observed between remotely sensed and inventory based AGB estimates when abundances of cover canopy density classes are removed from the list of potential explanatory variables: MODIS, (a); GLAS, (b); and ASAR, (c); density plots of observed vs predicted AGB differences between remotely sensed and inventory based AGB estimates: MODIS (d); GLAS (e); and ASAR data (f).

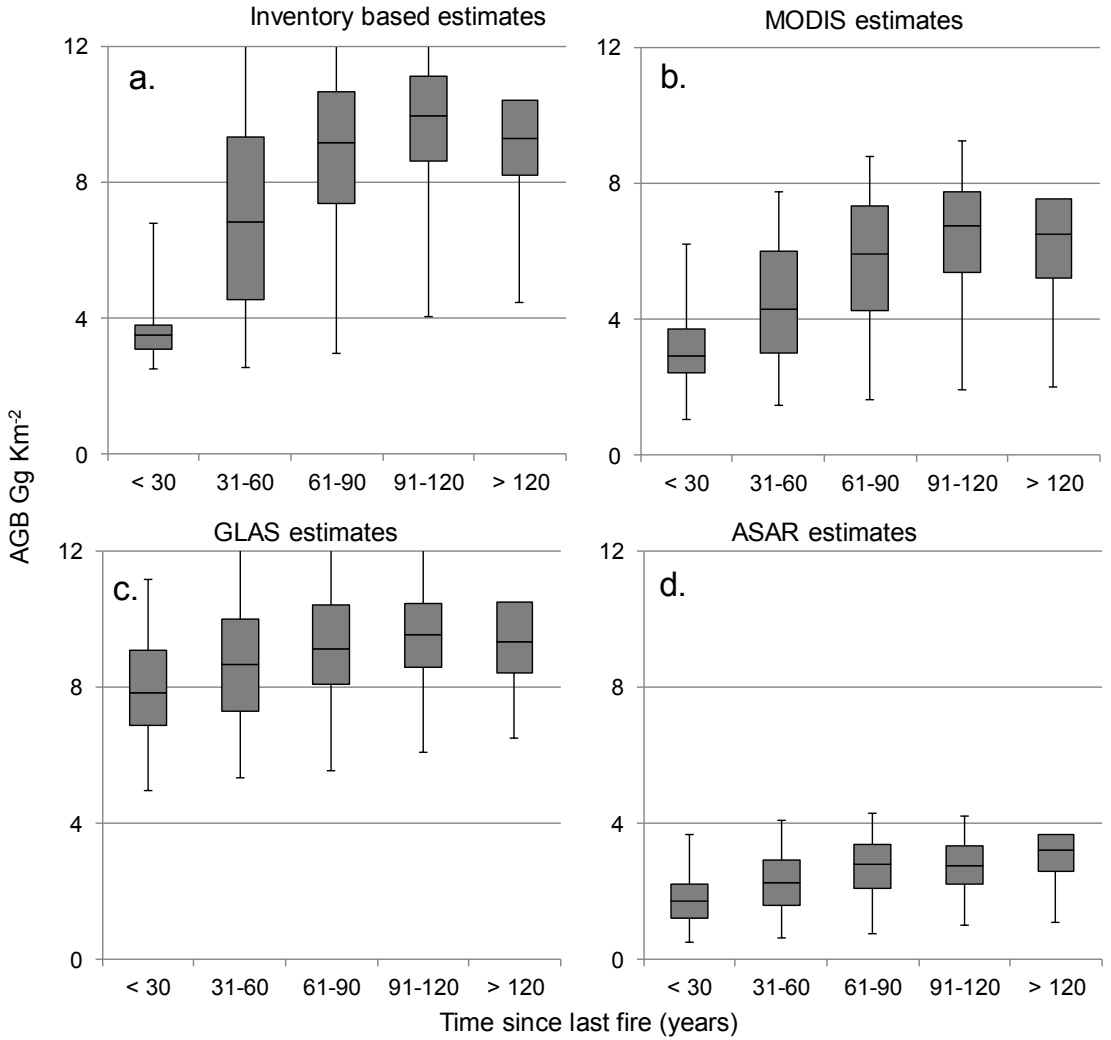

Figure 4.8. Box-and-whisker plots of AGB estimates based on inventory data (a), MODIS (b), GLAS (c), and ASAR data (d) as a function of TSLF at the 2-km^2 scale.

4.05 Discussion

4.05.01 Interpreting covariation and spatial distribution of biomass estimates

Our comparison results are affected by the different physical principles of data acquisition in sensors (optical, LiDAR and radar) at different spatial resolutions, sampling modes, and also methods used for generating AGB at a continental, national or regional scale. For example, with coarser scales, water, open areas, and infrastructure, etc. are subsumed in the pixels and influence the spectral response which affects AGB estimations. The GLAS (active optical, point-based) footprint size is 65 m, therefore sampling only 7% of the pixels, in which only a fraction of waveforms come from forest canopies. Furthermore, averaged canopy height values were predicted for areas not covered by GLAS waveform based on regression between footprint level LiDAR-derived canopy height estimates and spatially continuous ancillary variables from MODIS data (Simard et al., 2011). ASAR AGB estimates are based on a physical model of retrieval of growing stock volume from radar backscatter coefficient which was validated with ground data but only at a regional scale.

Our analysis revealed a low degree of consistency at the 2-km^2 scale between estimates that were based on field inventory data and remotely sensed biomass estimates (Figs. 4.5a-c), particularly in the case of ASAR data. This response can be attributed to the acquisition of ASAR estimates at the pan-terrestrial scale, while GLAS and MODIS estimates were obtained using forest inventory data or Canada's national forest inventory photo-plot data located within the study area. An another reason for low correlation between ASAR and inventory estimates is that ASAR biomass estimates were based upon generic biomass conversion factors from a global wood density database (Chave et al., 2009), while our inventory-based estimates were obtained using region-specific allometric equations.

Among the three remote sensing products, MODIS estimates exhibited the highest correlation with inventory-based estimates ($r = 0.54$, $P < 0.01$; Table 4.2) when compared to GLAS and ASAR estimates. The spatial gradient of biomass that was based on MODIS is similar to the patterns that were observed with the inventory data. MODIS estimates were obtained from Canada's National forest inventory photo-plots, which had been calibrated against provincial forest maps and standing volume data. In fact, MODIS and inventory-based AGB models use similar data, but differed in their modelling approaches, including different allometric equations to extrapolate AGB obtained from plots to the landscape. Despite such a high correlation, MODIS AGB estimates were consistently lower than inventory estimates all across our training area (Fig. 4.8b), and differences between inventory and MODIS biomass estimates were greatly related to observed TSLF (Figs. 4.7a, 4.7d). These differences were lower for recently disturbed cells (TSLF < 30 years) and increased with increasing TSLF, particularly for cells with TSLF equal to 60 to 90 years (Fig. 4.8b). The latter are linked to the abundance of closed canopy cover density estimates (> 75 %) with high biomass levels at a 2-km^2 scale within our training area (Fig. 4.6a; Irulappa Pillai

Vijayakumar et al., 2016). This may be related to the underestimation related to a saturation issue in the regions of high biomass (Beaudoin et al., 2014) and also to underestimation of large observed AGB values and overestimation of small observed AGB values, which is a typical problem of the k-NN method (Magnussen et al., 2010) used to generate the MODIS estimates.

We followed the approach of Zhang et al. (2014b) for developing an AGB model based upon GLAS data since they found a strong correlation (r = 0.70) between observed canopy height and AGB at the plot level (total *n* = 1968: 400 to 8092-m^2: n = 1478; 100 x 100 m: n = 490). Our analysis, in contrast, indicated only a moderate correlation (r = 0.43, P < 0.01) between observed canopy height and AGB of ground plots (400-m^2, *n* = 8739), together with weak model accuracy for AGB prediction at the plot level (R^2 = 0.29). Differences in plot selection can explain these contrasting results, since Zhang et al. (2014b) calibrated their relationships with 75% of plots that had been selected in regions of high productivity. Tree species in high productivity regions are generally taller and have higher volumes and biomass, whereas in less productive regions, other factors, such as stand density and species composition, might also become important (Irulappa Pillai Vijayakumar et al., 2016). This would imply that canopy height alone cannot fully explain variation of AGB variation for our region of study, which contains a range of site productivities.

AGB estimates and GLAS-measured canopy height were not correlated at the plot level in our training region (r = -0.03, P > 0.05) and this lack of a relationship may point to a difference in scale between forest inventory observations and GLAS acquisitions (e.g., Zhao et al., 2009). Canopy height may be an important variable to estimate biomass at the plot level but not at the spatial scale of 1 km^2. Because of this potential scale mismatch problem, the GLAS-derived biomass map (Fig. 4.4c) showed greatly contrasting spatial differences when compared to spatial patterns of AGB derived from MODIS, ASAR and inventory-based estimates. This mismatch can also explain the unexpectedly high values in areas that were recently disturbed by fire (Fig. 4.8d).

Nelson et al. (2010) calibrated airborne estimates of AGB with GLAS waveform metrics for the commercial forests in Quebec (area, 1.27 x 106 km^2). They found a weak relationship (R2 = 0.3-0.4, their Fig. 2) in the northern zone located between 47° N and 52° N, which corresponds to our study region (Fig. 4.2). R^2 values (GLAS heights vs airborne laser heights) were below 0.2 on average and maximum airborne laser heights of 6.6 m and 11.9 m, respectively. Pflugmacher et al. (2008) also suggested that GLAS estimates of biomass would be valuable on a global scale, but would differ from inventory estimates at a regional scale. Margolis et al. (2015), however, have reported higher R^2 values (0.59-0.79) for predicting AGB using GLAS height metrics across the boreal forest of North America (area, 3.7 million km^2), by scaling up airborne estimates of AGB with ICESAT-GLAS height metrics.

4.05.02 Consistency of results among comparable studies

Our results of weak to moderate correlations between remotely sensed biomass estimates for boreal forests in eastern Canada agree with those from similar studies. Mitchard et al. (2013) compared two aboveground biomass maps (Saatchi et al., 2011b; Baccini et al., 2012) for tropical forests in Africa, South America and Asia (area, 2.5 billion ha) obtained from GLAS data using different mapping methods. They found substantial differences between the two maps for particular regions, but estimates from both maps were consistent at the country level. For the Colombian Amazon forests (area of 165,000 km^2), the GLAS biomass maps of Saatchi et al. (2011b) and Baccini et al. (2012) overestimated AGB by 23% and 42 % when compared with the map of Asner et al. (2012), which was derived from field plots and airborne LiDAR. Mitchard et al. (2014) compared the GLAS biomass maps of Saatchi et al. (2011b) and Baccini et al. (2012) to a ground-plot dataset (*n* = 413, Amazon Forest inventory network; Malhi et al., 2002) across tropical forests of the Amazon basin (area, ~ 6.8 x 10^8 ha; Espírito-Santo et al., 2014). Both maps over- or under-estimated ground-based estimates of AGB by more than 25% and also showed different spatial patterns. The observed gradient of increasing AGB from SW to NE Amazonia was not replicated by either remote-sensed product. They indicated that the global relationships between GLAS and biomass could not capture variation in forest biomass throughout the Amazon forest because the map did not account for regional variation in wood density and tree diameter: height relationships.

Avitabile et al. (2011) compared six biomass maps that were based on Landsat, MODIS and global land cover datasets (Drigo, 2006; Gibbs and Brown, 2007; Baccini et al., 2008; Ruesch and Gibbs, 2008; Henry, 2010; Avitabile et al., 2012) for tropical forests in Uganda (area, 241,551 km^2) against a reference map that was based on country-specific field data (*n* = 3510 plots; size, 50 × 50 m) and a national land cover dataset. They found a lack of agreement between the remote sensing products (ranging from 343 to 2201 Tg, their Table 2) and also different mapped distribution patterns. The remote sensing products were also found to be biased (-4.8 Mg/ha to 51.1 Mg/ha; Avitabile et al., 2011, their Table. 3) with respect to the field plots. Finally, Margolis et al. (2015) compared GLAS AGB estimates of Neigh et al. (2003) with AGB estimates based on MODIS data (Beaudoin et al., 2014) for 3.7 million km^2 of the North American boreal forest. Differences in mean AGB densities between both maps (GLAS–MODIS) at the scale of World Wildlife Fund eco-regions for eastern Canadian forests and central Canadian Shield forests were 0.6 and 3.2 Mg ha^{-1}, respectively (Margolis et al., 2015, their Table 13). GLAS estimates of total eco-region AGB were consistently higher than MODIS estimates for 16 of 18 the eco-regions in Canada (Margolis et al., 2015).

4.05.03 Potential ancillary variables for remotely sensed AGB estimation

Our results reveal that the relative proportions of forest cover density classes were the most effective variables in reducing the differences between remotely sensed (MODIS, GLAS, ASAR) and inventory-based estimates. This is not surprising because cover density is linked with signal saturation in MODIS

and ASAR. This result underscores the absence of cover density in the AGB model that was based on GLAS data and which had much influence on inventory-based estimates.

Problems of scale-matching were also identified in the present study. In North American boreal ecosystems, successional dynamics are characterized by fire disturbances and post-fire vegetation recovery, which affect forest carbon stocks (Jones et al., 2013). Fire disturbances occur at a scale greater than most existing spatial resolutions of satellite data (Frolking et al., 2009; Bartels et al., 2016). In this regard, at a 2-km^2 scale, we found that TSLF could provide potential information for estimating biomass with single date reflectance data and also served proxy for canopy cover density in potentially rectifying problems of saturating signals. Disturbance history and vegetation recovery information, together with biophysical factors (surficial deposits), represent potential factors that require greater attention for more accurate estimations of AGB over large areas of the boreal forest.

The inclusion of ancillary variables when using remotely sensed data is well established. In mixed-conifer forests of Blue Mountains of eastern Oregon, USA (area, 830 km^2), Pflugmacher et al. (2014) demonstrated the importance of including a succession trajectory and adding disturbance histories prior to the dates on which estimates were made to improve AGB predictions. Main-Knorn et al. (2011) found that adding tree height or stand volume as predictors to Landsat TM data could significantly improve performance for estimating biomass in coniferous forests (area, ~116,000 ha) of the Carpathian Mountains (border regions of Poland, Czech Republic and Slovakia). For tropical forests of the Amazon basin (area, ~ 6.8 x 10^8 ha; Espírito-Santo et al., 2014), Mitchard et al., (2014) also illustrated the significance of adding spatial layers of species information to the GLAS data for more accurate estimates of biomass.

Forest disturbance and recovery play a major role in global C budgets (Houghton, 2005). In this context, our results of showing the potential interest of generating maps of TSLF, based on the understanding of forest succession dynamics are therefore also applicable to other ecosystems (tropical and temperate). Frolking et al. (2009) have likewise emphasized the importance of combining field data with remote sensing for generating information on disturbance histories and recovery patterns to accurately estimate biomass across forests world-wide. The current condition of a forest stand is related to its disturbance and recovery history (Pflugmacher et al., 2012). Time series analysis of satellite data would provide detailed information on prior canopy recovery/vegetation trend conditions that were based on disturbance histories (Main-Knorn et al., 2013; Ahmed et al., 2014; Madoui et al., 2015). Chu and Guo (2014) have proposed merging different remote sensing data with field data for generating high-quality and quantitative information on post-fire canopy recovery patterns.

4.06 Conclusion

We undertook this study to assess the spatial variation in AGB differences from models that were based on different remote sensing data collected over a large area of boreal forest. The basic goal was to help improve their accuracy. To do this, we compared MODIS, GLAS and ASAR estimates with inventory-based estimates that were derived from forest inventory plots and forest maps at a 2-km^2 scale over a large spatial extent (> 200,000 km^2). Correlations between remote sensing and inventory-based estimates were weak to moderate. Spatial distributions of AGB that were estimated from MODIS, inventory data and ASAR agreed with one another with an expected pattern that was related to fire regime; the spatial pattern provided by GLAS data was different. Our analysis for identifying ancillary variables indicated the potential for enhancing the relationship between reflectance data and AGB through the incorporation of disturbance histories and vegetation recovery trends. Not surprisingly, the relative proportion of canopy cover density that was linked to signal saturation can reduce the differences between inventory and remotely sensed biomass estimates. TSLF may represent a proxy for representing the relative proportion of canopy cover density at the 2-km^2 scale, which would potentially rectify problems of signal saturation.

Looking forward, the future of remote sensing of vegetation biomass relies on LiDAR technology for studying trees in a three-dimensional context. For instance, airborne LiDAR is preferred to spaceborne LiDAR to estimate AGB, but its use remains confined to relatively small study areas due to prohibitive acquisition costs (Zolkas et al., 2013). Combining airborne LiDAR metrics with spaceborne LiDAR measurements may by pass this problem of cost (e.g. Margolis et al., 2015) and in conjunction with information on disturbance history and surficial geological substrate information may provide still more accurate AGB estimates. Furthermore, we also have demonstrated the usefulness of scaling up to integrate ground plots with remotely sensed data up to a scale at which disturbances tend to occur. We also suggest that adequate measures of uncertainty should be provided with remotely sensed biomass estimates by using spatially exhaustive ground-plot data. Our results also show that vertical canopy structure information alone is insufficient for predicting biomass in our study region. We therefore propose the inclusion of metrics that relate to both horizontal and vertical canopy structures (Lu et al., 2014) and factors relevant for forest disturbance and recovery patterns (e.g. TSLF, surficial deposits) for AGB estimation.

4. 07 Acknowledgements

This study was supported by the Fonds Québécois de la Recherche sur la Nature et les Technologies. The Direction des inventaires forestiers, MFFPQ (Ministère de la Forêt, de la Faune et des Parcs du Québec), provided forest inventory plots, forest maps and the SOPFEU fire history map, for which we are grateful. We thank Héloïse Le Goff, Annie-Claude Bélisle and Daniel Lesieur for their fire history maps, and Glenda Russo for helping us to access AGB maps that were based on MODIS data from Canada's

National Forest Inventory portal. Martin Thurner graciously provided ASAR biomass estimates. We also thank Marc Simard for freely allowing us to access GLAS canopy height data. Rémi Saint-Amant provided the normal climate database from the NCEP-NCAR Twentieth Century Reanalysis project for the BioSIM simulations. We thank Dr. Mike Wulder (Research Scientist, Pacific Forestry Centre, Natural Resources Canada), Dr. Richard Fournier (Professor, Centre d'Applications et de Recherches en Télédétection, Université de Sherbrooke), Dr. Martin Schlerf (Senior Research Associate in Earth Observation, Luxembourg Institute of Science and Technology) and Dr. Steven Cumming (Professor, Département des sciences du bois et de la forêt, Université Laval) for providing very useful comments on the final version of this manuscript and W.F.J. Parsons (Centre d'Étude de la Forêt) for English editing.

4.08 References

Ahmed, O.S., Franklin, S.E., Wulder, M.A., 2014. Interpretation of forest disturbance using a time series of Landsat imagery and canopy structure from airborne lidar. Can. J. Remote Sens. 39, 521–542. http://dx.doi.org/10.5589/m14-004.

Amiro, B. D., Stocks, B. J., Alexander, M. E., Flannigan, M. D., Wotton. B. M., 2001. Fire, climate change, carbon and fuel management in the Canadian boreal forest. Int. J. Wildl. Fire 10, 405–413. http://dx.doi.org/10.1071/WF03066.

Asner, G P, Clark, J.K., Mascaro, J., Galindo García, G.A., Chadwick, K.D., Navarrete Encinales, D.A., Paez-Acosta, G., Cabrera Montenegro, E., Kennedy-Bowdoin, T., Duque, Á., Balaji, A., von Hildebrand, P., Maatoug, L., Phillips Bernal, J.F., Yepes Quintero, A.P., Knapp, D.E., García Dávila, M.C., Jacobson, J., Ordóñez, M.F., 2012. High-resolution mapping of forest carbon stocks in the Colombian Amazon. Biogeosciences 9, 2683–2696. http://dx.doi.org/10.5194/bg-9-2683-2012.

Asner, G.P., Mascaro, J., Muller-Landau, H.C., Vieilledent, G., Vaudry, R., Rasamoelina, M., Hall, J.S., van Breugel, M., 2012. A universal airborne LiDAR approach for tropical forest carbon mapping. Oecologia 168, 1147–1160. http://dx.doi.org/10.1007/s00442-011-2165-z.

Asner, G.P., Powell, G.V.N., Mascaro, J., Knapp, D.E., Clark, J.K., Jacobson, J., Kennedy-Bowdoin, T., Balaji, A., Paez-Acosta, G., Victoria, E., Secada, L., Valqui, M., Hughes, R.F., 2010. High-resolution forest carbon stocks and emissions in the Amazon. Proc. Natl. Acad. Sci. 107, 16738–16742. http://dx.doi.org/10.1073/pnas.1004875107.

Avitabile, V., Baccini, A., Friedl, M.A., Schmullius, C., 2012. Capabilities and limitations of Landsat and land cover data for aboveground woody biomass estimation of Uganda. Remote Sens. Environ. 117, 366–380. http://dx.doi.org/10.1016/j.rse.2011.10.012.

Avitabile, V., Herold, M., Henry, M., Schmullius, C., 2011. Mapping biomass with remote sensing: a comparison of methods for the case study of Uganda. Carbon Balance Manag. 6, 1–14. http://dx.doi.org/10.1186/1750-0680-6-7.

Baccini, A., Goetz, S.J., Walker, W.S., Laporte, N.T., Sun, M., Sulla-Menashe, D., Hackler, J., Beck, P.S.A., Dubayah, R., Friedl, M.A., Samanta, S., Houghton, R.A., 2012. Estimated carbon dioxide emissions from tropical deforestation improved by carbon-density maps. Nat. Clim. Chang. 2, 182–185. http://dx.doi.org/10.1038/nclimate1354.

Baccini, A., Laporte, N., Goetz, S.J., Sun, M., Dong, H., 2008. A first map of tropical Africa's above-ground biomass derived from satellite imagery. Environ. Res. Lett. 3, 45011. http://dx.doi.org/10.1088/1748-9326/3/4/045011.

Bartels, S.F., Chen, H.Y.H., Wulder, M.A, White, J., 2016. Trends in post-disturbance recovery rates of Canada's forests following wildfire and harvest. For. Ecol. Manage. 361, 194–207. http://dx.doi.org/10.1016/j.foreco.2015.11.015

Beaudoin, A., Bernier, P.Y., Guindon, L., Villemaire, P., Guo, X.J., Stinson, G., Bergeron, T., Magnussen, S., Hall, R.J., 2014. Mapping attributes of Canada's forests at moderate resolution through kNN and MODIS imagery. Can. J. For. Res. 44, 521–532. http://dx.doi.org/10.1139/cjfr-2013-0401.

Bélisle, A.C., Gauthier, S., Cyr, D., Bergeron, Y., Morin, H., 2011. Fire regime and old-growth boreal forests in central Québec, Canada: an ecosystem management perspective. Silva Fenn. 45, 889–908. http://dx.doi.org/10.14214/sf.77.

Bergeron, Y., Gauthier, S., Flannigan, M., Kafka, V., 2004. Fire regimes at the transition between mixedwood and moniferous boreal forest in northwestern Quebec. Ecology 85, 1916–1932. http://dx.doi.org/10.1890/02-0716.

Bergeron, Y., Leduc, A., Harvey, B.D., Gauthier, S., 2002. Natural fire regime: a guide for sustainable management of the Canadian boreal forest. Silva Fenn. 36, 81–95. http://www.metla.eu/silvafennica/full/sf36/sf361081.pdf.

Bouchard, M., Pothier, D., Gauthier, S., 2008. Fire return intervals and tree species succession in the North Shore region of eastern Quebec. Can. J. For. Res. 38, 1621–1633. http://dx.doi.org/10.1139/X07-201.

Boudreau, J., Nelson, R.F., Margolis, H.A., Beaudoin, A., Guindon, L., Kimes, D.S., 2008. Regional aboveground forest biomass using airborne and spaceborne LiDAR in Québec. Remote Sens. Environ. 112, 3876–3890. http://dx.doi.org/10.1016/j.rse.2008.06.003.

Bradshaw, C.J.A., Warkentin, I.G., 2015. Global estimates of boreal forest carbon stocks and flux. Glob. Planet. Change 128, 24–30. http://dx.doi.org/10.1016/j.gloplacha.2015.02.004.

Buech, R.R., Rugg, D.J., 1989. Biomass relations of shrub components and their generality. For. Ecol. Manage. 26, 257–264. http://dx.doi.org/10.1016/0378-1127(89)90086-8

Burkhart, H.E., Tomé, M., 2012. Modeling forest trees and stands. Springer Science & Business Media.

Chaieb, C., Fenton, N.J., Lafleur, B., Bergeron, Y., 2015. Can we use forest inventory mapping as a coarse filter in ecosystem based management in the black spruce boreal forest? Forests 6, 1195–1207. http://dx.doi.org/10.3390/f6041195.

Chave, J., Coomes, D., Jansen, S., Lewis, S. L., Swenson, N. G., Zanne, A. E., 2009. Towards a worldwide wood economics spectrum. Ecol. Lett. 12, 351-366. http://dx.doi.org/10.1016/ 10.1111/j.1461-0248.2009.01285.x.

Chi, H., Sun, G., Huang, J., Guo, Z., Ni, W., Fu, A., 2015. National forest aboveground biomass mapping from ICESat/GLAS Data and MODIS Imagery in China. Remote Sens. 7, 5534-5564.

Chu, T., Guo, X., 2014. Remote sensing techniques in monitoring post-fire effects and patterns of forest recovery in Boreal forest regions: A review. Remote Sens. 6, 470-520.

Compo, G.P., Whitaker, J.S., Sardeshmukh, P.D., Matsui, N., Allan, R.J., Yin, X., Gleason, B.E., Vose, R.S., Rutledge, G., Bessemoulin, P., Brönnimann, S., Brunet, M., Crouthamel, R.I., Grant, A.N., Groisman, P.Y., Jones, P.D., Kruk, M.C., Kruger, A.C., Marshall, G.J., Maugeri, M., Mok, H.Y., Nordli, Ø., Ross, T.F., Trigo, R.M., Wang, X.L., Woodruff, S.D., Worley, S.J., 2011. The twentieth century reanalysis project. Q. J. Roy. Meteorol. Soc. 137, 1–28. http://dx.doi.org/10.1002/qj.776.

Dobson, M. C., Ulaby, F. T., LeToan, T., Beaudoin, A., Kasischke, E. S., Christensen, N., 1992. Dependence of radar backscatter on coniferous forest biomass. IEEE Trans. Geosci. Remote Sens. 30, 412-415.

Dormann, C.F., Elith, J., Bacher, S., Buchmann, C., Carl, G., Carré, G., Garcia Marquéz, J.R., Gruber, B., Lafourcade, B., Leitão, P.J., Münkemüller, T., McClean, C., Osborne, P.E., Reineking, B., Schröder, B., Skidmore, A.K., Zurell, D., Lautenbach, S., 2013. Collinearity: a review of methods to deal with it and a simulation study evaluating their performance. Ecography, 36, 27–46. http://dx.doi.org/10.1111/j.1600-0587.2012.07348.x.

Drake, J.B., Knox, R.G., Dubayah, R.O., Clark, D.B., Condit, R., Blair, J.B., Hofton, M., 2003. Above-ground biomass estimation in closed canopy Neotropical forests using lidar remote sensing: factors affecting the generality of relationships. Glob. Ecol. Biogeogr. 12, 147–159. http://dx.doi.org/10.1046/j.1466-822X.2003.00010.x.

Drigo, R., 2006. WISDOM - East Africa. Woodfuel Integrated Supply/DemandOverview Mapping (WISDOM) Methodology. Spatial woodfuel production and consumption analysis of selected African countries. Wood Energy Working Paper: FAO Forestry Department http://agris.fao.org/agris-search/search.do?recordID=XF2007431847. (Accessed 1. 07. 2015)

Dunne, T., Leopold, L.B., 1978. Water in Environmental Planning. 1st ed. W.H. Freeman & Company, San Francisco. pp. 566–580.

Espírito-Santo, F.D.B., Gloor, M., Keller, M., Malhi, Y., Saatchi, S., Nelson, B., Junior, R.C.O., Pereira, C., Lloyd, J., Frolking, S., Palace, M., Shimabukuro, Y.E., Duarte, V., Mendoza, A.M., López-González, G., Baker, T.R., Feldpausch, T.R., Brienen, R.J.W., Asner, G.P., Boyd, D.S., Phillips, O.L., 2014. Size and frequency of natural forest disturbances and the Amazon forest carbon balance. Nat Commun 5, Art. No. 3434. http://dx.doi.org/10.1038 /ncomms4434.

FAO, 2015. Global Forest Resources Assessment 2015. How are the world's forests changing?. http://www.fao.org/3/a-i4793e.pdf. (Accessed 29.10.2015)

Farr, T. G., et al. 2007. The Shuttle Radar Topography Mission, Rev. Geophys. 45, RG2004, http://dx.doi.org/10.1029/2005RG000183.

Frelich, L.E., Reich, P.B., 1999. Neighborhood effects, disturbance severity, and community stability in forests. Ecosystems 2, 151–166. http://dx.doi.org/10.1007/s100219900066

Frolking, S., Palace, M.W., Clark, D.B., Chambers, J Q., Shugart, H.H., Hurtt, G.C., 2009. Forest disturbance and recovery: A general review in the context of spaceborne remote sensing of impacts on aboveground biomass and canopy structure. J. Geophys. Res.-Biogeo. 114, G2. http://dx.doi.org/10.1029/2008JG000911.

Gibbs, H. K., Brown, S. 2007. Geographical distribution of woody biomass carbon in tropical Africa: An Updated Database for 2000. Oak Ridge, Tennessee: Carbon Dioxide Information Center, Oak Ridge National Laboratory. http://cdiac.ornl.gov/epubs/ndp/ndp055/ndp055b. html. (Accessed 21. 10. 2015)

Gillis, M.D., Omule, A.Y., Brierley, T., 2005. Monitoring Canada's forests: The National Forest Inventory. For. Chron. 81, 214–221. http://dx.doi.org/10.5558/tfc81214-2.

Girardin, M.P., Ali, A.A., Carcaillet, C., Gauthier, S., Hely, C., Le Goff, H., Terrier, A., Bergeron, Y., 2013. Fire in managed forests of eastern Canada: Risks and options. For. Ecol. Manage. 294, 238–249. http://dx.doi.org/10.1016/j.foreco.2012.07.005.

Girardin, M.P., Guo, X.J., Bernier, P.Y., Raulier, F., Gauthier, S., 2012. Changes in growth of pristine boreal North American forests from 1950 to 2005 driven by landscape demographics and species traits. Biogeosci. Discuss. 9, 1021–1053. http://dx.doi.org/ 10.5194/bg-9-2523-2012.

Gower, S.T., Vogel, J.G., Norman, J.M., Kucharik, C.J., Steele, S.J., Stow, T.K., 1997. Carbon distribution and aboveground net primary production in aspen, jack pine, and black spruce stands in Saskatchewan and Manitoba, Canada. J. Geophys. Res. Atmos. 102, 29029–29041. http://dx.doi.org/10.1029/97JD02317.

Hansen, M., DeFries, R. S., Townshend, J. R. G., Carroll, M., Dimiceli, C., Sohlberg, R. A., 2003. Global percent tree cover at a spatial resolution of 500 meters: First results of the MODIS vegetation continuous

fields algorithm, Earth Interact. 7, 1–15, http://dx.doi.org/10.1175/1087-3562(2003)007<0001:GPTCAA>2.0.CO;2.

Harden, J.W., Trumbore, S.E., Stocks, B.J., Hirsch, A., Gower, S.T., O'neill, K.P., Kasischke, E.S., 2000. The role of fire in the boreal carbon budget. Glob. Chang. Biol. 6, 174–184. http://dx.doi.org/10.1046/j.1365-2486.2000.06019.x.

Henry M., 2010. Carbon stocks and dynamics in Sub-Saharan Africa. PhD Thesis, University of Tuscia, AgroParisTech/ENGREF; 2010 http://www.agroparistech.fr/geeft/Downloads/Pub/Theses/PhD/Henry_PhD_thesis.pdf (Accessed, September 6th, 2015)

Hijmans, R. J., Cameron, S. E., Parra, J. L., Jones, P. G., Jarvis, A., 2005. Very high resolution interpolated climate surfaces for global land areas, Int. J. Climatol. 25, 1965–1978. http://dx.doi.org/10.1002/joc.1276.

Hill, T. C., Williams, M., Bloom, A. A., Mitchard, E. T., Ryan, C. M., 2013. Are inventory based and remotely sensed above-ground biomass estimates consistent? PLoS ONE 8, e74170. http://dx.doi.org/10.1371/journal.pone.0074170

Houghton, R.A., 2005. Aboveground Forest Biomass and the Global Carbon Balance. Glob. Chang. Biol. 11, 945–958. http://dx.doi.org/10.1111/j.1365-2486.2005.00955.x.

Irulappa Pillai Vijayakumar, D. B., Raulier, F., Bernier, P. Y., Gauthier, S., Bergeron, Y., Pothier, D., 2015. Lengthening the historical records of fire history over large areas of boreal forest in eastern Canada using empirical relationships. For. Ecol. Manage. 347, 30–39. http://dx.doi.org/10.1016/j.foreco.2015.03.011.

Irulappa Pillai Vijayakumar, D. B., Raulier, F., Bernier, P. Y., Paré, D., Gauthier, S., Bergeron, Y., Pothier, D., 2016. Cover density recovery after fire disturbance controls landscape aboveground carbon biomass in the boreal forest of eastern Canada. For. Ecol. Manage. 360, 170–180. http://dx.doi.org/10.1016/j.foreco.2015.10.035.

Jenkins, J.C., Chojnacky, D.C., Heath, L.S., Birdsey, R.A., 2004. Comprehensive database of diameter-based biomass regressions for North American tree species. USDA Forest Service, Northeastern Research Station, Newton Square, PA. General Technical Report NE-319. 45 pp. http://svinet2.fs.fed.us/ne/durham/4104/papers/ne_gtr319_jenkins_and_others.pdf> (accessed 19.09.2014)

Jin, Y., Randerson, J.T., Goetz, S.J., Beck, P.S., Loranty, M.M., Goulden, M.L., 2012. The influence of burn severity on postfire vegetation recovery and albedo change during early succession in North American boreal forests. J. Geophys. Res.-Biogeo.117, G01036. http://dx.doi.org/10.1029/2011JG001886

Jones, M. O., Kimball, J. S., Jones, L. A., 2013. Satellite microwave detection of boreal forest recovery from the extreme 2004 wildfires in Alaska and Canada. Glob. Change Biol. 19, 3111–3122. http://dx.doi.org/10.1111/gcb.12288.

Johnson, E. A., Gutsell, S. L., 1994. Fire frequency models, methods and Interpretations. Adv. Ecol. Res. 25, 239–287.

Johnson, E.A., Miyanishi, K., Weir, J.M.H., 1998. Wildfires in the Western Canadian Boreal Forest: Landscape Patterns and Ecosystem Management. J. Veg. Sci. 9, 603–610. http://www.jstor.org/stable/3237276.

Johnstone, J.F., Hollingsworth, T.N., Chapin III, F.S., Mack, M.C., 2010. Changes in fire regime break the legacy lock on successional trajectories in Alaskan boreal forest. Glob. Change Biol. 16, 1281–1295. http://dx.doi.org/10.1111/j.1365-2486.2009.02051.x.

Kasischke, E.S., Melack, J.M., Dobson, M.C., 1997. The use of imaging radars for ecological applications—A review. Remote Sens. Environ. 59, 141-156. http://dx.doi.org/10.1016/S0034-4257(96)00148-4.

Kummerow, C., Barnes, W., Kozu, T., Shiue, J., Simpson, J., 1998. The Tropical Rainfall Measuring Mission (TRMM) sensor package, J. Atmos. Oceanic Technol. 15, 809–817. http://dx.doi.org/10.1175/1520-0426(1998)015<0809:TTRMMT>2.0.CO;2.

Kursa, M.B, Rudnicki, W.R., 2010. Feature selection with the Boruta package. Journal of Statistical Software 36, 1–13. http://www.jstatsoft.org/v36/i11.

Langner, A., Achard, F., Grassi, G., 2014. Can recent pan-tropical biomass maps be used to derive alternative Tier 1 values for reporting REDD+ activities under UNFCCC? Environ. Res. Lett. 9, 124008. http://dx.doi.org/10.1088/1748-9326/9/12/124008.

Lambert, M.C., Ung, C.-H., Raulier. F., 2005. Canadian national tree aboveground biomass equations. Can. J. For. Res. 35, 1996–2018. http://dx.doi.org/10.1139/x05-112.

Le Toan, T., Quegan, S., Davidson, M.W.J., Balzter, H., Paillou, P., Papathanassiou, K., Plummer, S., Rocca, F., Saatchi, S., Shugart, H. Ulander, L., 2011. The BIOMASS mission: Mapping global forest biomass to better understand the terrestrial carbon cycle. Remote Sens. Environ. 115, 2850-2860. http://dx.doi.org/10.1016/j.rse.2011.03.020.

Lecomte, N., Simard, M., Fenton, N., Bergeron, Y., 2006. Fire severity and long-term ecosystem biomass dynamics in coniferous boreal forests of eastern Canada. Ecosystems 9, 1215–1230. http://dx.doi.org/10.1007/s10021-004-0168-x.

Le Goff, H., Flannigan, M.D., Bergeron, Y., Girardin, M.P., 2007. Historical fire regime shifts related to climate teleconnections in the Waswanipi area, central Quebec, Canada. Int. J. Wildland Fire 16, 607–618. http://dx.doi.org/10.1071/WF06151.

Lefsky, M.A., Cohen, W.B., Harding, D.J., Parker, G.G., Acker, S.A., Gower, S.T., 2002. Lidar remote sensing of above-ground biomass in three biomes. Glob. Ecol. Biogeogr. 11, 393–399. http://dx.doi.org/10.1046/j.1466-822x.2002.00303.x.

Lefsky, M.A., Harding, D.J., Keller, M., Cohen, W.B., Carabajal, C.C., Del Bom Espirito-Santo, F., Hunter, M.O., de Oliveira, R., 2005. Estimates of forest canopy height and aboveground biomass using ICESat. Geophys. Res. Lett. 32, L22S02. http://dx.doi.org/10.1046/ 10.1029/2005GL023971.

Lesieur, D., Gauthier, S., Bergeron, Y., 2002. Fire frequency and vegetation dynamics for the south-central boreal forest of Quebec, Canada. Can. J. For. Res. 32, 1996–2009. http://dx.doi.org/10.1139/x02-113.

Lu, D., 2006. The potential and challenge of remote sensing-based biomass estimation. Int. J. Remote Sens. 27, 1297–1328. http://dx.doi.org/10.1080/01431160500486732.

Lu, D., Chen, Q., Wang, G., Liu, L., Li, G., Moran, E., 2014. A survey of remote sensing-based aboveground biomass estimation methods in forest ecosystems. Int. J. Digit. Earth, 1-43. http://dx.doi.org/10.1080/17538947.2014.990526.

McGuire, A.D., 2002. Ecosystem element cycling. Pages 614–618 in A. H. El-shaarawi and W. W. Piegorsch, editors. Encyclopedia of Environmetrics. John Wiley and Sons Ltd., Chichester, UK.

Madoui, A., Gauthier, S., Leduc, A., Bergeron, Y., Valeria, O., 2015. Monitoring forest recovery following wildfire and harvest in boreal forests using satellite imagery. Forests, 6, 4105-4134. http://dx.doi.org/10.3390/f6114105.

Magnussen, S., Tomppo, E., McRoberts, R.E., 2010. A model-assisted k-nearest neighbour approach to remove extrapolation bias. Scand. J. For. Res. 25, 174–184. http://dx.doi.org/10.1080/02827581003667348.

Main-Knorn, M., Moisen, G.G., Healey, S.P., Keeton, W.S., Freeman, E.A., Hostert, P., 2011. Evaluating the remote sensing and inventory-based estimation of biomass in the Western Carpathians. Remote Sens. 3, 1427-1446. http://dx.doi.org/10.3390/rs3071427.

Main-Knorn, M., Cohen, W.B., Kennedy, R.E., Grodzki, W., Pflugmacher, D., Griffiths, P., Hostert, P., 2013. Monitoring coniferous forest biomass change using a Landsat trajectory-based approach. Remote Sens. Environ. 139, 277-290. http://dx.doi.org/10.1016/ j.rse.2013.08.010.

Malhi, Y., 2012. The productivity, metabolism and carbon cycle of tropical forest vegetation. J. Ecol. 100, 65–75. http://dx.doi.org/10.1111/j.1365-2745.2011.01916.x.

Malhi, Y., Phillips, O.L., Lloyd, J., Baker, T., Wright, J., Almeida, S., et al., 2002. An international network to monitor the structure, composition and dynamics of Amazonian forests (RAINFOR). J. Veg. Sci. 13, 439-450. http://dx.doi.org/10.1658/1100-9233(2002)013[0439:AINTMT]2.0.CO;2.

Mansuy, N., Gauthier, S., Robitaille, A., Bergeron, Y., 2010. The effects of surficial deposit–drainage combinations on spatial variations of fire cycles in the boreal forest of eastern Canada. Int. J. Wildland Fire 19, 1083–1098. http://dx.doi.org/10.1071/WF09144.

Mansuy, N., Gauthier, S., Robitaille, A., Bergeron, Y., 2012. Regional patterns of postfire canopy recovery in the northern boreal forest of Quebec: interactions between surficial deposit, climate, and fire cycle. Can. J. For. Res. 42, 1328–1343. http://dx.doi.org/10.1139/x2012-101.

Mansuy, N., Thiffault, E., Lemieux, S., Manka, F., Paré, D., Lebel, L., 2015. Sustainable biomass supply chains from salvage logging of fire-killed stands: A case study for wood pellet production in eastern Canada. Appl. Energy 154, 62–73. http://dx.doi.org/ 10.1016/j.apenergy.2015.04.048.

Mitchard, E.T., Feldpausch, T.R., Brienen, R. J., Lopez-Gonzalez, G., Monteagudo, A., Baker T.R., et al., 2014. Markedly divergent estimates of Amazon forest carbon density from ground plots and satellites. Glob. Ecol. Biogeogr. 23, 935-946. http://dx.doi.org/ 10.1016/10.1111/geb.12168.

Mitchard, E.T., Saatchi, S.S., Baccini, A., Asner, G.P., Goetz, S.J., Harris, N.L., Brown, S., 2013. Uncertainty in the spatial distribution of tropical forest biomass: a comparison of pan-tropical maps. Carbon Balance Manag. 8, 1-13. http://dx.doi.org/10.1186/1750-0680-8-10.

Margolis, H.A., Nelson, R.F., Montesano, P.M., Beaudoin, A., Sun, G., Andersen, H.-E., Wulder, M.A., 2015. Combining satellite lidar, airborne lidar, and ground plots to estimate the amount and distribution of aboveground biomass in the boreal forest of North America. Can. J. For. Res. 45, 838–855. http://dx.doi.org/10.1139/cjfr-2015-0006.

Neigh, C.S., Nelson, R.F., Ranson, K.J., Margolis, H.A., Montesano, P.M., Sun, G., et al., 2013. Taking stock of circumboreal forest carbon with ground measurements, airborne and spaceborne LiDAR. Remote Sens. Environ. 137, 274-287. http://dx.doi.org/10.1016/ j.rse.2013.06.019.

Nelson, R., 2010. Model effects on GLAS-based regional estimates of forest biomass and carbon. Int. J. Remote Sens. 31, 1359-1372. http://dx.doi.org/10.1080/01431160903380557.

Pan, Y., Birdsey, R.A., Fang, J., Houghton, R., Kauppi, P.E., Kurz, W.A., Phillips, O.L., Shvidenko, A., Lewis, S.L., Canadell, J.G., Ciais, P., Jackson, R.B., Pacala, S.W., McGuire, A.D., Piao, S., Rautiainen, A., Sitch, S., Hayes, D., 2011. A large and persistent carbon sink in the World's forests. Science 333, 988–993. http://dx.doi.org/10.1126/science.1201609.

Pelletier, G., Dumont, Y., Bédard, M., 2007. SIFORT: Système d'Information FORestière par Tesselle, Manuel de l'usager. Ministère des Ressources naturelles et de la Faune du Québec. Québec, QC, Canada. https://www.mffp.gouv.qc.ca/publications/forets/fimaq/usager.pdf (accessed 2.10. 2014)

Pflugmacher, D., Cohen, W., Kennedy, R., Lefsky, M., 2008. Regional applicability of forest height and aboveground biomass models for the Geoscience Laser Altimeter System. For. Sci. 54, 647-657.

Pflugmacher, D., Cohen, W.B., Kennedy, R.E., 2012. Using Landsat-derived disturbance history (1972–2010) to predict current forest structure. Remote Sens. Environ. 122, 146-165. http://dx.doi.org/10.1016/j.rse.2011.09.025.

Pflugmacher, D., Cohen, W.B., Kennedy, R.E., Yang, Z., 2014. Using Landsat-derived disturbance and recovery history and lidar to map forest biomass dynamics. Remote Sens. Environ. 151, 124-137. http://dx.doi.org/10.1016/j.rse.2013.05.033.

Popescu, S. C., Zhao, K., Neuenschwander, A., Lin, C. 2011. Satellite lidar vs. small footprint airborne lidar: Comparing the accuracy of aboveground biomass estimates and forest structure metrics at footprint level. Remote Sens. of Environ. 115, 2786-2797. http://dx.doi.org/10.1016/j.rse.2011.01.026.

Ruesch, A., Gibbs, H.K., 2008. New IPCC Tier-1 Global biomass carbon map for the year 2000. Oak Ridge, Tennessee: Carbon Dioxide Information Analysis Center, Oak Ridge National Laboratory. http://cdiac.ornl.gov/epubs/ndp/global_carbon/carbon_documentation.html. (accessed 5.10. 2014)

Régnière, J., St-Amant, R., 2008. BioSIM 9 user's manual. Natural Resources Canada, Canadian Forest Service, Laurentian Forestry Centre, Quebec, QC, Canada. Information Report LAU-X-134E. https://cfs.nrcan.gc.ca/publications?id=28768.(accessed 7.10. 2014)

Saucier, J.-P., Grondin, P., Robitaille, A., Gosselin, J., Morneau, C., Richard, P.J.H., Brisson, J., Sirois, L., Leduc, A., Morin, H., Thiffault, E., Gauthier, S., Lavoie, C., Payette, S., 2009. Écologie forestière - Chapitre 4. Pages 167–315 Manuel de Foresterie (2ème édition). Éditions M. Québec.

Santoro, M., Beer, C., Cartus, O., Schmullius, C., Shvidenko, A., McCallum, I., Wegmüller, U. Wiesmann, A., 2011. Retrieval of growing stock volume in boreal forest using hyper-temporal series of Envisat ASAR ScanSAR backscatter measurements. Remote Sens. Environ. 115, 490–507. http://dx.doi.org/10.1016/j.rse.2010.09.018.

Saatchi, S.S., Harris, N.L., Brown, S., Lefsky, M., Mitchard, E.T., Salas, W., et al. 2011a. Benchmark map of forest carbon stocks in tropical regions across three continents. Proc. Natl Acad. Sci. 108, 9899-9904. http://dx.doi.org/10.1073/pnas.1019576108.

Saatchi, S., Marlier, M., Chazdon, R. L., Clark, D. B., Russell, A. E. 2011b. Impact of spatial variability of tropical forest structure on radar estimation of aboveground biomass. Remote Sens. Environ.115, 2836-2849.

Simard, M., Pinto, N., Fisher, J.B., Baccini, A., 2011. Mapping forest canopy height globally with spaceborne lidar. J. Geophys. Res. Biogeosciences 116, G04021. http://dx.doi.org/ 10.1029/2011JG001708.

Sun, G., Ranson, K. J., Guo, Z., Zhang, Z., Montesano, P., Kimes, D., 2011. Forest biomass mapping from lidar and radar synergies. Remote Sens. Environ. 115, 2906-2916.

Tedeschi, L.O., 2006. Assessment of the adequacy of mathematical models. Agric. Syst. 89, 225–247. http://dx.doi.org/10.1016/j.agsy.2005.11.004.

Ter-Mikaelian, M.T., Korzukhin, M.D.,1997. Biomass equations for sixty-five North American tree species. For. Ecol. Manage. 97, 1–24. http://dx.doi.org/10.1016/S0378-1127(97)00019-4.

Thompson, J.R., Spies, T.A., 2009. Vegetation and weather explain variation in crown damage within a large mixed-severity wildfire. For. Ecol. Manage. 258, 1684–1694. http://dx.doi.org/10.1016/j.foreco.2009.07.031.

Thurner, M., Beer, C., Santoro, M., Carvalhais, N., Wutzler, T., Schepaschenko, D., Shvidenko, A., Kompter, E., Ahrens, B., Levick, S. R. Schmullius, C., 2014. Carbon stock and density of northern boreal and temperate forests. Glob. Ecol. Biogeogr. 23, 297–310. http://dx.doi.org/10.1016/10.1111/geb.12125.

Ung, C.H., Bernier, P., Guo, X.-J., 2008. Canadian national biomass equations: new parameter estimates that include British Columbia data. Can. J. For. Res. 38, 1123–1132. http://dx.doi.org/10.1139/X07-224.

Van Zyl, J.J. 2001. The Shuttle Radar Topography Mission (SRTM): a breakthrough in remote sensing of topography. Acta Astronautica 48, 559–565. http://dx.doi.org/10.1016/S0094-5765(01)00020-0.

Wu, J., David, J.L., 2002. A spatially explicit hierarchical approach to modeling complex ecological systems: theory and applications. Ecol. Model. 153, 7–26. http://dx.doi.org/10.1016/S0304-3800(01)00499-9.

Zhang, G., Ganguly, S., Nemani, R.R., White, M.A., Milesi, C., Hashimoto, H., Wang, W., Saatchi, S., Yu, Y., Myneni, R.B., 2014a. Estimation of forest aboveground biomass in California using canopy height and leaf area index estimated from satellite data. Remote Sens. Environ. 151, 44–56. http://dx.doi.org/ 10.1016/j.rse.2014.01.025.

Zhang, J., Huang, S., Hogg, E.H., Lieffers, V.J., Qin, Y., He, F., 2014b. Estimating spatial variation in Alberta forest biomass from a combination of forest inventory and remote sensing data. Biogeosciences 11, 2793–2808. http://dx.doi.org/10.5194/bg-11-2793-2014.

Zhao, K., Popescu, S., 2009. Lidar-based mapping of leaf area index and its use for validating GLOBCARBON satellite LAI product in a temperate forest of the southern USA. Remote Sens, Environ. 113, 1628-1645. http://dx.doi.org/10.1016/j.rse.2009.03.006.

Zhao, K., Popescu, S., Nelson, R. 2009. Lidar remote sensing of forest biomass: A scale-invariant estimation approach using airborne lasers. Remote Sens. Environ. 113, 182-196. http://dx.doi.org/10.1016/j.rse.2008.09.009.

Zhao, S.Q., Liu, S., Li, Z., Sohl, T.L., 2010. A spatial resolution threshold of land cover in estimating terrestrial carbon sequestration in four counties in Georgia and Alabama, USA. Biogeosciences 7, 71–80. http://dx.doi.org/0.5194/bg-7-71-201.

Zolkos, S. G., Goetz, S. J., Dubayah, R., 2013. A meta-analysis of terrestrial aboveground biomass estimation using lidar remote sensing. Remote Sens. Environ. 128, 289-298. http://dx.doi.org/10.1016/j.rse.2012.10.017.

4.09 Supplementary material

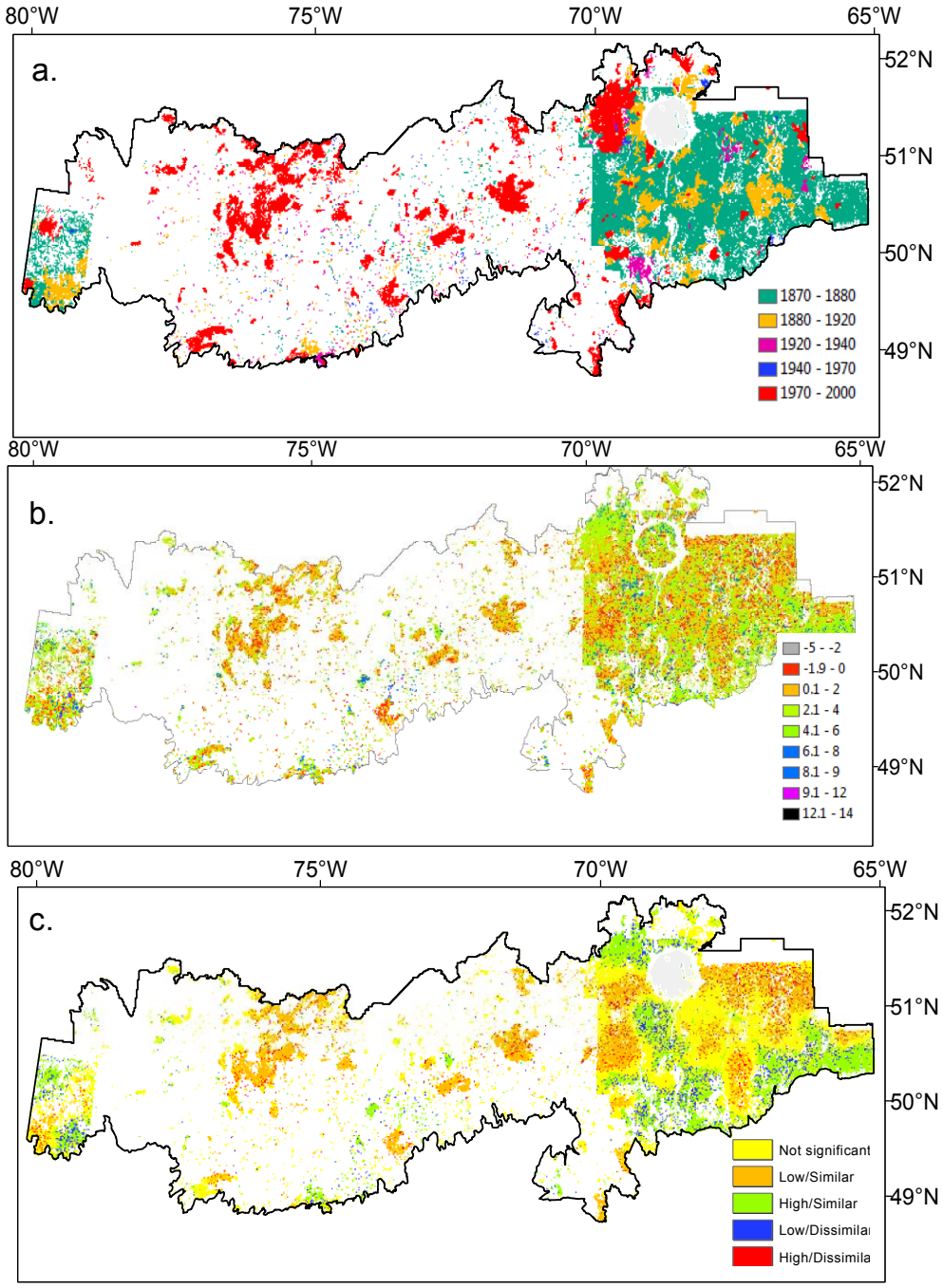

Fig. A.1. a) Map of time since last fire in the training areas; b) the map of observed AGB differences (Gg km^{-2}) between inventory and MODIS estimates; c) spatial clusters of the differences between inventory and MODIS estimates.

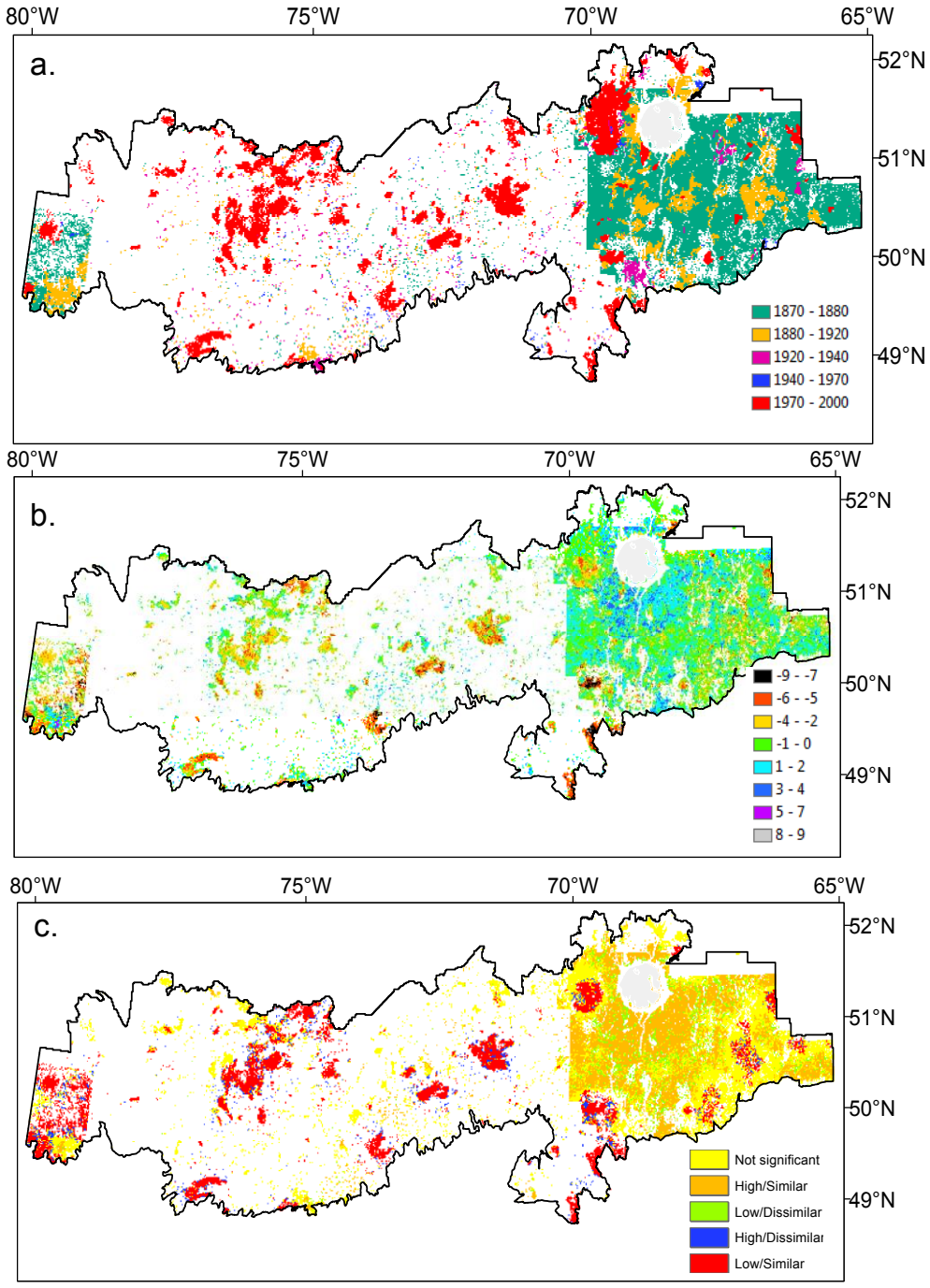

Fig. A.2. a) Map of time since last fire in the training areas; b) the map of observed AGB differences (Gg km^{-2}) between inventory and GLAS estimates; c) spatial clusters of the differences between inventory and GLAS estimates

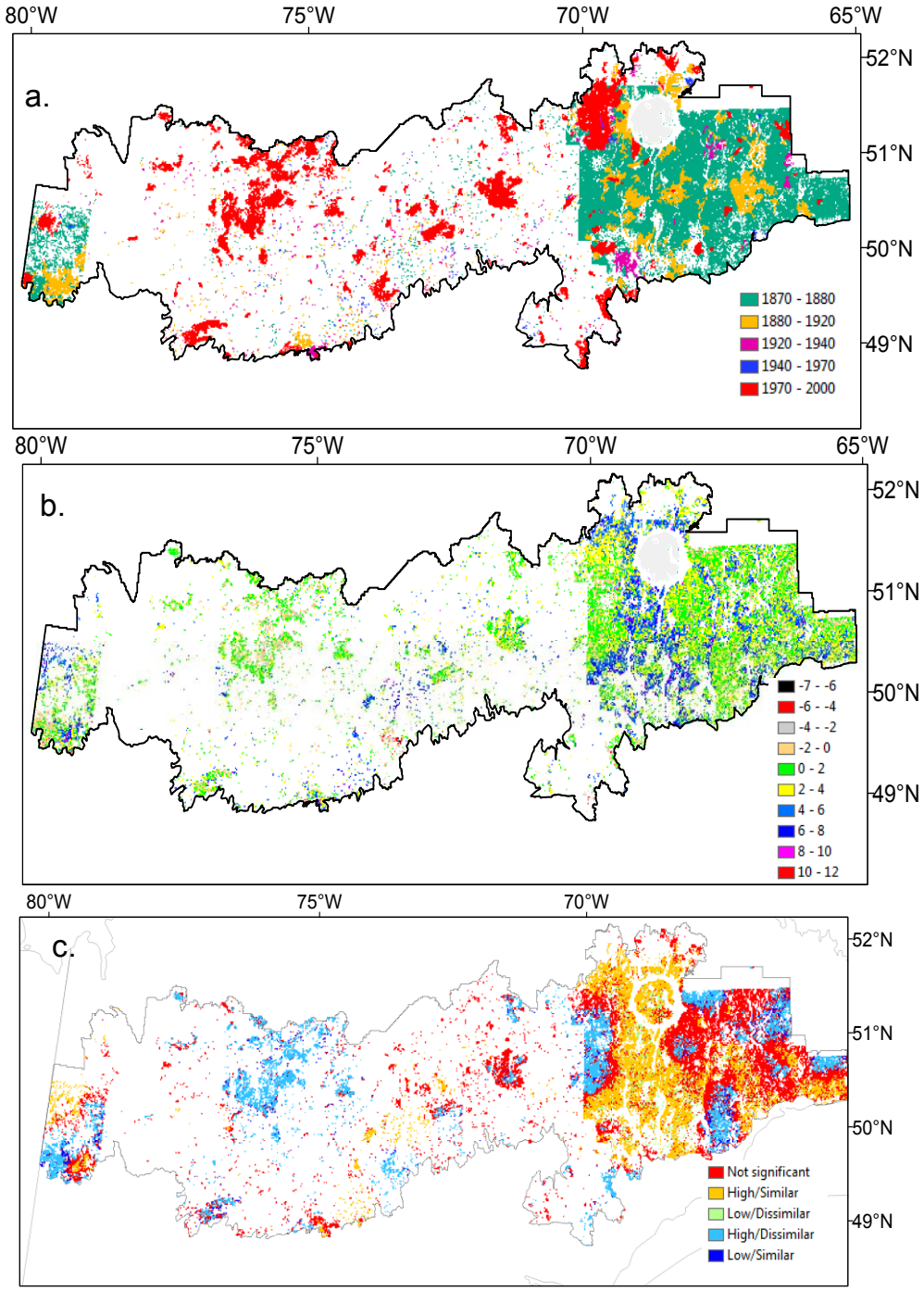

Fig. A.3. a) Map of time since last fire in the training areas; b) the map of observed AGB differences (Gg km^{-2}) between inventory and ASAR estimates; c) spatial clusters of the differences between inventory and ASAR estimates

5. General Conclusion

Studies of carbon storage in any part of boreal forests generally lack wall to wall TSLF information over a long temporal scale (Balshi et al., 2007). For this reason, our understanding of the interaction between TSLF, vegetation composition and structure, climate and environmental factors on aboveground biomass carbon (ABC) at a regional scale across the boreal forest remains fragmentary.

In our study region, we had the privilege to use most of the available fire history maps that allowed us to devise a method for mapping TSLF (1880-2000, 120 years) over a large forest area through deriving empirical relationships between existing historical fire records, forest inventory and climate data at a coarse spatial scale (2-km^2). The selection of a large spatial scale (2-km^2) allowed circumventing the heterogeneity of burning and severity of fire at that scale and detection problems of past burns. Furthermore, we analyzed the contribution of TSLF to predict aboveground biomass carbon (ABC) at plot level and coarse spatial scale (2-km^2). The results of this work revealed the following: 1) the need for lengthening the historical records of fire records for assessing past carbon dynamics and also to evaluate long-term changes of fire regime and 2) at such a coarse scale (2-km^2), ABC is not directly related to stand age and therefore TSLF, but rather to the speed of post-fire canopy recovery, through which TSLF exerts an indirect control on ABC.

Existing carbon budget models (e.g., Kurz et al., 2009, Seely et al., 2002) use growth and yield curves as a function of stand age at a fine spatial scale (plot or stand scale). At such a scale, forest successional dynamics is difficult to observe and our results point to the necessity of developing landscape ABC yield curves that consider forest succession dynamics. Contrary to parametric carbon yield curves, we have developed through a hybrid modelling approach non-parametric empirical models without any assumptions about the structure of data and also based on process understanding. The selection of scale (2-km^2) in agreement with the major disturbance agent in our study area of interest allowed us to analyze emergent outcomes of the interactions existing between TSLF, forest composition, structure and climate on ABC at that scale. We detected that post-fire vegetation recovery is controlling landscape aboveground forest carbon stocks at a scale coarser than that of forest inventory plots or of existing remote sensing data. We have drawn conclusions at one coarse scale only over large spatial extent (> 200,000 km^2), which may change could we reduce or enlarge the study area or change of scale. A further multi-scale research would be necessary to expand or generalize these results.

Further studies should analyze more directly how post-fire dynamics controls biomass recovery after fire over a large spatial extent to inform carbon budget models. In addition, classifying and identifying trajectories of forest recovery over extensive areas and finding their link with standing carbon stocks remain to be explored. Biomass dynamics in tropical and temperate forests are also related to post-fire vegetation recovery legacies that depend on human-induced disturbances/land use (e.g., Letcher et al.,

2009) or major natural disturbances (e.g., Chambers et al., 2007) respectively. Therefore, global monitoring of post-fire vegetation response and recovery seems to be a prerequisite for better understanding biomass recovery and also biomass spatial distribution.

We did not incorporate soil carbon pools, which are important C pools in the boreal forest ecosystems, containing enormous amounts of C, particularly in peatlands and permafrost soils. Further studies also should apply our method for soil carbon pools and total ecosystem carbon content and results may change.

We incorporated the knowledge obtained from the above two studies with a study on remotely sensed biomass estimates for improving their accuracy. Remote sensing is very useful when there is a scarcity of ground inventory data. But the relationship between single date reflectance and biomass is weak under high leaf area conditions and closed canopy conditions (saturation). Our analysis indicated that the discrepancy existing between remote sensing and inventory based estimates could be reduced by incorporating disturbance histories and vegetation recovery trends. The trajectories of forest structure recovery information could be derived from long-term time series data (e.g. Pflugmacher et al., 2012). MODIS burned area products (Giglio et al., 2006) and existing fire polygons data from forest inventory area are potential data to be used in biomass estimation (e.g. Margolis et al., 2015). Chu et al. (2014) proposed the integration of different remote sensing data with field data to support monitoring of post-fire forest recovery patterns.

The future of remote sensing is on studying trees in a three-dimensional view (Shugart et al., 2010). Currently, ICESat GLAS is not functional and data were produced only from 2003 to 2009. ICESat-2 will be launched in 2017 (http://icesat.gsfc.nasa.gov/) and has the mission objective to provide vegetation heights. LiDAR is limited to sampling and profile measurement and must be fused with other remote sensing data to provide information on forest structure (Saatchi et al., 2010). For developing a potential method to estimate biomass, it would be necessary to follow an upscaling approach by integrating AGB information from ground plots with remote sensing data (e.g. Margolis et al., 2015), along with disturbance history and recovery information, from long-term records of observations.

5.01 References

Balshi, M. S., A. D. McGuire, Q. Zhuang, J. Melillo, D. W. Kicklighter, E. Kasischke, C. Wirth, M. Flannigan, J. Harden, and J. S. Clein. 2007. The role of historical fire disturbance in the carbon dynamics of the pan-boreal region: A process-based analysis. Journal of Geophysical Research: Biogeosciences (2005–2012), 112.

Chambers, J. Q., Fisher, J. I., Zeng, H., Chapman, E. L., Baker, D. B., Hurtt, G. C., 2007. Hurricane Katrina's carbon footprint on US Gulf Coast forests. Science, 318, 1107-1107.

Chu, T., Guo, X., 2014. Remote sensing techniques in monitoring post-fire effects and patterns of forest recovery in Boreal forest regions: A review. Remote Sensing, 6(1), 470-520.

Frolking, S., Palace, M. W., Clark, D. B., Chambers, J. Q., Shugart, H. H., Hurtt, G. C., 2009. Forest disturbance and recovery: A general review in the context of spaceborne remote sensing of impacts on aboveground biomass and canopy structure. Journal of Geophysical Research, 114(G00E02).

Giglio, L., Van der Werf, G. R., Randerson, J. T., Collatz, G. J., Kasibhatla, P. 2006. Global estimation of burned area using MODIS active fire observations. Atmospheric Chemistry and Physics, 6(4), 957-974.

Kurz, W., Dymond, C., White, T., Stinson, G., Shaw, C., Rampley, G., Smyth, C., Simpson, B., Neilson, E., Trofymow, J., 2009. CBM-CFS3: A model of carbon-dynamics in forestry and land-use change implementing IPCC standards. Ecological Modelling. 220(4), 480-504.

Letcher, S. G., Chazdon, R. L. 2009. Rapid recovery of biomass, species richness, and species composition in a forest chronosequence in northeastern Costa Rica. Biotropica, 41(5), 608-617.

Margolis, H. A., Nelson, R. F., Montesano, P. M., Beaudoin, A., Sun, G., Andersen, H. E., & Wulder, M. 2015. Combining Satellite Lidar, Airborne Lidar and Ground Plots to Estimate the Amount and Distribution of Aboveground Biomass in the Boreal Forest of North America. Canadian Journal of Forest Research.

Pflugmacher, D., Cohen, W. B., Kennedy, R. E., 2012. Using Landsat-derived disturbance history (1972–2010) to predict current forest structure. Remote Sensing of Environment, 122, 146-165.

Saatchi, S. S., 2010. Synergism of optical and radar data for forest structure and biomass Sinergismo entre dados ópticos e de radar da estrutura da floresta e biomassa. Ambiência, 6(4), 151-166.

Seely, B., Welham, C., Kimmins, H., 2002. Carbon sequestration in a boreal forest ecosystem: results from the ecosystem simulation model, FORECAST. Forest Ecology and Management, 169(1), 123-135.

Shugart, H. H., Saatchi, S., & Hall, F. G. 2010. Importance of structure and its measurement in quantifying function of forest ecosystems. Journal of Geophysical Research: Biogeosciences (2005–2012), 115(G2).